IDENTIFICATION OF DIFFERENTIALLY EXPRESSED PROTEINS AS A RESULT OF RAF KINASE ACTIVITY

By

SARAH ANN REED

A THESIS PRESENTED TO THE GRADUATE SCHOOL
OF THE UNIVERSITY OF FLORIDA IN PARTIAL FULFILLMENT
OF THE REQUIREMENTS FOR THE DEGREE OF
MASTER OF SCIENCE

UNIVERSITY OF FLORIDA

2006

This document is dedicated to my Grandpa, who always believed I could do anything.

ACKNOWLEDGMENTS

Foremost, I would like to thank my advisor, Dr. Sally Johnson, who believed in me enough to first employ me and then accept me as a student. Her ever present guidance, expert advice, and friendship were crucial to the completion of my degree. I also thank my committee members, Dr. Lesley White and Dr. William Buhi, for their excellent suggestions and ideas as well as for reviewing my thesis.

I could not have completed this research without the aid of my former and present lab mates: Jeanine Page, Jessica Starkey, Xu Wang, Dane Winner, Jennelle McQuown, Ju Li, and Sara Ouellette. Dr. Alan Ealy was gracious enough to assist with the statistical analysis and introduce me to Dr. Johnson. In addition, Dr. Stan Stevens and Scott McClung were extremely helpful in troubleshooting and assisting the protein identification.

My Mom, Dad, and brother have shown more love and support than I could ever ask for, for which I thank them endlessly. Most importantly, I thank my husband Jared and my dogs, Annie and Bella. They have kept me smiling through the hard times and have been sounding boards for ideas and frustrations. Jared has graciously dealt with my unending pre-occupation, supported every decision I made, and kept me focused.

TABLE OF CONTENTS

LIST OF TABLES

LIST OF FIGURES

Abstract of Thesis Presented to the Graduate School
of the University of Florida in Partial Fulfillment of the
Requirements for the Degree of Master of Science

IDENTIFICATION OF DIFFERENTIALLY EXPRESSED PROTEINS AS A RESULT OF RAF KINASE ACTIVITY

By

Sarah Ann Reed

May 2006

Chair: Sally E. Johnson
Major Department: Animal Sciences

Satellite cells exist in the quiescent state in healthy muscle. Upon stimuli, they become active and subsequently enter the cell cycle. In the absence of appropriate mitogenic signals, these cells have the ability to exit the cell cycle and return to the quiescent state, replenishing the satellite cell pool. The events that lead to reversible cell cycle exit are largely unknown. 23A2RafER^{DD} myoblasts withdraw from the cell cycle upon initiation of high levels of Raf activity. Phosphorylation of ERK1/2 occurs within the first hour of Raf activation. High levels of Raf activity induce a growth arrest within 24 hours without causing senescence or apoptosis. This growth arrest is reversible upon removal of stimuli, resembling the process of satellite cell self-renewal. Two dimensional PAGE followed by mass spectrometry identified changes in nuclear protein expression after one hour of Raf activity. E2F5 and LEK1 translocate to the nucleus in response to high Raf activity. This response is specific to ERK1/2 phosphorylation and is a specific response of these proteins, as E2F4 expression profiles were unaffected. In

addition, pRb, a pocket protein capable of interaction with E2F transcription factors and LEK1, also translocated to the nucleus in response to ERK1/2 activation. Interestingly, two additional pocket proteins associated with maintenance of quiescence, p107 and p130, are unaffected at this early time. These data indicate that the relocation of E2F5 and LEK1 to the nucleus may be an important early step in the progression from G_1 to G_0.

CHAPTER 1
INTRODUCTION

Satellite cells are responsible for muscle growth and regeneration. These muscle stem cells exist in a quiescent state in normal muscle tissue. Upon appropriate stimuli, satellite cells activate prior to proliferation and subsequent fusion into myotubes. An important characteristic of satellite cells is the ability to self-renew. Following activation or proliferation, one or more daughter cells are capable of returning to the quiescent state to replenish the satellite cell population. To elucidate the potential mechanism of self-renewal, Raf induced quiescence was examined in 23A2RafER^{DD} myoblasts. This cell line contains a Raf molecule fused to a mutated estrogen receptor that responds specifically to 4-hydroxytamoxifen. High levels of Raf stimulation inhibit the myogenic program (139). In addition, these myoblasts also express Pax7 protein, suggesting that they are more akin to muscle satellite cells than myoblasts (Ouellette et al. unpublished data).

The objectives of this work are to (1) characterize the cell cycle response to high levels of Raf activity leading to quiescence and (2) identify changes in nuclear protein expression that may play a role in cell cycle exit.

CHAPTER 2
LITERATURE REVIEW

Satellite Cells: Definition and History

In 1961, Alexander Mauro described the first noted satellite cells. In electron micrograph studies of frog skeletal muscle, Mauro discovered mononucleated cells existing between the plasma membrane and basal lamina (Figure 1). These cells had a low cytoplasm to nucleus ratio, and were fewer in number than normal myonuclei. Mauro named these cells "satellite cells" due to their position relative to the muscle fiber and proposed that these cells are "remnants from the embryonic development of the multinucleate muscle cell which results from the process of fusion of individual myoblasts." He put forth the theory that satellite cells were "dormant myoblasts that failed to fuse" and were "ready to recapitulate the embryonic development of skeletal muscle fiber when the main multinucleate cell is damaged" (89, p. 493-494).

Seventeen years later, Schultz et al. furthered the basic knowledge of the satellite cell population. Confirming that these cells exist in a mononucleated state under the basal lamina, this group found that upon ^{3}H-thymidine perfusion into adult muscle, very few (0.07%) incorporated radiolabeled nucleotides into DNA, indicating that few cells existed in S phase. Together with the organelle poor cytoplasm and abundance of condensed chromatin, this group concluded that satellite cells exist in a quiescent state until needed (117).

Bischoff investigated the *in vitro* activation of satellite cells in their natural position using isolated myofibers from rats. When isolated fibers were destroyed,

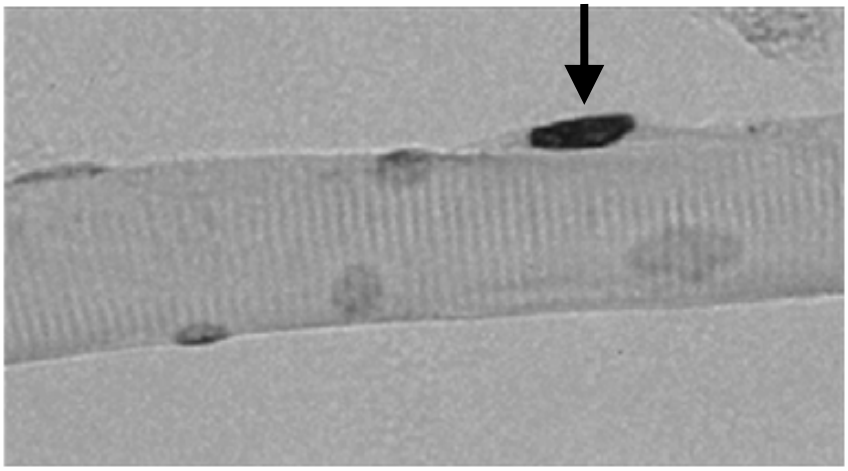

Figure 1. Location of muscle satellite cells. Arrow indicates satellite cell located adjacent to the sarcolemma and under the basal lamina (141).

virtually all satellite cells (>97%) were mitotically active after 24 and 48 hours as determined by ^{3}H-thymidine incorporation. Subsequent fusion of these satellite cells into elongated syncytia confirmed their myoblast nature and ability to recapitulate the entire myogenic program. Because muscle injury stimulated satellite cell mitosis/proliferation, Bischoff proposed that damaged muscle fibers release growth factors and/or mitogens that enable cell proliferation. After 15 hours of exposure to soluble protein extracts of crushed muscles (CME), satellite cells on living fibers became proliferative. This time period shortened considerably to five hours on dead fibers. However, in the absence of CME, no proliferation occurred, regardless of the amount of serum present. Satellite cells on basement membrane shells that were stimulated briefly with CME and subsequently incubated in basal medium proliferated during the following 48 hours, indicating that CME is necessary for the initial activation of satellite cells, but not for continued proliferation. Interestingly, contact with a live fiber is enough to reverse or limit the cell cycle commitment of satellite cells (16).

Mauro found satellite cells to be fewer in number than normal myofiber nuclei. Confirmation of this occurred in 1976, when Schmalbruch and Hellhammer found that only 3.8% of nuclei were satellite cells in varied muscle groups of ten human subjects of both sexes, aged 7-73 (116). In young rats (17-18 days), more satellite cells incorporated thymidine after mincing than did satellite cells in old rats (35-40 days) (128). In Moss and Leblond's study, 12% of satellite cells incorporated thymidine in 14-17 day old rats following injury. These cells proceeded to divide and fuse to existing myofibers in increasing numbers. This group concluded that upon injury, satellite cells are activated

and work to replace the damaged myonuclei – something Mauro had theorized ten years earlier (93).

Distinguishing Features of Satellite Cells

The identification of satellite cells was initially based on anatomical location. In order to study pure populations of satellite cells, these cells had to be distinguished from other mononucleated cells residing in muscle tissue. To this end, a number of protein markers have been identified that are specific to satellite cells alone or in combination with other proteins. These markers include cell membrane receptors, signaling molecules, adhesion molecules, and transcription factors. It is important that these proteins be expressed specifically in satellite cells and not in the adjacent myofiber or myonuclei to best identify satellite cells.

c-Met

The first protein marker identified in satellite cells was the membrane receptor c-Met. Originally identified as a protein encoded by the oncogene *met*, this tyrosine kinase receptor is the receptor for hepatocyte growth factor (HGF) and is necessary for proper migration of hepatocytes and liver regeneration (21, 65, 94). C-Met is a transmembrane tyrosine kinase receptor composed of α and β chains linked by disulfide bonds. The α chain is highly glycosylated and entirely extracellular while the β chain has a large extracellular region, a transmembrane region and an intracellular tyrosine kinase domain. Binding of the extracellular ligand results in autophosphorylation of intracellular tyrosine residues and subsequent phosphorylation of downstream proteins (94). This receptor is found on all quiescent satellite cells but is not expressed in myofibers. Satellite cells identified by anatomic location were positive for c-Met transcripts (141). The c-Met (+) cells had a narrow band of darkly stained cytoplasm located around the nuclei.

Following crush injury, mononucleated cells surrounding the necrotic fiber express c-Met protein. C-Met colocalizes with hepatocyte growth factor (HGF) in actively proliferating satellite cells and is responsible for conducting the HGF signal (132). Isolated cells negative for the surface marker CD34 but positive for c-Met were capable of giving rise to myotubes in culture (113). C-Met null mouse embryos exhibit no skeletal muscle precursor cells in the limb buds or diaphragm, in contrast to the normal formation of the axial muscles (19). This indicates that c-Met is necessary for proper limb and diaphragm skeletal muscle formation.

Pax7

A member of the paired box family of transcription factors, Pax7 is expressed in proliferating primary myoblasts. Pax7 protein levels are down-regulated upon myoblast differentiation (118, 119). Pax7 co-localizes with myostatin, c-Met, and m-cadherin in satellite cells resting beneath the basal lamina (60, 84, 90, 111, 119). While Pax 7 is restricted to satellite cells in the post-natal animal, not all satellite cells, identified by c-Met expression, contain Pax7. The heterogeneity of Pax7 in daughter cells does not correlate with differences in MyoD expression (96, 111). Satellite cells quickly down-regulate Pax7 upon commencement of terminal differentiation (96). Myoblasts immunostaining Pax7(+) and MyoD(-) may return to quiescence to replenish the satellite cell pool while myoblasts that acquire MyoD proliferate and fuse to form myotubes (147). Myofiber nuclei in chicks immunostain negative for Pax7 but positive for MyoD and myogenin (60). Whether myoblasts express Pax7 and myogenin simultaneously is the source of some debate. Olguin and Olwin found Pax7 and myogenin to be mutually exclusive, while Pax7, Myf-5, and MyoD may be present in the same myoblast (96). In contrast, Halevy et al. and Zammit et al. found few cells that were positive for both Pax7

and myogenin indicating that these may be an intermediate population that is exiting the cell cycle and entering terminal differentiation (60, 147) .

In myogenic cell lines, quiescent, undifferentiated myoblasts appear to be uniquely marked with high levels of Pax7. Overexpression of Pax7 in satellite cells induces cell cycle exit, prevents incorporation of BrdU, decreases expression of MyoD, and prevents the induction of myogenin. However, the loss of Pax7 does not induce differentiation, indicating that other factors must be present or absent for myoblasts to commence terminal differentiation. While myogenic conversion induced by MyoD is inhibited by Pax7, MyoD remains nuclear. However, Pax7 was unable to inhibit the effects of a MyoD-E47 heterodimer, indicating that Pax7 may interfere with MyoD function or compete for proteins necessary for MyoD-dependent transcription (96).

Adult Pax7-/- mice are smaller in size and have smaller myofibers than wild type counterparts (100). Fibers isolated from Pax 7 null mice give rise to no quiescent satellite cells in culture systems. In addition, no quiescent satellite cells could be identified in more than 300 sublaminar nuclei from gastrocnemius muscles in 7-10 day old knockout mice or day 18 embryos (119). Oustanina et al. indicated that Pax7 null mice have satellite cells, but these are very few and the numbers decrease with age (100). The mitotically active satellite cells express *MyoD* and divide at rates comparable to wild types suggesting that Pax7 may be needed for maintenance of the satellite cell population rather than proliferation. Pax7-/- myoblasts demonstrate a reduced differentiation capacity *in vitro* (100). Importantly, injury in adult Pax7 null mice indicates that regeneration is not as efficient or complete as wild type or heterozygous individuals as indicated by a lengthened time of healing and the presence of residual necrotic material.

This may be due to the decreasing number of satellite cells and/or inefficient differentiation.

CD34

CD34 as a true marker of satellite cells remains controversial. CD34 positive cells express no cardiac, hematopoietic, or skeletal muscle cell mRNA transcripts, indicating a lack of lineage. By contrast, skeletal muscle progenitor cells lacking CD34 express c-Met but no other skeletal muscle transcripts, indicative of a muscle cell lineage. After 14-21 days in culture, both CD34(+) and (-) myoblast populations fuse and exhibit spontaneous contractile behavior, expressing MyoD, myocyte nuclear factor α (MNFα), and desmin. Thus, both CD34 (+) and CD34 (-) progenitor cells may give rise to myotubes *in vitro* (113). Single fiber isolates from mice contain mononucleated cells that express both CD34 and m-cadherin. After five days of differentiation, some cells remain mononucleated and express CD34 but are MyoD and Myf5 negative. After 48 hours in culture, CD34 expression declines in satellite cells that migrate and have begun to proliferate. This group did note that CD34, Myf-5, and m-cadherin do not mark all satellite cells (15).

CD34 may mark a population of satellite cells that is less committed to the myogenic lineage. Muscle-derived stem cells isolated from mice that express CD34 lack Pax7 and m-cadherin expression. These cells are capable of contributing to regeneration of *mdx* muscle at low passage numbers but lose this ability with time (39). In mouse gastrocnemius sections, CD34 expressing cells constitute a small population of muscle-derived cells located under the basal lamina co-expressing m-cadherin (85). Jankowski et al. found CD34 expressing primary myoblasts to be more efficient at participating in regeneration, although CD34(-) cells had a higher fusion index in vitro (68).

Interestingly, mononucleated cells remaining after cultures were induced to differentiate expressed high levels of CD34. Myoblasts expressed similar levels of myogenic proteins (MyoD, myogenin, MRF4, m-cadherin) regardless of the presence of CD34.

m-cadherin

Several groups have identified the Ca-dependent cell adhesion molecule m-cadherin in both quiescent and activated satellite cells (15, 31, 35, 84). Cells expressing m-cadherin account for 5.3% of sublaminar nuclei in the six week old mouse hind limb (31). The number of m-cadherin positive cells increases upon satellite cell activation (35). Following cardiotoxin injury, cells staining positive and negative for m-cadherin express MyoD, although cells lacking m-cadherin stain less intensely for MyoD. All cells expressing Myf-5 also express m-cadherin (31). M-cadherin expressing cells also express CD34 (15).

Myocyte Nuclear Factor

Expressed in cardiac and skeletal muscle, myocyte nuclear factor (MNF) was identified in a screen of binding proteins for the myoglobin CCAC box. This transcription factor has also been identified as Foxk1. Two forms of MNF were identified as having reciprocal expression during regeneration (52, 144). MNFα is a 90kDa protein expressed in committed myoblasts and myotubes. A splice variant of MNFα, MNFβ expression peaks on day two of *in vitro* differentiation and then wanes (144). Further characterization showed MNFβ expression primarily in quiescent satellite cells while MNFα occurred predominantly in proliferating cells. MNF protein is present as early as 8.5 days post coitum (dpc) in the heart tube and rostral somites. By 10.5 dpc, MNF is abundantly expressed in the myotome of the somite and cells migrating to the limb bud and two days later can be found throughout the limb bud and axial musculature.

Expression in differentiated myotubes wanes around 16 dpc but persists in small mononucleated cells in the limbs and body wall. Approximately 2-5% of sublaminar nuclei in post-natal sections contain MNF. Electron microscopy of post natal sections shows MNF expression in the nuclei of satellite cells as classified by location beneath the basal lamina yet above the sarcolemma. Upon cardiotoxin injury, the number of positively stained MNF cells expands and expression persists in the central nuclei of regenerating fibers (53).

MNF null mice show significant growth retardation, at ~60% the size of wild type littermates. These mice also have impaired regeneration; three weeks following cardiotoxin injury, a hypercellular myonecrotic response remained. The regeneration that did occur was accompanied by extensive replacement of muscle tissue with fat (52). Myoblasts isolated from MNF null animals can differentiate into myotubes but proliferate much more slowly than heterozygous or wild type cells (52). In addition, progenitor cells that are capable of differentiation are able to co-express MNFα and CD34 (113). When crossed with *mdx* mice, the resulting MNF -/- *mdx* mouse is born even smaller than MNF-/- or *mdx* littermates. Compared to littermates, these mice also are less active and appear to be more fragile. Upon closer investigation, the chest wall and diaphragm have widespread myonecrosis and fibrosis. MNF-/-*mdx* mice die within the first few weeks of life (52).

V-CAM1 and N-CAM

Two cell adhesion molecules, vascular cell adhesion molecule 1 (V-CAM1) and neuronal cell adhesion molecule (N-CAM) have been identified in satellite cells (69, 88, 118). V-CAM1 is expressed in endothelial and skeletal muscle cells in adult animals, and in skeletal muscle is limited to quiescent satellite cells and activated muscle precursor

cells *in vivo*. A possible interaction between cells staining positive for V-CAM1 and infiltrating lymphocytes may increase cytokine accumulation, which is required for satellite cell activation and muscle precursor cell proliferation and differentiation during regeneration (69).

Little information is available regarding N-CAM expression in satellite cells. Malm et al. used N-CAM (CD56) as a marker for activated satellite cells following exercise in human skeletal muscle (88). Ectopic expression of human N-CAM in mouse muscle resulted in an increased size of the neuromuscular junction and an increase in the number of terminal sprouts in the absence of denervation (138). Ectopic N-CAM enhanced regeneration of the neuromuscular junction following denervation by increasing the length of the sprouts and the number of secondary sprouts.

Syndecan 3/4

Syndecan 3 and 4 are cell surface transmembrane heparin sulfate proteoglycans involved in FGF signaling. Both proteins are implicated in satellite cell maintenance and regeneration. Syndecan 3 immunostaining is present in the skeletal muscle of the mouse forelimb throughout development and in young adult skeletal muscle. Syndecan 3 appears at embryonic day (dE) 14.5 in individual myoblasts and by dE18.5 individual myoblasts and myotubes are outlined with syndecan 3. By neonatal day 2, syndecan 3 is becoming localized to discrete sites at the myotube periphery and becomes even more localized in young adult skeletal muscle (33). Syndecan 4 is present around the lumen in developing myoblasts at dE14.5 and at the periphery of myotubes at dE18.5. While expression becomes localized in young adult cells, it is not as restricted as syndecan 3.

Syndecan 3 and 4 are both associated with a subset of myonuclei. Co-staining syndecan 3/4 expressing cells with c-met shows complete overlap of staining in quiescent

and proliferating cells. Laminin staining locates the cells between the basal lamina and myotube. In young adult muscle syndecan 3 staining colocalizes with FGFR1, staining satellite cells exclusively. These proteins are expressed prior to detectable MyoD expression and remain after MyoD induction and proliferation. Primary mouse satellite cells require heparan sulfate for normal proliferation. When signaling events requiring heparan sulfate (including syndecan signaling) are blocked, activation and initiation of myogenesis is delayed *in vitro* (33).

Syndecan 3 null mice have extensive fatty infiltrates between and within muscle fibers. Quiescent satellite cells appear normal in morphology in terms of size, position, and marker gene expression. However, the knockout mouse has approximately 6.7 times the number of satellite cells/100 myofiber nuclei than the wild type mouse. There also is an increase in the number of differentiated myonuclei compared to wild type but no difference in the fiber number/muscle or the average fiber diameter. The appearance of significantly more central nuclei in mature fibers suggests that regeneration is occurring in the absence of experimental damage. These observations are consistent with the defects in hind limb locomotion exhibited by these animals. Upon activation of satellite cells, fewer satellite cells from syndecan 3 null mice expressed MyoD at 96 hours than wild type. This lower expression is accompanied by a mislocation of MyoD to the cytoplasm rather than the nucleus. Satellite cells from syndecan 3 null mice proliferate extensively but form large, irregular syncytia rather than fibers. These cells do not express MyoD or MyHC (34).

Syndecan 4 null mice also have adipose infiltrates between fibers, but unlike syndecan 3 null mice, have none within the fibers. Satellite cells in syndecan 4 null mice

have decreased c-Met and syndecan 3 immunostaining along with a decreased thickness and increased disorder of the basal lamina. Unlike the syndecan 3 null mouse, the syndecan 4 null mouse has only a slight increase in central myonuclei above the wild type mouse. There is no difference in the number of satellite cells or mature myonuclei in syndecan 4 null mice and wild type. Satellite cells in these mice are delayed in activation and proliferation, and after proliferation myoblasts appear in large, aberrant clusters. Few cells express MyoD at 96 hours post stimulation and those that do express the protein cytoplasmically. These results indicate that syndecan 4 is required for normal activation and proliferation. Isolated colonies of satellite cells from syndecan 4 null mice are delayed in adhesion, fail to express MyoD and MyHC, and fail to fuse. Addition of exogenous heparan partially rescues the syndecan 3 null mouse by correcting the MyoD localization but fails to correct syndecan 4 defects (34).

Notch

The Notch signaling pathway is an evolutionarily conserved signaling cascade that is involved in tissue development in a multitude of organisms. The binding of an extracellular ligand (such as Delta or Serrate) to a transmembrane receptor of the Notch family results in the enzymatic cleavage of the intracellular domain of the receptor. This cleavage product represents the active form of Notch and translocates to the nucleus where it affects gene transcription through association with various transcription factors. Muscle injury results in the increased expression of desmin and activated Notch 1 in the injured tissue. However, desmin and Notch1 are co-expressed in mononucleated cells only at the site of injury. Therefore, muscle injury results in the activation of Notch 1 and expansion of Notch1 and Desmin expressing myoblasts *in vivo*. Interestingly, Numb is expressed asymmetrically in crescent shaped patterns. During cell division, Numb

localizes to one pole, thus only one daughter cell receives Numb. Myofibers were isolated 72 hours after injury and cultured overnight. Numb and Pax3 (a premyoblast gene) were mutually exclusive in satellite cells on the cultured myofibers. The exclusion of Numb in Pax3 expressing satellite cells indicates that these cells are less committed to a specific phenotype. In contrast, Numb expressing cells also expressed Pax7, suggesting that Pax7 is a marker of a more committed cell. The expression of a constitutively active Notch1 resulted in the up regulation of Pax3 and the down regulation of Myf-5, MyoD, and desmin as well as a modest reduction in Pax7. Over expression of Numb resulted in the down regulation of Pax3 and the up regulation of Myf-5 and desmin. Notch 1 appears to promote a less committed myogenic phenotype while Numb may promote progression along the myogenic lineage (29).

Side Population Cells

A fraction of muscle-derived stem cells, side population cells are theorized to contribute marginally to muscle regeneration. This population of cells is derived from bone marrow. Side population cells may reside in skeletal muscle but do not assume the typical satellite cell position in healthy muscle tissue (9, 83). However, upon gamma irradiation, bone marrow derived side population cells may reside in the satellite cell niche and assume a myogenic lineage, expressing c-met and Myf-5 (83). Side population cells injected into injured muscle contribute to regeneration (32, 41, 83). Isolated bone marrow cells that are $CD45^{+}Lin^{-}c\text{-}kit^{+}$ contribute to muscle regeneration (41). Expression of CD34 or Sca1 did not distinguish cells capable of assisting regeneration. The side population cells residing in muscle are also capable of giving rise to hematopoietic cells, unlike satellite cells (9).

Satellite Cell Activation: Progression from G_0 to G_1

In normal adult muscle, satellite cells exist in the quiescent state (G_0). Upon injury or hypertrophic stimulus, these cells are activated and enter the cell cycle. Satellite cell activation occurs during the lag phase from the first extracellular signal to cell cycle entrance. This phase is often incorrectly grouped with the proliferative state: they are two separate stages. In essence, the activation phase is the preparation for cell cycle entry. It is important to note that activation does not imply or lead to proliferation. Early inhibition may return the satellite cell to the quiescent state.

Hepatocyte Growth Factor

The first satellite cell activating factor was identified by Richard Bischoff in 1986. The soluble material obtained from crushed rat leg muscles was capable of inducing proliferation of satellite cells on single fibers in culture without stimulating proliferation of the surrounding fibroblasts. Crushed muscle extract (CME) also enhanced proliferation of myogenic cells isolated from 19 day old rat embryos and promoted differentiation in these cells. Satellite cells stimulated with CME enter S phase after 18 hours and proliferate with a generation time of 12 hours. When injected into the flexor digitorum brevis (FDB) muscle of 1 week old rat pups, CME caused a significant increase in muscle growth reflected by increased DNA content (18). Satellite cells on living fibers proliferated 15 hours after CME exposure, but only 5 hrs after exposure on degenerating fibers. Satellite cells on killed fibers that briefly were stimulated with CME and then incubated in basal medium proliferated over the following two days. Contact with a live fiber was enough to reverse or limit the cell cycle commitment (16). In primary cultures of satellite cells isolated from three week and nine month old rats, CME increased PCNA expression, indicating cell cycle re-entry (71).

Immunoblotting of CME identified two bands of hepatocyte growth factor (HGF), a 90 kDa uncleaved and 60 kDa cleaved alpha chain. In fibers isolated from normal adult rat tibialis anterior (TA) muscle, c-Met positive cells were elongated and located under the basal lamina in the typical satellite cell position. In regenerating muscle, c-Met and HGF co-localize to the cytoplasm of satellite cells with levels of both proteins decreasing as the cells enter terminal differentiation (132). HGF is present in the extracellular matrix of muscle (131). The HGF message was detectable from 12-72 hr in culture of adult rat satellite cells. At 12 hrs, HGF appears to be predominantly located on the cell surface but is intracellular at 72hr. Serum-free conditioned medium contained HGF, indicating that it was synthesized, secreted, and dissociated from activated cells (122). In the presence of anti-HGF, satellite cells stimulated with CME do not re-enter the cell cycle at rates comparable to controls, indicating that HGF is responsible for activation. HGF injection into uninjured rat hind limbs causes satellite cell proliferation (over 50% more than that caused by IGF/FGF2) (132). Conditioned medium from stretched fibers stimulated BrdU incorporation into satellite cells on unstretched fibers, indicating the release of an activating factor. Addition of anti-HGF to the conditioned medium inhibited S-phase entry of satellite cells on unstretched fibers (133). The addition of exogenous HGF in isolated chick satellite cells increased satellite cell DNA synthesis and resulted in an earlier entry into S-phase. Exogenous HGF also inhibited transcription from muscle-specific reporter genes as well as *MyoD* and *myogenin* expression. Inhibition of differentiation through these pathways suggests that HGF may regulate differentiation through inhibition of the myogenic regulatory factors (49). Injection of exogenous HGF on the day of muscle injury results in significantly more myoblasts

although there is no difference in the regenerative ability of the fibers. Multiple injections of HGF (once daily for three days) result in a large area devoid of regenerated myofibers. Those fibers that do regenerate have a significantly smaller cross sectional area. After washout of exogenous HGF, muscle regeneration returns to normal (92). Thus, while HGF promotes satellite cell proliferation, it inhibits differentiation, allowing enlargement of the pool of muscle precursor cells.

Age differences

Differences in the extent and the length of time for muscle regeneration in the elderly are a common cause of age-related myopathies such as sarcopenia and polymyositis. Several differences in the satellite cell population are readily apparent, such as the lag time until activation and the size of the nuclear domain. Many age-related myopathies are related to muscle atrophy and lack of regeneration. Old rats (24 mos) incur more sarcopenia than adult (9 mos) or young (1 mos) rats (12). The relative muscle weight (muscle weight/body weight) decreases from adult (6-20 mos) to elderly (20-32 mos) in rats. Hind limb suspension decreases muscle weight in young and old rats, causing a muscle mass loss due to inactivity that is similar to the loss that occurs during aging. Intermittent reloading of the suspended muscle decreases atrophy in rats of 6 and 20 months, but not of 32 months of age (50).

While the number of satellite cells present in young adult, adult, and old animals remains the same, the number of cells that can be isolated from these animals tends to decrease with age, most likely due to changes in activation. Because these animals have the same number of satellite cells prior to activation, the difference in proliferative cells is a decline in the activation of satellite cells, not the total number present (12, 20, 27).

The percent of quiescent cells per fiber was similar in all three groups (young adult, adult, aged) (12).

Important in maintaining proper protein production, the amount of cytoplasm a nucleus controls is termed the nuclear domain. Nuclear domain tends to differ in aged and young muscle. The number of myonuclei per fiber is lower in younger individuals than in older individuals, resulting in a larger nuclear domain in younger muscle (72). Similarly, Gallegly et al. found that despite the decline in muscle size and strength in old rats, the number of nuclei present remains similar between groups. The smaller nuclear domain (nuclei/mg protein) is reflected in a lower myofiber cross sectional area per nucleus (50).

In addition to the differences in nuclear domain size, satellite cells from older animals take longer to become mitotic following stimuli. Satellite cells isolated from young rats re-enter the cell cycle 24-30hr post plating, while satellite cells isolated from old rats remain quiescent for 42-48 hours (12, 70, 112, 143). G_0 exit is accompanied by a higher number of c-Met positive cells upon serum stimulation in young rats as compared to old rats and an overall higher percentage of PCNA positive cells in young rats (12, 87). Similar to rodents, no significant difference was found in the proliferation or fusion rates of myogenic cells isolated from 60-69 and 70-79 yr old humans (20).

Conboy et al. completed a rather elegant set of experiments with parabiotic pairings between young and old mice (28). The young partners in each pair were either transgenic for green fluorescent protein (GFP) or expressed a distinct CD45 allele to confirm blood chimaerism. Mice were paired isochronically (young-young and old-old) or heterochronically (young-old). After five weeks of parabioses, a hind limb on each

mouse was injured. Five days after injury, young mice in isochronic and heterochronic parabioses exhibit regenerating muscles as indicated by central nuclei in embryonic myosin heavy chain (eMHC) expressing myotubes. Old isochronic pairs exhibited poor muscle regeneration with few proliferating cells, prominent fibrosis, and incomplete myofiber formation. Injured muscle in old mice (19-26 months) exposed to a young systemic environment through heterochronic parabiotic pairing with a young mouse regenerated similarly to injured muscle in young mice. This regeneration was due almost exclusively from the activation of aged satellite cells, not from grafts from the young mouse.

Exercise

The act of exercise evokes stress upon muscle fibers through stretching, as well as physiological changes in pH, changes in growth factor concentration, and occasionally injury to the myofibrils or myofibers. The amount of damage caused to the cell (and therefore the level of satellite cell activation) is dependent upon the type of exercise as well as the intensity and duration.

Both endurance and resistance training activate satellite cells. Mice participating in daily exercise show a significant increase in the number of proliferating satellite cells. Daily exercise resulted in the addition of significantly more new myonuclei than one bout or no exercise (127). The number of satellite cells increased gradually (but significantly) over 90 days of resistance training in young men and ten weeks of strength training in young women (73, 74). After 30 days of detraining, satellite cell number gradually decreased to pre-training levels. mRNA for the cell cycle markers cyclin D1 and p21 increased following the first 30 days of training and returned to basal levels during de-training. Along with changes in satellite cell number and muscle cross sectional area,

acute resistance loading (RL) increased mechano growth factor (MGF) mRNA expression, the muscle-specific form of IGF-1. Acute RL also induced an overall increase in levels of cyclin D1 gene expression and inhibited *myostatin* expression (78). There was no significant change in the number of myonuclei following resistance training or during the detraining period in contrast to changes that occur during endurance exercise. The gradual increase in the CSA gained during training (significant by 90 days) decreased during detraining. The significant increase in cross sectional area (CSA) coupled with little increase in myonuclear number resulted in a larger myonuclear domain during training in the vastus lateralis (which consists of type I and type II fibers), indicating that the number of nuclei present were capable of handling the increased myonuclear domain (73). In a previous study, this group indicated that the fibers of the trapezius in women increased by 36% following a ten week resistance exercise protocol. The increased CSA was concurrent with an increase in myonuclei to CSA ratio in accordance with the myonuclear domain theory. The differences between these two studies may be the differences in the percentage of cross sectional area gained (17% in the 2004 study, 36% in the 2000 study) (74).

Maximal voluntary exercise stimulus in humans is not enough to cause myofiber lesions in most individuals, however it is enough for satellite cell activation. There was a significant increase in the number of cells positive for N-CAM following a single bout of high intensity exercise (four and eight days post exercise) concurrent with a significant increase in the percent of mononuclear cells expressing Fetal Antigen 1 (FA1) in the exercised leg. FA1 is expressed in undifferentiated mononucleated cells in fetal skeletal muscle. Following high intensity eccentric exercise, there was a significant increase in

the number of cells positive for FA1. FA1 colocalizes with Pax7 in mononuclear cells in damaged adult muscle fibers but is not present in healthy adult fibers (36).

Irradiation attenuates satellite cell proliferation in mouse hind limbs. In healthy muscle, eccentric contraction-induced injury causes regeneration demonstrated by centrally located nuclei. Muscles irradiated prior to eccentric contraction-induced or freeze-induced injury had few fibers with central nuclei. Not only does irradiation affect regeneration, it also prevents the recovery of muscle strength following injury. Even after 35 days of recovery, muscle that was irradiated and then injured did not recover the same amount of strength (compared to pre-irradiation/injury) as non-irradiated injured muscle (108).

Spinal cord transection causes a rapid and progressive decrease in the cross sectional area of soleus and extensor digitorum longus (EDL) in rats. The CSA of the soleus declines more rapidly and to a greater extent than the EDL. Exercise following spinal cord transection results in an increase in the CSA of soleus fibers to nearly control values but has no effect on the EDL. While all three fiber types are affected in the soleus muscle, only types IIx and IIa are affected in the EDL but these fibers aren't stimulated enough to offset the atrophy caused by a lack of neural input. Satellite cell activation occurs in the soleus and EDL muscles following spinal cord transaction regardless of exercise regime (42).

Both muscle contraction and stretching occur during exercise, so it follows that mechanical stretch may activate satellite cells in a similar manner to the stretch and contraction caused by exercise. Both Tatsumi et al. and Wozniak et al. noted that stretch activated satellite cells on isolated fibers although not all cells were activated (133, 141).

Satellite cell activation peaked at thirty minutes and two hours after stretching (141). The differences in activation resulting from stretch may occur because of differences in the intensity or duration of stretch.

Nitric Oxide

Recent work has focused on the interaction between nitric oxide (NO) release and satellite cell activation. Anderson was the first to show an effect of NO on satellite cells. Using L-Arginine, a stimulus for nitric oxide synthase (NOS) and L-NAME, a NOS inhibitor, this group showed that the presence of NO (through the addition of L-Arg) increased the cell yield (presumably from activated satellite cells) following muscular injury. Treatment with L-NAME both restricted and delayed the normally rapid changes in size and position of activated satellite cells. Thin cells that were c-Met positive but expressed no HGF immediately following injury were present in L-NAME treated mice. By 10 minutes post injury, enlarged, HGF expressing satellite cells were present but these were fewer in number than in control muscles. The persistence of necrotic fiber segments in mice supplemented with L-NAME during 6 days of repair indicated inefficient regeneration (5). Inhibition of satellite cell activation by L-NAME was restored with the addition of HGF (5, 133). The combination of CME and L-NAME treatments increased activation above control levels, but only to approximately half the level of CME alone. Addition of HGF or L-Arg increased activation two fold. Stretch and injury both released HGF to bind the c-met receptor through a NO dependent mechanism (4). Satellite cells on unstretched fibers were activated with SNP, a NO generating compound. NO increased as early as 1 hr after muscle fiber stretch and continued to be present as long as 20 hr (133).

On fibers isolated from the FDB, many c-Met(+) mononucleated cells remained attached to the fiber for 44-48 hours post plating. However, some c-Met expressing cells lifted from the fibers and entered the cell cycle. The percentage of proliferative cells increased to 55% at 48 hours post plating. The addition of CME to fibers increased the number of proliferating cells 76% by 48 hours post plating. While CME increased activation by three fold, the addition of L-NAME decreased satellite cell activation and proliferation (4).

Mdx mice treated with L-Arg and deflazacort (a corticosteroid used to treat Duchene's muscular dystrophy) resulted in earlier myoblast differentiation. The positive effects of deflazacort and L-Arg are positively correlated with NOS-Iμ expression in regenerating muscles. Deflazacort treatment alleviated dystrophy, decreased the central nucleation index, and increased fiber diameter. NOS inhibition decreased myotube formation and decreased or blocked the c-Met and myf-5 increase that occurs with satellite cell activation (7).

Daily L-Arg injections over four weeks increased the nNOS activity and nitric oxide levels in *mdx* mice, although there were no changes in the number of central nuclei. The percent of fibers taking up Evans Blue Dye decreased from 10% to 4% in mdx mice in the absence or presence respectively of L-Arg, indicating that L-Arg increases the stability of the fibers. L-Arg protected *mdx* mice against damage caused by eccentric contraction, had positive effects on the force frequency relationship, and increased utrophin (a substitute for dystrophin) in *mdx* fibers (14).

Overload of the rat plantaris causes an increase in skeletal α-actinin and MyHC type I mRNA as well as a higher expression of HGF, IGF-I, MGF, and VEGF mRNA.

TRIM (a specific inhibitor for iNOS and nNOS) doubled IGF-I and MGF mRNA expression in overloaded but not control muscle and eliminated the increase of skeletal α-actinin and MyHC type I mRNA seen in overloaded muscle. L-NAME and TRIM increased phosphorylation of p70s6k in overloaded muscles which correlated to increased protein synthesis (120).

Notch

In 2002, Conboy and Rando used a mouse myofiber explant system to monitor satellite cell activation and proliferation. No bromodeoxyuridine (BrdU) incorporation was seen before 24 hours *in vitro*. Proliferation gradually increased from 24-72 hr *in vitro* and then increased dramatically between 72 and 96 hr *in vitro*. Full length Notch1 was present at 0 hours *in vitro*. Activated Notch1 was undetectable at 0 hours, but increased between 0 and 96hr. The Notch1 ligand Delta also was undetectable at 0 hours *in vitro* and increased until 96 hr *in vitro*. At 96 hours *in vitro*, Notch1, Delta, and Numb were present in the majority of mononucleated cells associated with the myofiber. Notch1 activation and the increased expression of Delta are coincident with satellite cell activation (29).

The Notch1/Numb balance also effects myoblast proliferation and differentiation. Overexpression of Numb, an inhibitor of intracellular Notch, resulted in lower cell proliferation, while a constitutively active Notch1 enhanced proliferation of primary mouse myoblasts. The constitutively active Notch1 continued to promote proliferation even upon serum withdrawal. In addition to increased proliferation, Notch1 appears to inhibit differentiation, significantly reducing the expression of eMHC and production of multinucleated myotubes. The use of RNAi to inhibit Notch1 signaling decreased the rate of BrdU incorporation by two fold. These transient effects were most severe in

rapidly proliferating, recently established myoblast cultures. Cells deprived of serum expressed more Numb and withdrew from the cell cycle (29).

Resting muscle expresses little of the Notch ligand, Delta1, but has increased levels of Numb and baseline levels of Notch1 regardless of the age of mouse from which it was isolated. However, in response to injury Delta1 expression increases in young and adult satellite cells but fails to do so in old cells. The increase in Delta1 is associated with a decrease in Numb expression and an increase in proliferation (identified through increased PCNA expression). When satellite cells are activated in culture, similar levels of Notch1 are expressed, but cells from old mice have consistently lower levels of activated Notch (27).

After injury, Delta expression in young animals is induced in satellite cells and at the periphery of myofibers adjacent to the injury as well as in cells ~300 μm caudal to the injury. Very little *Delta* up-regulation occurs in older animals and none occurs at a distance from the injury site. Inhibition of Notch1 signaling by a soluble Jagged-Fc fusion protein blocked satellite cell activation in young injured muscle and resulted in a reduced number of regenerating myotubes. By contrast, activation of Notch1 by an antibody directed to its extra-cellular domain increased cell proliferation and inhibited differentiation. Forced Notch1 activation markedly improved regeneration of injured old muscle and significantly enhanced formation of regenerated fibers (27).

Basic Fibroblast Growth Factor

Basic fibroblast growth factor (bFGF or FGF2) stimulates myoblast proliferation while inhibiting differentiation into mature myofibers. bFGF represses differentiation while stimulating proliferation in MM14 myoblasts and is 30 times more effective at maintaining a proliferative state than acidic FGF. bFGF is required for the initiation of a

new cell cycle (26). MM14 and C2C12 myoblasts exhibit specific bFGF binding. Differentiating cells lose expression of the fibroblast growth factor receptor and therefore lose the ability to bind bFGF while serum-starved quiescent cells retain high levels of FGFR on the cell surface (97). Unlike differentiating MM14 myoblasts, proliferating MM14 myoblasts express bFGF mRNA. Addition of exogenous bFGF inhibits differentiation. Transfection of a bFGF cDNA into MM14 myoblasts inhibits differentiation and increases BrdU incorporation. Transfection also affects neighboring cells which incorporated BrdU in the presence of bFGF expression, suggesting a paracrine action (61). Addition of HGF and bFGF to C2C12 myoblasts has a synergistic effect on proliferation (137). 23A2 myoblasts supplemented with TGF-β or bFGF were incapable of fusion. Removal of the inhibitory growth factor resulted in fusion and troponin I expression (134).

Inhibition of FGF signaling through overexpression of a dominant negative FGF receptor 1 (dnFGFR1) resulted in withdrawal from the cell cycle and the formation of small myotubes containing few nuclei. A small number (7%) of cells continued to proliferate, indicating the presence of FGF independent myoblasts. Inhibition of FGFR1 resulted in a decrease in muscle mass during embryonic development due to decreased numbers of myoblasts. No change in fiber diameter was observed, however a 50% decrease in packing density in dnFGFR1 limbs existed corresponding to an increased space between fibers (46).

bFGF is a heparin binding growth factor that can signal through a variety of intracellular signaling pathways. bFGF stimulated the mitogen activated protein kinase kinase 1 (MEK1, a dual specificity protein kinase upstream of ERK1/2 in the

Raf/MEK/ERK pathway) but not ERK1/2 or S6 kinase in MM14 myoblasts. However, addition of bFGF following ten hours of serum starvation resulted in the activation of MEK, MAPK, and S6 kinase indicating that the response to this growth factor may be dependent upon the extracellular environment (23). Syndecans are heparan sulfate proteoglycans (HSPGs) implicated in the binding of growth factor and extracellular matrix components. Proliferating but not differentiating MM14 myoblasts express syndecan 3/4. Chlorate treatment reduces the low affinity binding of ^{125}I-aFGF and ^{125}I-bFGF to HSPGs. This effect is reversed by the restoration of glycosaminoglycan sulfation. Chlorate induces terminal differentiation in bFGF supplemented cells, indicating that it blocks the bFGF driven inhibition of differentiation. Addition of heparin to chlorate treated cells restores bFGF action (98).

In addition to affecting myoblasts, bFGF increases satellite cell proliferation, promoting muscle regeneration (71, 86, 121, 143). Proliferating rat satellite cells express FGFR1/2/3/4 mRNA with 1 and 4 being the most prominent. Addition of bFGF to isolated adult rat satellite cells elicited a greater mitogenic response than IGF-I or TGF-β. The combination of bFGF and HGF acted in an additive manner with regard to proliferation (121). Addition of bFGF increases proliferation and PCNA expression in satellite cells isolated from three week old rats but not from 9 month old rats (71). High affinity FGF binding did not occur until 42 hours post-plating in adult rat satellite cells, occurring only 18 hours after plating in cells from young rats. The activated receptors were capable of generating the intracellular signaling through tyrosine phosphorylation characteristic of the bFGF signaling cascade (70).

In healthy mouse muscle, bFGF is expressed around the fiber periphery, around myonuclei, and in non-muscle cells (6). Mononucleated cells in *mdx* mice are positive for bFGF and myogenin (mgn), especially around and within damaged fibers (51). Twelve hours after muscle injury, disrupted myofibers express bFGF, particularly in regions of hypercontraction (6). There is a corresponding increase in the number of mononucleated cells distal to the injury that express bFGF. This population likely includes inflammatory cells. bFGF also is present in newly formed myotubes (51). Injection of bFGF into the TA of male *mdx* mice at the time of the first round of spontaneous necrosis results in enhanced satellite cell proliferation (86). The number of regenerated fibers is positively correlated to the dose of bFGF. Addition of bFGF to satellite cells isolated from rats increased the number of activated cells, possibly by allowing an increased number of satellite cells to enter the cell cycle or shortening the time it takes to undergo division thus, achieving more cells in the same amount of time (143).

Faster proliferating satellite cells isolated from the pectoralis major of the turkey expressed higher levels of bFGF and FGFR1 earlier than slower proliferating cells and produced more HSPG. The faster proliferating satellite cells also showed a greater mitogenic responsiveness to bFGF than slower proliferating cells. Expression of HSPG decreased as differentiation proceeded (91).

Satellite cells isolated from the extensor digitorum longus and tibialis anterior of rat hind limbs were most responsive to bFGF when added at a concentration of 2 ng/ml. The addition of heparin to cultures supplemented with bFGF had no effect on the number of PCNA (+) cells (77). As in myoblasts, bFGF stimulated a strong mitogenic signal in

isolated satellite cells and isolated myofibers by increasing proliferation and inhibiting differentiation (3, 17, 58, 59, 146).

Chicken anterior latissimus dorsi muscle expressed decreased levels of FGF1, normal levels of bFGF, and increased levels of FGFR1 after 11 days of stretching when compared to unstretched muscle. After 11 days of stretch, increases were seen immunohistochemically in bFGF and FGF4 protein levels within the endomysium and perimysium. Nuclear bFGF localization was identified in a specific population of mononucleated cells at the fiber periphery. Chronic low frequency electrical stimulation over five days resulted in a 3 fold increase in FGF1 and bFGF mRNA. In addition, FGFR1 increased two fold, while FGFR4 only slightly increased in response to electrical stimulation (43).

Insulin-like Growth Factor 1

Similar to bFGF, insulin like growth factor I (IGF-I) increases satellite cell proliferation *in vitro* and *in vivo* (1, 3, 76). IGF-I stimulated proliferation of isolated satellite cells even in the presence of TGF-β. However, TGF-β decreased the proliferation rate in a dose dependent manner. In the absence of TGF-β, IGF-I greatly stimulated satellite cell differentiation although high amounts of IGF-I could not induce differentiation in the presence of TGF-β (3). The presence of IGF-I increased the magnitude of the proliferative response elicited by bFGF as well as stimulating differentiation alone (59). IGF-I binding protein (IGFBP) 3 and IGFBP 5 are produced by satellite cells but not fibroblasts *in vitro*. IGFBP3 and 5 expression were increased by addition of IGF-I, TGF-β, and bFGF. IGF-I was the most potent stimulus for IGFBP5, while TGF-β greatly stimulated IGFBP3. IGF binding proteins extend the half life of IGFs and serve as a reservoir for IGF-I in the blood (146). The addition of estrogen or

trenbolone to bovine satellite cell cultures resulted in increased amounts of IGF-I mRNA and an increase in cell proliferation (76).

Infusion of IGF-I into rat TA muscles caused no systemic effects. IGF-I infusion over two-three weeks resulted in a ~9% increase in muscle mass as well as an increase in muscle DNA content (1). Muscles recovering from atrophy (hind limb suspension) regained more muscle mass than control recovering muscles when infused with IGF-I during regeneration. Colonies from satellite cells isolated from atrophied muscles treated with IGF-I were larger than colonies isolated from control atrophied muscles. Satellite cells with the highest potential for replication appeared to be lost with repeated atrophy-regeneration. The addition of IGF-I to cells after repeated atrophy-recovery resulted in larger colonies with a greater potential for replication, indicating that IGF-I may help restore the replicative capacity of these cells (24). In young rats, overloaded muscles have increased IGF-I receptor mRNA. A significant increase in mechano growth factor mRNA occurs in all ages following muscle overload (101).

While muscles injected with rAAV-IGF-I demonstrated increased muscle mass, gamma irradiation prior to IGF-I injection suppressed the increase in size. A small muscle mass increase did occur in muscles that were irradiated and subsequently injected with IGF-I, indicating that not all of the hypertrophy was due to satellite cells. This increased muscle mass may result from the ability of differentiated fibers to produce more protein by increasing the myonuclear domain without the addition of new myonuclei (13).

Transforming Growth Factor β

One of the most potent inhibitors of myoblast proliferation and differentiation, the transforming growth factor β (TGF-β) family of growth factors also elicit dramatic

effects on satellite cells. TGF-β greatly inhibits differentiation and to a lesser extent, proliferation, of satellite cells (2, 47, 59, 107, 129). The inhibition of fusion caused by TGF-β is dose dependent and reversible. Removal of the growth factor allows myoblasts to fuse and express myosin heavy chain as well as creatine kinase (47, 129). While the inhibition of fusion is not overcome by addition of IGF-I, bFGF is capable of overcoming at least a portion of the inhibition of proliferation resulting from TGF-β activation (3).

In Sol 8 mouse myoblasts addition of anti-TGF-β was capable of blocking the inhibition of differentiation resulting from addition of exogenous TGF-β (2). Supplementation with bFGF or TGF-β blocked differentiation of C2C12 myoblasts. These cells accumulated cyclin D1 protein, a cyclin active in mid-G1 of the cell cycle. Cyclin D3 responded to bFGF or TGF-β in a biphasic manner, decreasing 2-4 hours post stimulation and increasing 32-64 hours post stimulation. Ectopic expression of cyclin D1 inhibited differentiation when expressed at low levels but had no effect on fusion at high levels of expression. Activation of muscle gene transcription by myogenic basic helix-loop-helix regulators also is prevented by the ectopic expression of cyclin D (107).

Both TGF-β and family member GDF8 (myostatin) increase IGFBP3 mRNA and protein expression. IGFBP3 suppresses proliferation of porcine embryonic myogenic cells. Antibody neutralization of IGFBP3 relieved 50-70% of the suppression of proliferation caused by TGF-β or GDF8 (75).

Portacaval anastomosis (PCA) rats mimic the muscle atrophy seen in liver cirrhosis. PCA rats exhibit decreased expression of myosin heavy chain, MyoD, myogenin, Myf5, and PCNA protein levels. Myostatin levels are three times higher in PCA than control mice, coinciding with increases in activinR2b, the myostatin receptor,

and CDKI p21 which mediates the effects of myostatin. Changes in mRNA levels are consistent with the identified protein changes (38).

CHAPTER 3
MATERIALS AND METHODS

Myoblast Culture

Stock cultures of 23A2RafER^{DD} embryonic mouse myoblasts (139) were maintained on 10 cm plastic plates coated with 0.1% w/v gelatin and passaged at approximately 70-75% confluency. Cells were cultivated in basal medium eagle (BME) supplemented with 15% v/v fetal bovine serum (FBS), 1% v/v L-glutamine, 1% v/v penicillin/streptomycin, 0.1% v/v gentamycin reagent solution, and 10mM puromycin and incubated in 5% CO_2 at 37ºC. All cell culture media, supplements, and sera were purchased from Invitrogen (Carlsbad, CA). Cells (3.5×10^4) for immunofluorescence were cultured on 35 mm glass-bottomed plates (World Precision Inst., Sarasota, FL) coated with 10% v/v BD Matrigel Matrix HC (BD Biosciences, San Jose, CA).

Raf Protein Expression

23A2RafER^{DD} myoblasts stably express a tamoxifen-inducible chimeric Raf protein (139). The estrogen receptor-Raf kinase domain chimera is unstable in the absence of the estrogen analog. Addition of 4-hydroxy-tamoxifen (4HT) binds to the estrogen receptor and allows for a dose-dependent increase in Raf protein expression and kinase activity. Sub-confluent 23A2RafER^{DD} myoblasts were washed twice with phosphate buffered saline (PBS), treated with 10μg/mL protamine sulfate (CalBioChem, San Diego, CA) in serum-free BME for 10 minutes, and washed twice with PBS. Cells were starved in serum free BME for one hour. For long term (>2hr) Raf induction, cells were treated with 1μM 4-hydroxy-tamoxifen (4HT; Sigma, St. Louis, MO) in 2% FBS

BME. For short term induction (≤ 2 hr) cells were treated with 1μM 4HT in serum free BME. Control cells were maintained in the appropriate media supplemented with ethanol. When necessary, cells were pulsed with bromodeoxyuridine (BrdU) during the last thirty minutes of treatment and then fixed with methanol.

Western Blots

Following Raf activation, plates were washed twice with PBS. Cells were lysed in 4X SDS PAGE sample buffer. Lysates were briefly sonicated, heated for 5 minutes at 95ºC and stored frozen at -20ºC until further use. Equal amounts of protein were separated through 10% polyacrylamide gels. Blots were incubated in 5% w/v non fat dry milk (NFDM) in TRIS-buffered saline – Triton X (TBS-T; 10 mM Tris, pH 8.0, 150 mM NaCl, 0.1% v/v Tween 20) for thirty minutes at room temperature. Primary antibodies were diluted in blocking solution and incubated with the blots overnight at 4ºC. After washing three times for five minutes each in TBS-T, peroxidase conjugated anti-mouse (or rabbit) antibodies diluted 1:5000 in blocking solution were added to the blots for sixty minutes at room temperature. Blots were washed a further three times for five minutes each in TBS-T. Immunoreactive complexes were visualized by enhanced chemi-luminescence (Amersham Biosciences, Piscataway, NJ) and X-ray film.

Acidic β-galactosidase Staining

Following Raf activation, myoblasts cells were stained for acidic β-galactosidase to visualize senescent cells. Myoblasts were fixed in 2% v/v formaldehyde, 0.2% v/v glutaraldehyde in PBS for 4 minutes at room temperature. Plates were incubated overnight at 37ºC in β-galactosidase staining solution (20% v/v citric acid sodium phosphate solution [126mM sodium phosphate, 36.8mM citric acid, pH 6.0], 150mM NaCl, 2mM $MgCl_2$, 5mM potassium ferricyanide, 5mM potassium ferrocyanide, 1mg/ml

X-galactosidase, to 100ml with H_20). Staining was viewed by light microscopy the following day after three five minute washes with PBS.

Growth Arrest and Recovery

23A2RafER^{DD} myoblasts were culture in 2% fetal bovine serum containing 1 μM 4HT or vehicle only. After 48 hours, cells were washed twice with PBS and placed in normal growth media (15% FBS BME, no 4HT) for 24 hours. Cells were pulsed with 10 μM BrdU for 30 minutes prior to fixing in methanol.

Nuclear Protein Extracts

Myoblasts were rinsed in cold TBS and scraped from the plates into hypotonic buffer (25 mM Tris, pH7.5, 1 mM MgCl2, 5 mM KCl, 0.05% v/v NP40, 5 mM orthovanadate, 5 mM sodium fluoride, 5 mM pyrophosphate, 1 mM PMSF, 10 mg/ml aprotinin). Cells were allowed to swell for 15 minutes on ice in polypropylene Falcon tubes (Fisher, Pittsburgh, PA). Lysates were centrifuged at 3220 x g for 10 minutes at 4ºC in a swinging bucket rotor to recover nuclei. Nuclei were resuspended in high salt buffer (20 mM Tris, pH8.0, 20% v/v glycerol, 300 mM NaCl, 1.5 mM MgCl2, 200 μM EDTA, 1 mM DTT, 1 mM PMSF, 10 mg/ml aprotinin, 5 mM orthovanadate, 5 mM pyrophosphate, 5 mM sodium fluoride, 1% v/v NP40, 0.01% v/v SDS) and rocked at 4ºC for one hour. DNA and debris were pelleted for 15 minutes at 16,100 x g at 4ºC. The supernatants containing the nuclear proteins were frozen at -80ºC until further use.

Protein Desalting and Concentration

Resin from D-Salt Excellulose Desalting columns (Pierce, Rockford, IL) was added to small spin columns (Pierce, Rockford, IL). The resin was centrifuged at 1500 x g for one minute. Isoelectric focusing (IEF) sample buffer (4% w/v CHAPS, 7M urea, 2M thiourea) was passed through the column at 1500 x g for one minute. The column

wash was repeated twice, with the final spin lasting two minutes. Nuclear proteins were applied to the resin bed and the column was centrifuged at 1500 x g for two minutes. Eulates were stored at -80 ºC or used immediately for isoelectric focusing. Alternatively, salts were removed from the nuclear protein extracts by dialysis (Slide-a-lyzers; Pierce, Rockford, IL) into water followed by IEF sample buffer.

Nuclear proteins were concentrated by acetone precipitation. In brief, an equal amount of acetone was added to the extracts and proteins were precipitated at -20ºC for two hours. Proteins were collected by centrifugation at 16,100 x g for 10 minutes at 4ºC. The pellet was washed in 70% ethanol, vortexed and centrifuged at 16,100 x g for 10 minutes at 4ºC. After a second wash, the pellet was allowed to air dry before resuspension in IEF sample buffer at 25% of the original volume. Protein concentration was measured using the Bradford method (Pierce, Rockford, IL).

Two Dimensional Polyacrylamide Gel Electrophoresis (2D-PAGE)

Isoelectric focusing was performed using the Ettan IPGphor II system (Amersham Biosciences, Piscataway, NJ) Precast gel strips with a fixed pI range of 4-7 or 6-11 (Amersham Biosciences, Piscataway, NJ) were loaded with 250 µg of protein for 13 cm gels and 100 µg of protein for 7 cm gels in IEF sample buffer plus 0.4% v/v IPG buffer (Amersham Biosciences, Piscataway, NJ) and 0.01% bromophenol blue. IEF strips were placed in the electrophoresis unit and proteins were separated as follows: (1) Rehydration, 16 hours, 50 V; (2) 500V, 500Vhr; (3) 1000V, 1,000Vhr; and (4) 8000V, 16,000Vhr. Maximum amperage of 50 µA and temperature of 20°C were maintained throughout the course of IEF. Focused gel strips were equilibrated with equilibration buffer (50 mM Tris HCl, pH8.8, 6 M Urea, 2% w/v SDS, bromphenol blue) for 15 minutes with 1% w/v dithiothreitol (Fisher, Pittsburgh, PA) and alkylated for 15 minutes

with 2.5% w/v iodoacetamide (Sigma, St. Louis, MO). The gel strips were overlayed on to 10% SDS polyacrylamide gels and sealed in place with 1% w/v agarose in SDS-PAGE running buffer. Proteins were separated through the polyacrylamide gels at constant amperage (30 mA). Subsequently, gels were fixed in 20% v/v methanol, 10% v/v acetic acid for one hour at room temperature. Proteins were detected by modified silver staining methodology. Gels were incubated sequentially with gentle shaking as follows: (1) 30% v/v methanol, 2% w/v sodium thiosulfate and 6.8% w/v sodium acetate for one hour (2) washed five times for eight minutes each in ddH_2O (3) 0.25% w/v silver nitrate solution for one hour (4) washed four times for one minute in ddH_2O (5) 0.025% (w/v) sodium carbonate, 0.004% formaldehyde (37% stock) until satisfactory color is attained. Development was stopped with ethylenediaminetetraacetic acid (EDTA; 3.65g EDTA w/v in 250 ml water) for 45 minutes. Gels were then washed in water.

Mass Spectrophotometry

Proteins of interest were rated based on the intensity of staining as determined by comparison with equally stained gels. Intensely stained proteins were excised and subjected to in-gel tryptic digestion prior to analysis by MALDI-TOF or MALDI MS/MS by the University of Florida Protein Chemistry Core. The type of analysis was determined by the perceived staining intensity of the proteins of interest. For intensely stained proteins, mass spectrometric analysis of the tryptic digests was accomplished by a hybrid quadrupole time-of-flight instrument (QSTAR, Applied Biosystems, Foster City, CA) equipped with the o-MALDI ionization source. A two-point mass calibration was performed in MS/MS mode of operation using the known fragment ion masses of [Glu]-Fibrinopeptide (*m/z* 175.119 and *m/z* 1056.475). Peptide mass fingerprint data generated via the QSTAR were searched against the NCBI nr sequence database

using the Mascot (Matrix Science, Boston, MA) database search engine. Probability-based MOWSE scores above the default significant value were considered for protein identification in addition to validation by manual interpretation of the mass spectra.

Proteins stained with moderate intensity were analyzed by capillary rpHPLC separation of protein digests performed on a 10 cm x 75 um i.d. PepMap C18 column (LC Packings, San Francisco, CA) in combination with a home-built capillary HPLC System operated at a flow rate of 200 nL/min. Inline mass spectrometric analysis of the column eluate was accomplished by a quadrupole ion trap instrument (LCQ, ThermoFinnigan, San Jose, CA) equipped with a nanoelectrospray source. Fragment ion data generated by data dependent acquisition via the LCQ were searched against the NCBI nr sequence database using the SEQUEST (ThermoFinnigan) and Mascot (Matrix Science, Boston, MA) database search engines. In general, the score for SEQUEST protein identification was considered significant when dCn was equal to 0.08 or greater and the cross-correlation score (Xcorr) was greater than 2.2. MASCOT probability-based MOWSE scores above the default significant value were considered for protein identification in addition to validation by manual interpretation of the tandem MS data.

The least intensely stained proteins were analyzed by capillary rpHPLC separation of protein digests performed on a 15 cm x 75 um i.d. PepMap C18 column (LC Packings, San Francisco, CA) in combination with an Ultimate Capillary HPLC System (LC Packings, San Francisco, CA) operated at a flow rate of 200 nL/min. Inline mass spectrometric analysis of the column eluate was accomplished by a hybrid quadrupole time-of-flight instrument (QSTAR, Applied Biosystems, Foster City, CA) equipped with a nanoelectrospray source. Fragment ion data generated by Information Dependent

Acquisition (IDA) via the QSTAR were searched against the NCBI nr sequence database using the Mascot (Matrix Science, Boston, MA) database search engine. Probability-based MOWSE scores above the default significant value were considered for protein identification in addition to validation by manual interpretation of the tandem MS data.

Phosphorylated Protein Isolation

Phosphorylated proteins were purified using the PhosphoProtein Purification Kit (Qiagen, Valencia, CA) according to manufacturer's recommendations. In brief, myoblasts were rinsed twice with ice-cold TBS and scraped into TBS. Cell pellets were collected by centrifugation and resuspended in lysis buffer. Lysates were incubated at 4ºC for 30 minutes with vortexing every 10 minutes. Cell debris and insoluble material was removed by centrifugation at 10,000 x g for 30 minutes at 4ºC. The supernatant was collected and diluted (1:5) with lysis buffer before application to immobilized metal ion resin. The column resin bed was washed with lysis buffer once before elution of the phosphoproteins. The eluate was concentrated and exchanged into 10mM Tris, pH 7.0 using Nanosep columns (Qiagen, Valencia, CA). Protein concentration was determined using the Bradford method. Proteins were frozen at -20ºC until use.

Immunocytochemistry

23A2RafER^{DD} myoblasts were fixed with 4% v/v paraformaldehyde for 20 minutes at room temperature. For the detection of LEK1, myoblasts were fixed with 70% v/vethanol for 15 minutes at room temperature. Non specific antigen sites were blocked by incubation in 5% v/v horse serum, 0.1% v/v Triton X-100 in PBS for 60 minutes at room temperature. Antibody dilutions, sources, and conditions are listed in Table I. After exhaustive washes with PBS, AlexaFluor 488 conjugated anti-mouse and anti-mouse antibodies diluted 1:500 were added for 60 minutes at room temperature. Hoechst

dye was included as a nuclear stain. After washing with PBS representative images were captured using a DM1200F digital camera.

Table I. Primary antibodies used for immunocytochemistry.

Antigen	Antibody Type	Source	Dilution
LEK1	Rabbit polyclonal	D. Bader	1:300
Phospho-ERK1/2	Mouse monoclonal IgG_1	Sigma	1:100
MyoD	Mouse polyclonal IgG_1	Novo Castra	1:30
Myogenin	Mouse monoclonal IgG	Developmental Hybridoma Bank	1:2000
E2F5	Mouse monoclonal IgG_1	Santa Cruz	1:50
pRb	Rabbit polyclonal	Santa Cruz	1:50
p130	Rabbit polyclonal	Santa Cruz	1:50
p107	Rabbit polyclonal	Santa Cruz	1:50

CHAPTER 4
RESULTS

Raf Induced Growth Arrest is Rapid and Reversible

Previous work from this lab has demonstrated that high levels of Raf activity inhibit mouse myogenesis (139). To clarify the mechanisms behind this effect, 23A2RafER^{DD} myoblasts were treated with 1 μM 4HT in low serum media for 48 hours to induce high levels of Raf protein expression and kinase function. After 48 hours, control and treated myoblasts were fixed and cell numbers measured. Total cell number in plates treated with 4HT remained similar to t=0 hour plates, while the cell number in vehicle-only plates increased two-fold (Figure 2, $p<0.01$). Total cell number in 4HT-treated plates never decreased below the number of cells at t=0 indicating Raf signaling during the treatment period was not lethal. To determine how soon the negative effect on mitosis occurs, myoblasts were treated with 1 μM 4HT for 24 hours and pulsed with 10 μM bromodeoxyuridine (BrdU) during the final thirty minutes. Myoblasts were fixed and immunostained for BrdU. 23A2RafER^{DD} myoblasts containing elevated amounts of Raf incorporate significantly less BrdU than control myoblasts, indicating fewer cells in S phase (Figure 3, $p<0.02$). Coincident with the abrupt cessation of proliferation are subtle changes in cell morphology. Control and 4HT treated 23A2RafER^{DD} myoblasts were fixed and stained with phalloidin to visualize the actin cytoskeleton (Figure 4). Myoblasts that synthesized abundant Raf kinase display an ordered, distinct localization of actin filaments. Control myoblasts posses a more diffuse acting staining pattern surrounding the periphery of the cell.

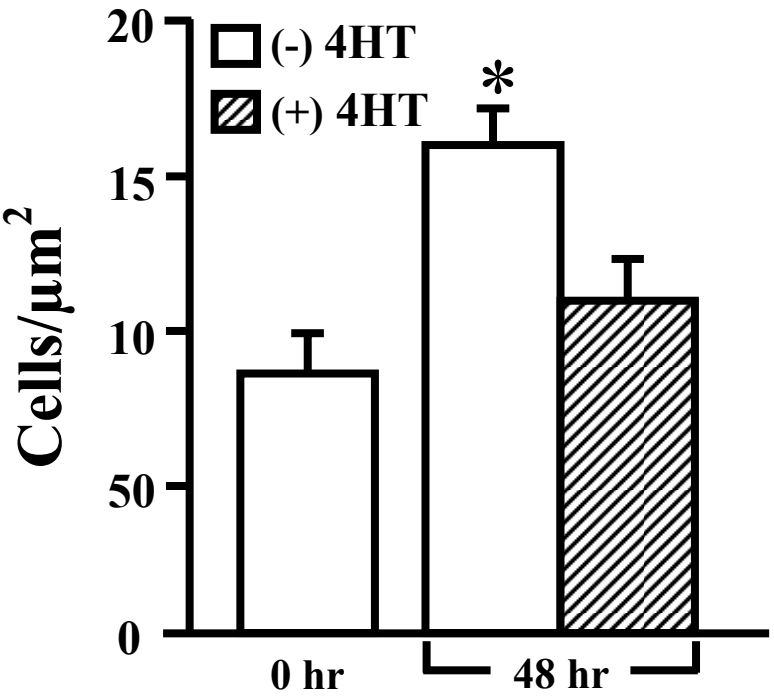

Figure 2. High levels of Raf activity inhibit cell number increases. 23A2RafER^{DD} myoblasts treated with 1μM 4HT or vehicle-only for 48 hours in low serum media do not proliferate to the same extent as untreated cells. Asterisk indicates significant difference, $p<0.01$.

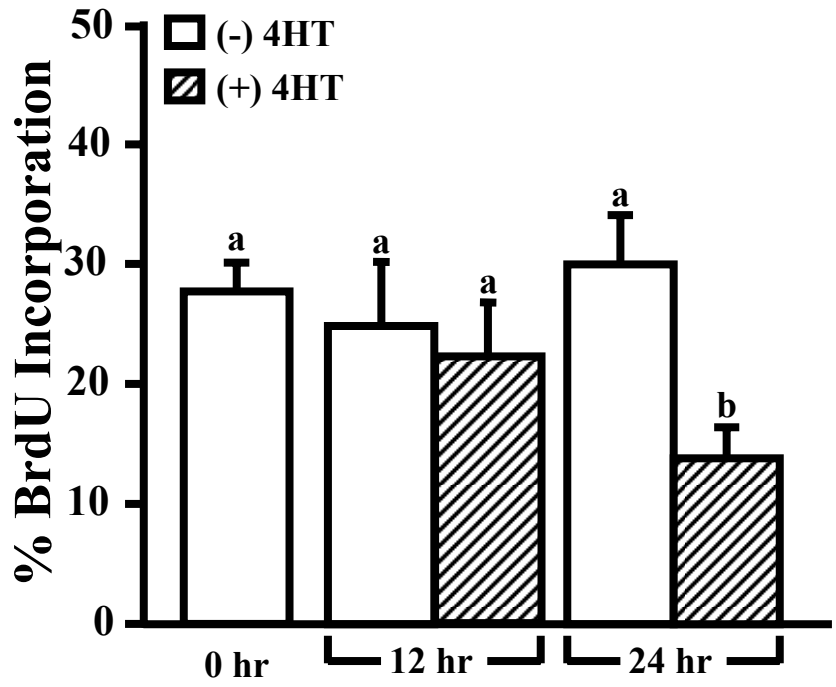

Figure 3. High levels of Raf activity inhibit BrdU incorporation. 23A2RafER^{DD} myoblasts were treated for 12 or 24 hours with 1μM 4HT or vehicle-only in low serum media and pulsed with BrdU for the last thirty minutes of the incubation. Letters indicate significant difference, $p<0.02$.

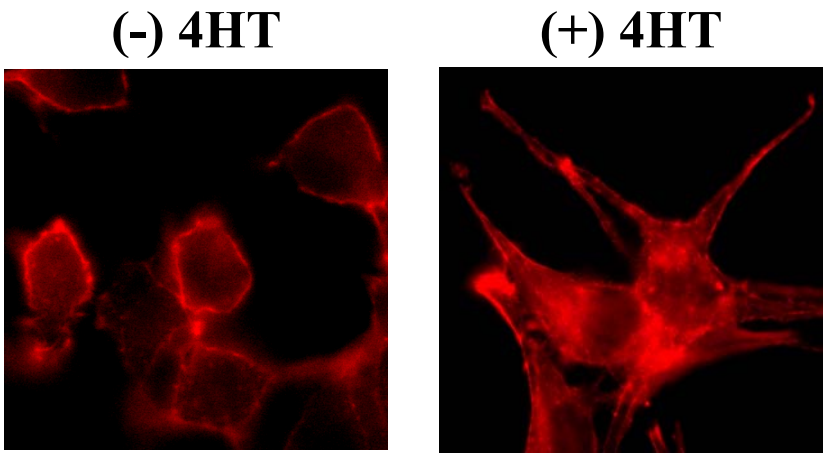

Figure 4. High levels of Raf activity result in morphological changes. 23A2RafER^{DD} myoblasts treated with 1μM 4HT or vehicle-only for 48 hours in low serum were subsequently immunostained for phalloidin, highlighting the morphological changes.

Elevated Raf signaling in human fibroblasts causes senescence typified by irreversible growth arrest. Myoblasts senescence was measured in 23A2RafER^{DD} cells treated with 4HT or vehicle only. After 48 hours in low serum media in the presence of 4HT, the culture media was replaced with fresh growth media containing 15% FBS. Cultures were fixed and myoblast cell number measured at 24 hour intervals. After 48 hours in 4HT, cell number was not different from t=0 (Figure 5). Control myoblasts doubled over the 48 hour time-frame. Replacement of media with fresh growth media lacking 4HT caused a two-fold increase in cell number ($p<0.01$). In data not shown, 23A2RafER^{DD} myoblasts treated for 48 hours with 1 μM 4HT failed to express detectable amounts of acidic galactosidase, a hallmark of cellular senescence. Satellite cells exiting the cell cycle enter the quiescent state, from which cell cycle re-entry is possible. Alternatively, myoblasts exiting the cell cycle often enter the senescent state, in which proliferation is no longer an option. Interestingly, high serum medium prevents Raf-induced growth arrest. Myoblasts were treated with 4HT in 15% FBS for 48 hours. Cultures were fixed at 24 hour intervals and cell number measured (Figure 6). No difference in cell number was apparent between control and 4HT treated myoblasts, indicating that high serum concentration is sufficient to prevent the growth arrest caused by elevated levels of Raf activity.

Raf-Initiated ERK1/2 Activation is Sustained at 60 Minutes

The rapid reversible growth arrest imposed by Raf is a similar feature of myogenic stem cells. Skeletal muscle stem cells or satellite cells exist in mature muscle as quiescent precursors that reactivate the myogenic program during periods of growth and regeneration. Thus, 23A2RafER^{DD} myoblasts may be a useful model to examine

early events during entry into G_0 or self-renewal. To clarify the early events associated with Raf induced quiescence, the temporal activation of ERK1/2 was examined. 23A2RafER^{DD} myoblasts were treated with 1 μM 4HT and proteins from three replicates of parallel plates were isolated at 15 minute intervals. Total cell lysates prepared from equal numbers of cells were electrophoretically separated through 10% polyacrylamide denaturing gels. Proteins were transferred to nitrocellulose and analyzed for total and phospho-ERK1/2 expression by Western blot. No phosphorylation of ERK1/2 was observed in 23A2RafER^{DD} cells treated with vehicle-only (Figure 7, representative blot). Phosphorylation of ERK1 occurs as early as 15 minutes in 23A2RafER^{DD} cells treated with 4HT and continues to be phosphorylated over the next two hours. ERK2 phosphorylation occurs at 30 minutes and is strongly phosphorylated at one hour. ERK1/2 phosphorylation does not occur in 23A2 myoblasts treated with 4HT (139). Sustained activation of both ERK1 and ERK2 was detected at 60 minutes post Raf induction. Based upon the strong sustained phosphorylation of ERK1/2 at 60 minutes, this time point was selected for the identification of proteins uniquely expressed in the nucleus during entry into G_0. The preferred method of protein identification involves 2D-PAGE separation and MALDI-TOF or MALDI MS/MS identification. Several parameters were refined to accomplish our goals.

Identification of Nuclear Proteins: Protocol Definition

Because the use of two-dimensional polyacrylamide gel electrophoresis was a new technique for this laboratory, it was necessary for the protocol to be refined to suit our needs. Protocol definition included sample preparation, isoelectric focusing and subsequent vertical PAGE, and silver staining techniques.

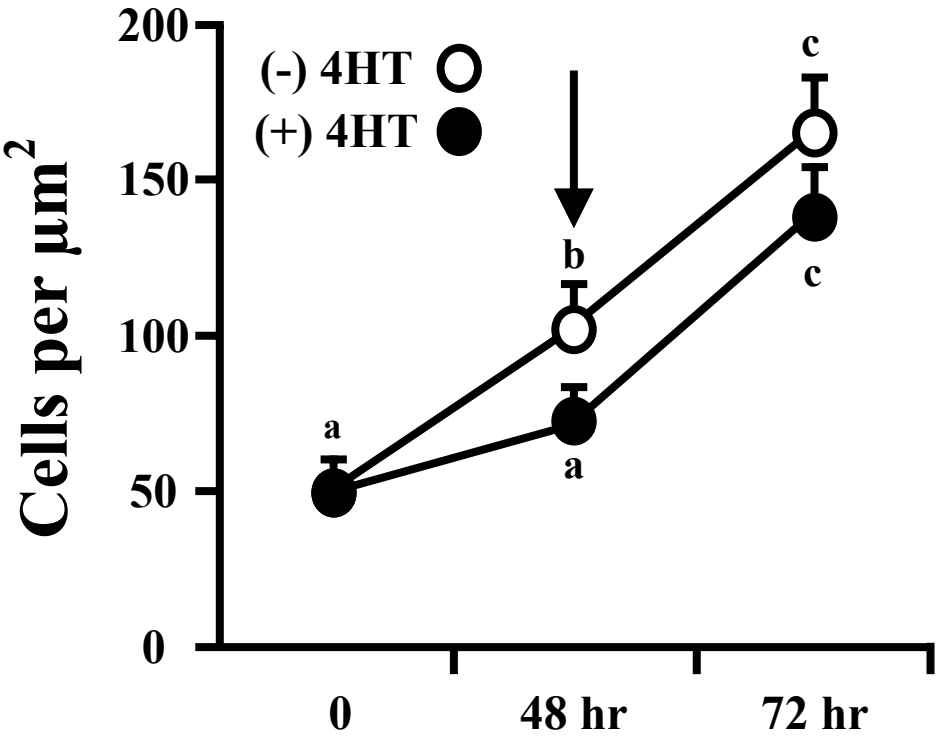

Figure 5. Raf induced growth arrest is reversible. 23A2RafER^{DD} myoblasts were treated with 1μM 4HT or vehicle-only in low serum media for 48 hours. Treatment media was replaed with normal growth media lacking tamoxifen. Arrow indicates replacement of low serum treatment media with high serum growth media. Different letters indicate significant difference, $p<0.05$.

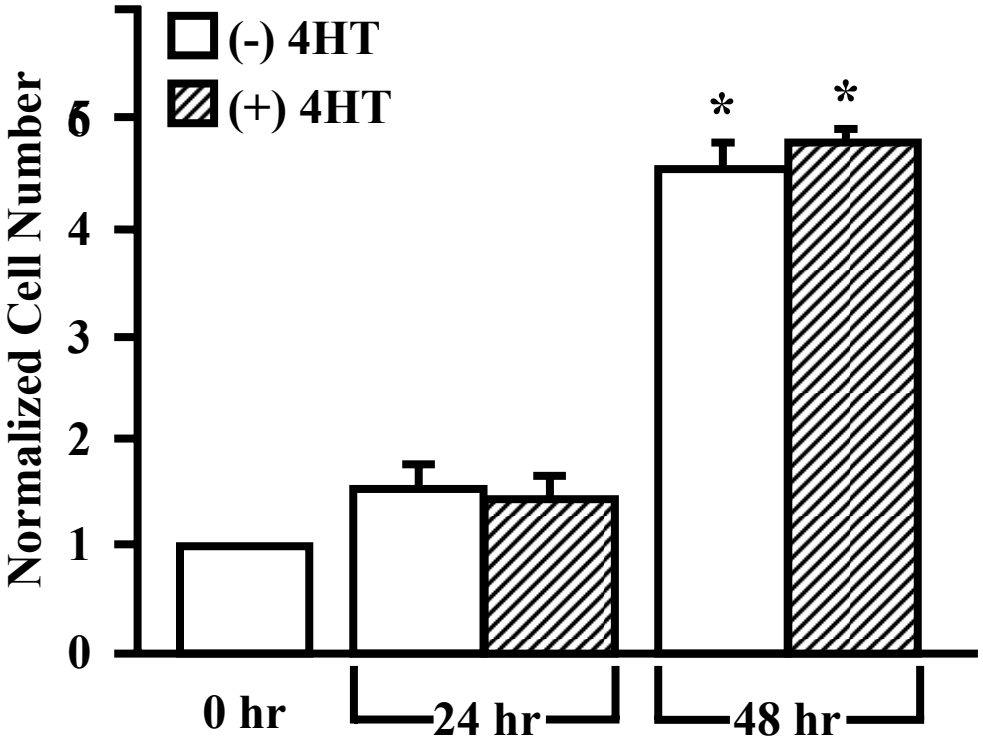

Figure 6. Raf induced growth arrest is negated by the presence of high serum concentrations. 23A2RafER^{DD} myoblasts were cultured in high serum media with 1μM 4HT or vehicle-only. Cell numbers have been normalized to one based on the t=0 cells. Asterisk indicates significant difference, $p<0.01$.

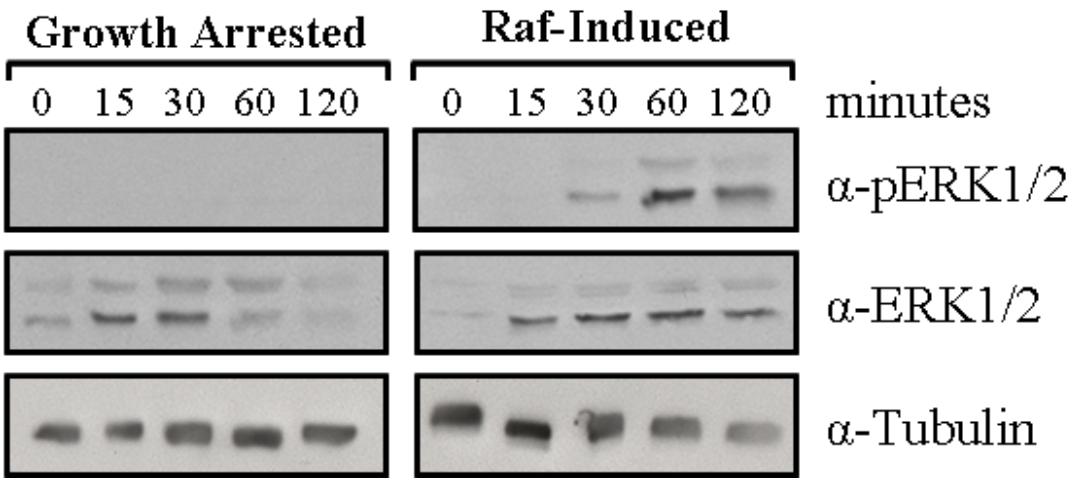

Figure 7. Time course of ERK1/2 activity. 23A2RafER^{DD} myoblasts were treated with 1μM 4HT (Raf-Induced) or vehicle-only (Growth Arrested) over the times shown. Cell lysates were probed for phosphorylated and total ERK1/2 and tubulin (loading control).

Removal of Salts

Proteins from control and Raf induced nuclei were extracted using 3M NaCl, a solute incompatible with isoelectric focusing and 2D-PAGE. Three methods of salt removal were tested. First, nuclear proteins were precipitated with an equal volume of ice-cold acetone. Recovery of proteins using this method was approximately 20% of original concentration. Second, proteins were dialyzed against IEF sample buffer. This method efficiently removed salt and retained protein. However, the final protein concentration was too dilute and required an additional concentration step. The third, and preferred, method of salt removal involves the use of D-Salt Excellulose resin. Recovery of protein was similar to dialysis with regard to final amount of protein recovered. This method was chosen due to the ease of use and time savings.

Isoelectric Focusing (IEF)

Separation of proteins based upon their isoelectric point was accomplished using the Ettan IPGphor system. Two protocols were tested to determine optimum focusing times and voltages using 3-10 non-linear pI gradients. The first protocol used a fixed time period protocol and the second protocol used fixed voltages (Table II). Identical samples (250 μg) were electroporetically separated using each protocol. Proteins were visualized by silver stain. The fixed time protocol occasionally produced gel strips that failed to reach maximum voltage and resulted in poor protein focusing and separation (Figure 8). The fixed voltage protocol resulted in sharper protein spots and less vertical smearing. Therefore all experimental isolations and 2D-PAGE were performed at fixed voltage.

The overwhelming number of protein spots on each gel posed a limitation to excision of single proteins for further identification. Therefore, pI 4-7 and pI 6-11 Immobiline dry strips were tested for focusing sharpness as well as protein patterns. pI 6-11 gel strips were difficult to electrophoresis, often failing to reach maximum voltage or taking an extraordinary amount of time to resolve. The proteins on pI 6-11 gels resolved poorly and two vertical streaks of proteins were evident at ~pI 8 and pI 10 (Figure 9). Separation of proteins with a pI 4-7 gradient resulted in a sharper resolution of protein. A vertical streak was present on the extreme basic side of the gel, representing the accumulation of proteins with pIs outside of the covered range.

To estimate the molecular weight and isoelectric points of proteins of interest, carbamylytes were run in parallel with nuclear protein samples. Calibration standards included carbonic anhydrase (CA; MW 30kDa, pI range 4.8-6.7), creatine phosphokinase (CP; MW 40kDa, pI range 4.9-7.1), and glyceraldehyde-3-phosphate dehydrogenase (GAPDH; MW 36kDa, pI range 4.7-8.3). Carbamylytes are trains of the same protein with different isoelectric points. The positively charged amino groups of each protein interact with urea upon heating, forming protein derivatives with a lower pI. These three carbamylytes resulted in protein trains of 20-30 spots each, providing a good estimate of pI values (Figure 10). In summary, the final protocol for purification, electrophoresis and visualization of nuclear proteins uses desalting resin, pI 4-7 IEF gel strips, electrophoresis at a constant voltage (Table II), and silver staining.

Activation of Raf/ERK1/2 Causes Changes in Nuclear Protein Expression Profiles

To determine specific changes in protein expression, nuclear proteins isolated from control and Raf-induced cells were separated by 2D PAGE and visualized by silver staining. Gel images were analyzed by Melanie (GeneBio), a software program that

allows comparisons of 2D PAGE pattern profiles. Protein landmarks were used to align gels, orient molecular weight, and calculate pI. A number of similar proteins were present in high levels in both the control and treated gels, making them ideal as landmarks. Unique proteins were excised from the control and treated gels (Figures 11 and 12). A total of 57 protein spots were excised from the treatment groups, 24 from the

Table II. Isoelectric focusing parameters.

	Fixed Time	**Fixed Voltage**
Rehydration	50V, 16 hours	50V, 16 hours
Step One	500V, 1 hour	500V, 500Vhr
Step Two	1000V, 1 hour	1000V, 1000Vhr
Step Three	8000V, 2 hours	8000V, 16,000Vhr

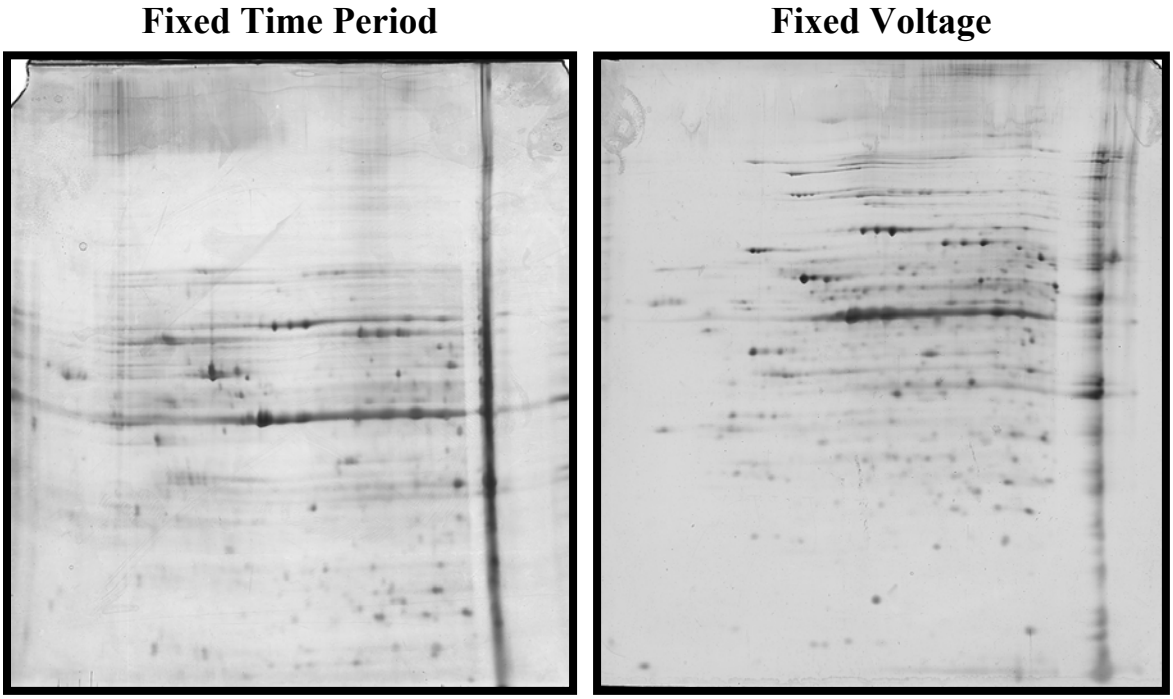

Figure 8. Comparison of IEF protocols. First dimension separation protocols were tested for optimum focusing conditions. The fixed time period protocol was based on maximum amperage for a pre-determined amount of time. The fixed voltage protocol used a set amount of volt hours and maximum voltage.

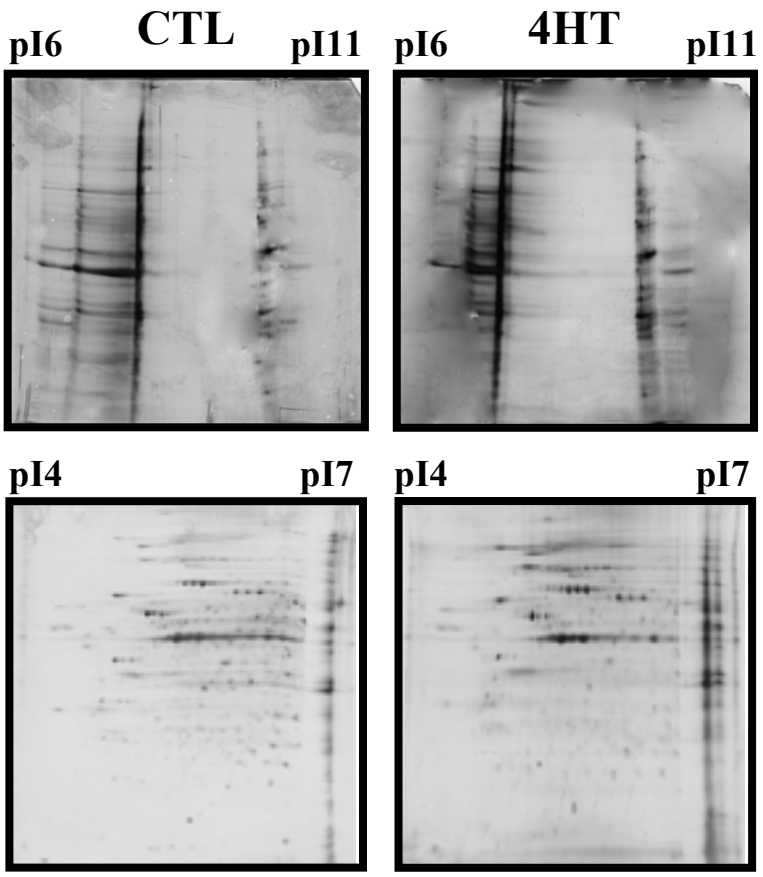

Figure 9. Representative pI 6-11 and pI 4-7 two dimension gels of control and Raf induced cells. 23A2RafER^{DD} myoblasts were treated with 1μM 4HT or vehicle-only for one hour. Nuclear proteins were isolated and separated over pI6-11 or pI4-7 first dimension gels and subsequently separated down a 10% SDS gel.

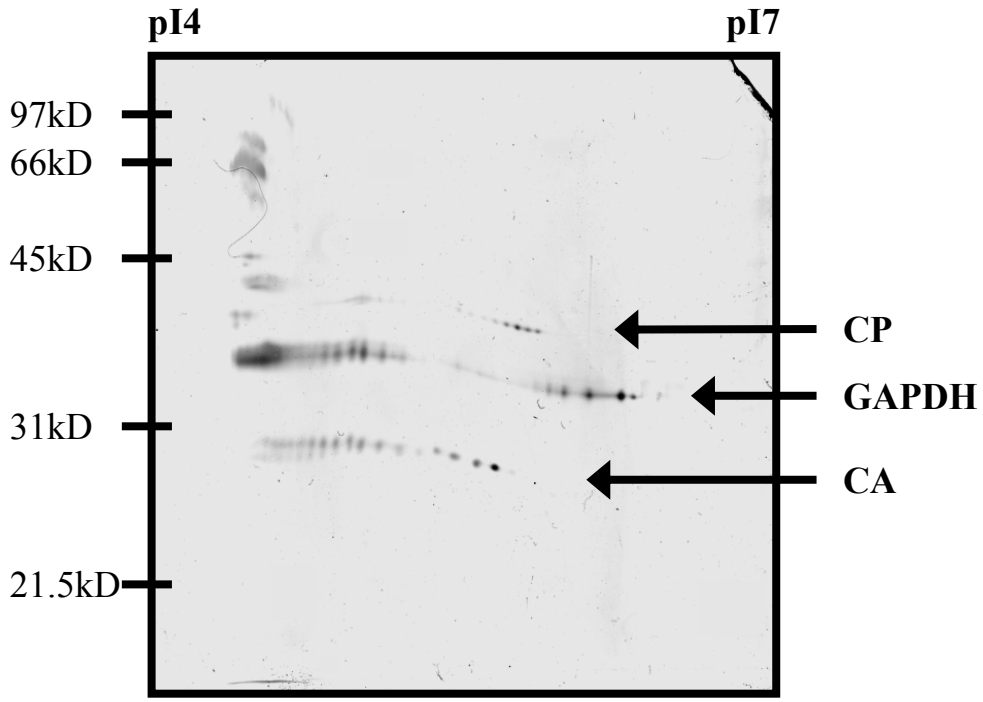

Figure 10. Carbamylyte two dimension gel. Creatine phosphokinase (CP), glyceraldehydes-3-phosphate dehydrogenase (GAPDH), and carbonic anhydrase (CA) carbamylytes were separated over a 10% SDS gel and silver stained.

Raf-induced proteins and 33 from the control proteins. A minimum of four gels were analyzed for each group (control, 4HT). Proteins were digested in gel with trypsin and peptides were identified by MALDI-TOF and MS/MS at the University of Florida Protein Chemistry Core facility. Identification was verified by the presence of the protein in at least three gels in the correct location relative to pI and molecular weight. Twelve unique proteins were identified in the Raf-induced cells and ten unique proteins were identified in the control cells (Table III).

Raf Signaling Causes Nuclear Translocation of E2F5 and LEK1

LEK1 and E2F5, two proteins of interest identified in extracts from the Raf expressing myoblasts, were chosen for further analysis (Figure 12). E2F5 and LEK1 are pocket protein binding proteins that are involved in cell cycle control (44, 104, 115, 145). E2F5 and LEK1 proteins are located in the nucleus of Raf-induced myoblasts (Figure 13). On closer inspection, LEK1 was localized throughout the cytoplasm and nucleus in control serum starved myoblasts. Treatment with 1 μM 4HT treatment caused a marked redistribution of LEK1 to the nucleus. Residual cytoplasmic LEK1 immunoreactivity was apparent in Raf induced myoblasts. E2F5 expression was similar to LEK1. In control myoblasts, E2F5 appeared primarily cytoplasmic, entering the nucleus upon Raf induction. Nuclear accumulation of E2F5 begins as early as 15 minutes post Raf induction, but does not occur at anytime during the one hour treatment in serum starved controls (Figure 14).

The translocation of E2F5 and LEK1 prompted the examination of ERK1/2 localization in response to Raf activity. Surprisingly, phosphorylated ERK1/2 remained cytoplasmic throughout the first hour of Raf induction (Figure 15). This was confirmed through Western blotting of nuclear extracts for phospho-ERK1/2 (Figure 16). To verify

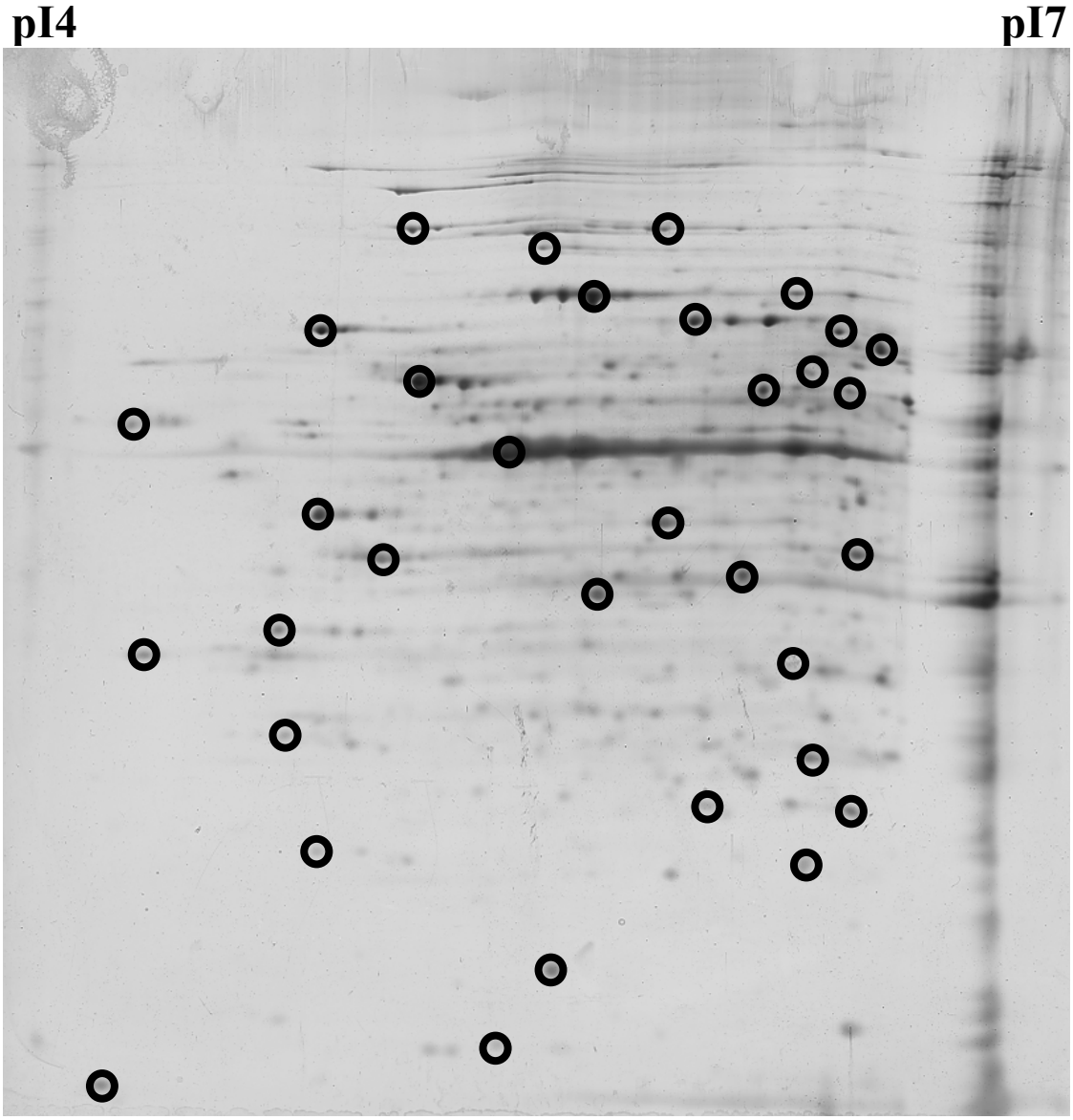

Figure 11. Representative two dimension gel of nuclear extracts from control cells. Nuclear extracts from vehicle-only treated cell were separated over a pI4-7 gel strip and subsequently over a 10% SDS gel and silver stained. Circled proteins are those excised for identification.

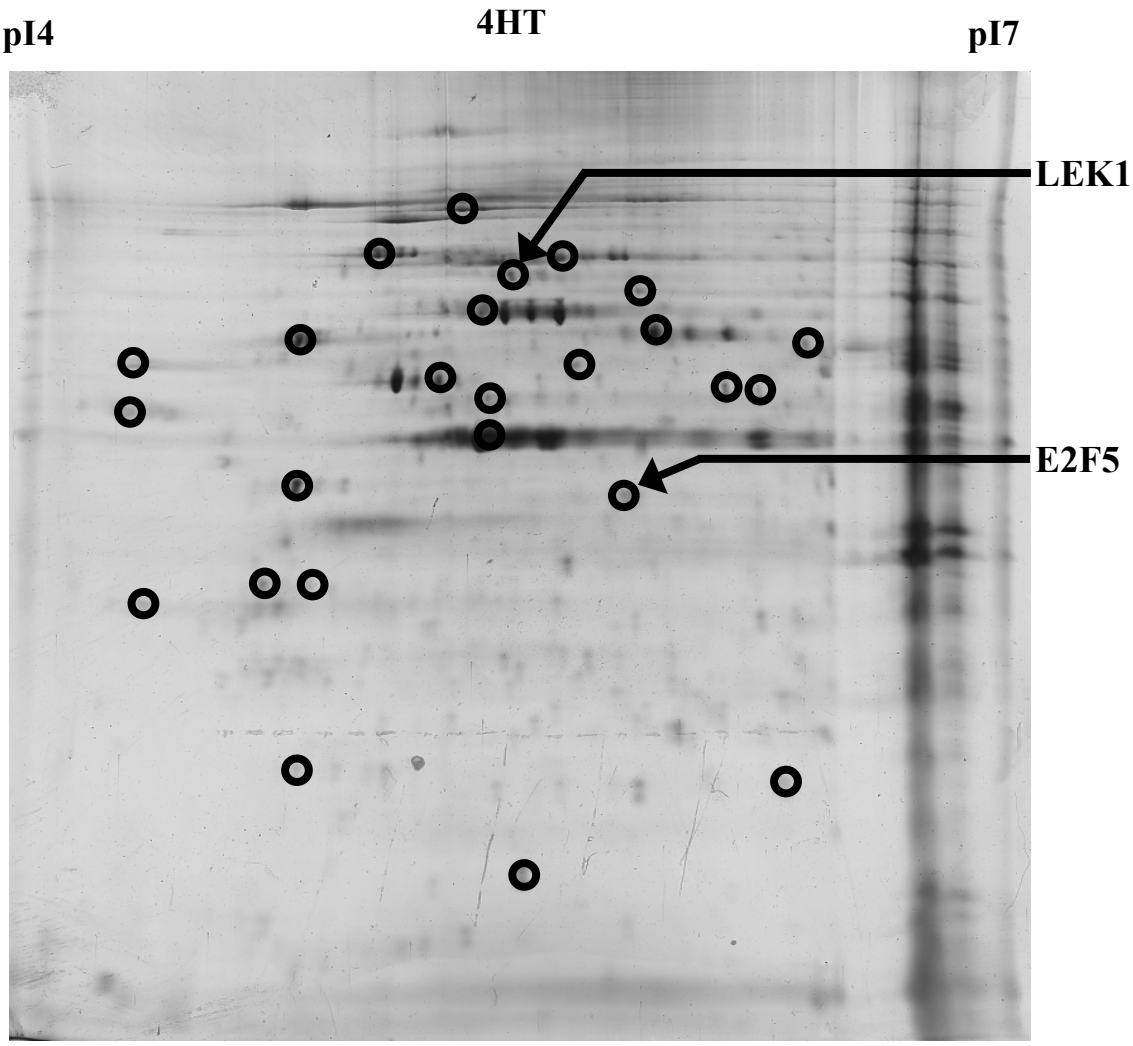

Figure 12. Representative two dimension gel of nuclear extracts from Raf induced cells. Nuclear extracts from Raf induced cells were separated over a pI4-7 gel strip, a 1-% SDS gel and subsequently silver stained. Circled proteins are those excised for identification. LEK1 and E2F5 were chosen for further analysis.

Table III. Unique proteins identified from control and Raf-induced nuclear extracts.

Control				Raf induced			
Protein	**MW**	**pI**	**Ascension #**	**Protein**	**MW**	**pI**	**Ascension #**
Aldehyde Dehydrogenase	57kD	7.53	P47738	Dihydrolipoamide s-acetyltransferase	59kD	5.71	AAL02400
Annexin A1	39kD	7.15	P10107	E2F5	37kD	5.17	Q61502
Annexin A2	39kD	7.53	P07356	gprin1	96kD	6.79	AAH57044
Calumenin	37kD	4.49	O35887	LEK1	284kD	4.94	Q9QZ84
Casein Kinase α1	41kD	9.5	Q8BK63	Tumor rejection antigen gp96	92kD	4.74	P08113
Chaperonin β	58kD	5.97	AAH26918	Txndc7	48kD	5.05	BC006865
Lipocortin 1	39kD	6.57	NP 034860	YL2	31kD	4.77	Q8R5L1
Reticulocalbin	37kD	4.7	Q05186	U8	51kD	8.74	BAA79193
SNEV	56kD	6.14	Q99KP6	Nad+specific Isocitrate dehydrogenase	40kD	6.46	Q9D6R2
TNFα induced protein 1	37kD	8	NP 891995				
Msx2 interacting Nuclear target protein	389k	8.	AF156529				

that the phosphorylation and cytoplasmic location of ERK1/2 was a result of Raf activation, myoblasts were treated with 50 μM PD98059, a MEK1/2 inhibitor. In the presence of both 4HT and the MEK inhibitor, no phosphorylated ERK1/2 was present in the cytoplasm (Figure 17).

E2F5 and LEK1 both interact with members of the pocket protein family of proteins. To determine whether these proteins are involved in the early events leading to quiescence, Raf induced cells were immunostained for pRb, p130, and p107 expression (Figure 18). No apparent changes in p130 or p107 localization or expression level occur within the first hour of Raf induction. This was surprising, as p130 and E2F5 are commonly found localized in the nucleus of quiescent cells (55). This suggests that while p130 may be required for the maintenance of quiescence, it is not immediately necessary for the induction of the quiescent state. However, pRb appears to localize to the nucleus following one hour of 4HT stimulation, although some cytoplasmic staining remains. The number of cells expressing nuclear pRb is increased significantly in treated cells (Figure 19, $p<0.01$). Immunostaining was verified with nuclear extracts, which appeared to show increased levels of pRb in the nucleus of Raf induced myoblasts but no apparent changes in p130 or p107 concentration in response to Raf activity (Figure 20A). However, upon quantification with densitometry, no significant changes in intensity were apparent, although pRb tended to increase with 4HT treatment (Figure 20B). The western blots may be more sensitive than the immunocytochemistry, as p130 and p107 could be detected in the nuclear extracts and more nuclear pRb was detected in control myoblasts. Further work should be completed to define the effects of Raf activity on pRb localization. E2F5 is often examined in conjunction with E2F4, the other major

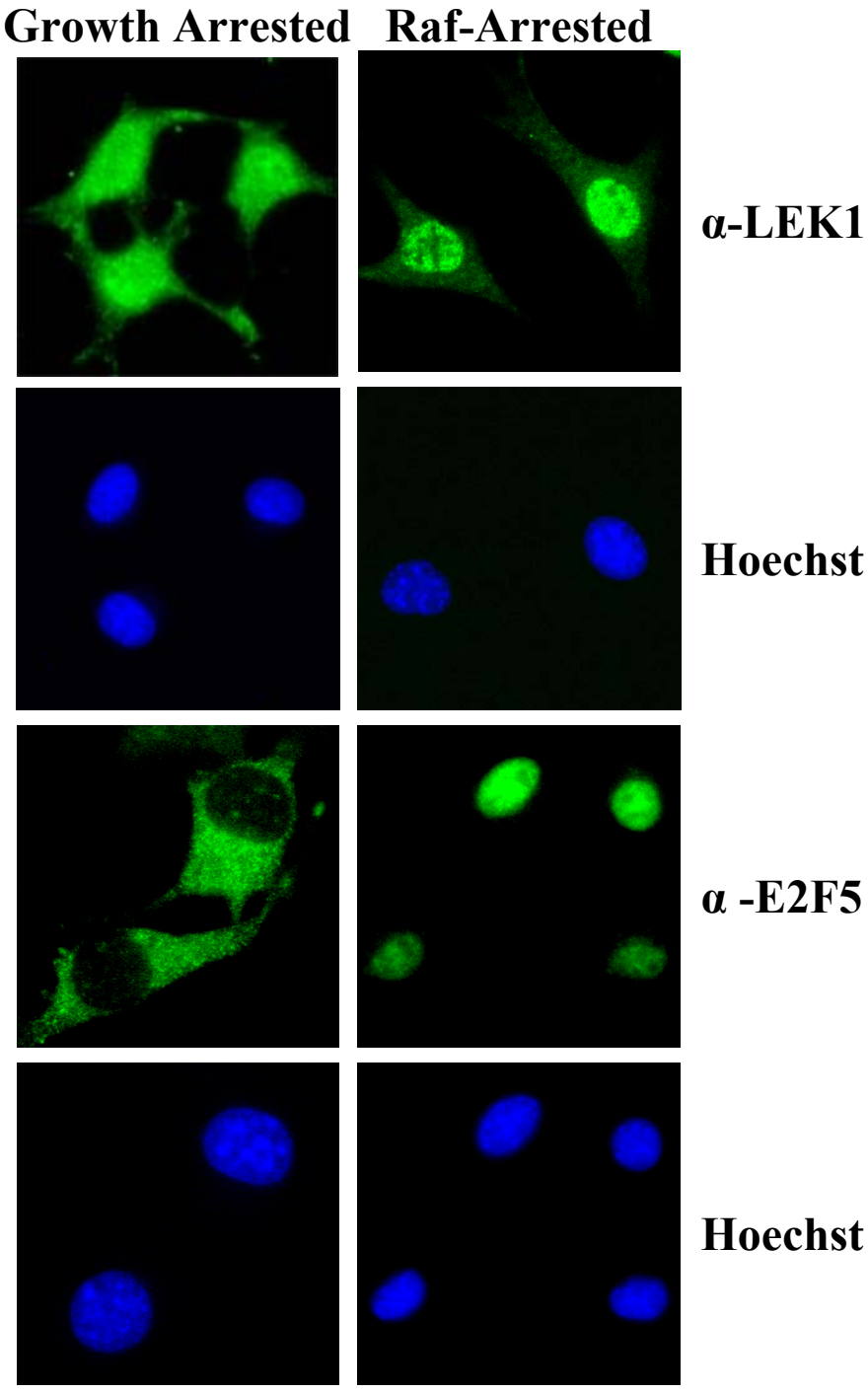

Figure 13. Localization of LEK1 and E2F5. 23A2RafER^{DD} myoblasts were treated with 1μM 4HT or vehicle only for one hour prior to immunostaining with LEK1 or E2F5.

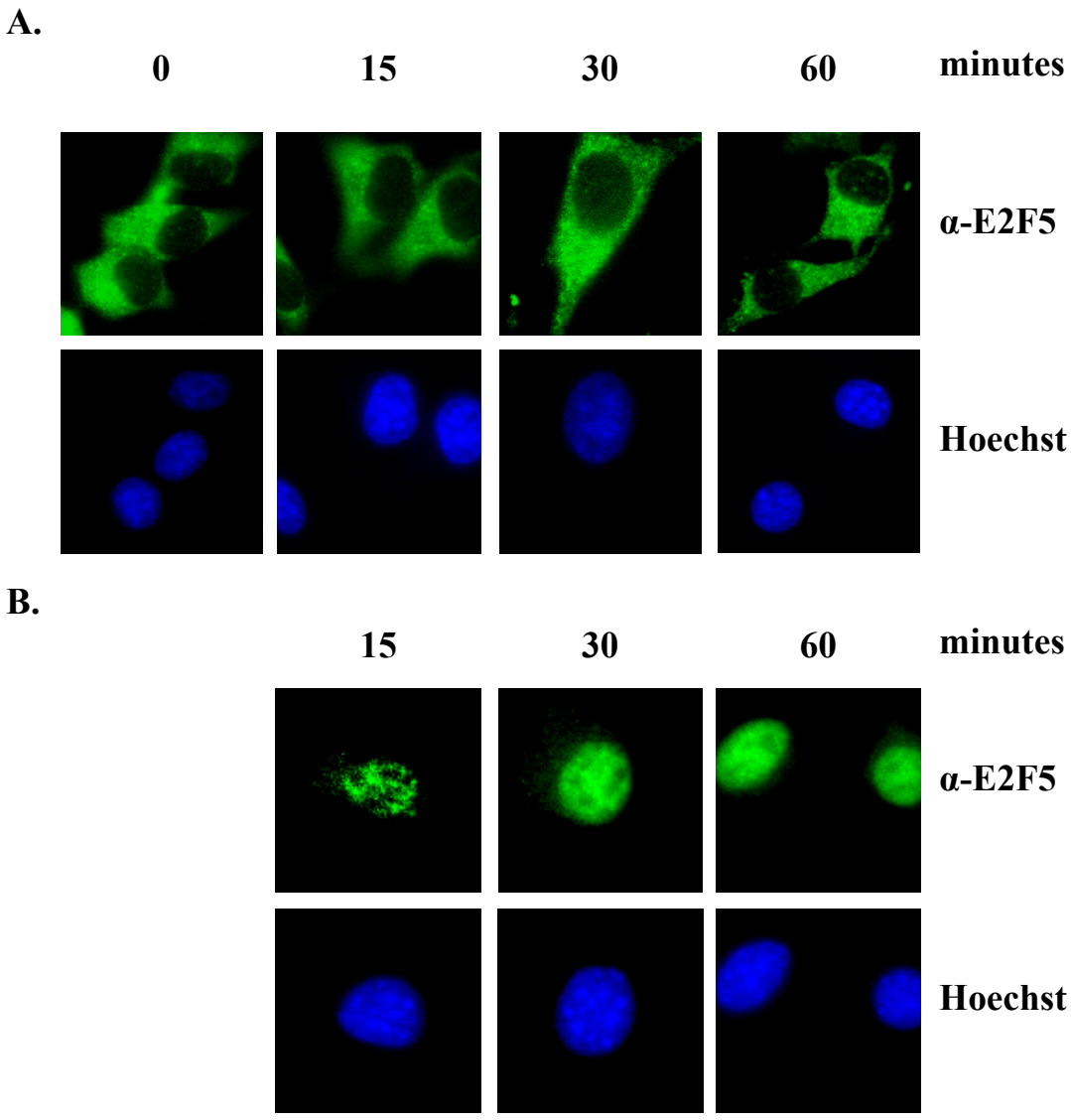

Figure 14. Localization of E2F5 over time. 23A2RafER^{DD} myoblasts were treated with 1μM 4HT or vehicle-only for times stated and immunostained for E2F5.

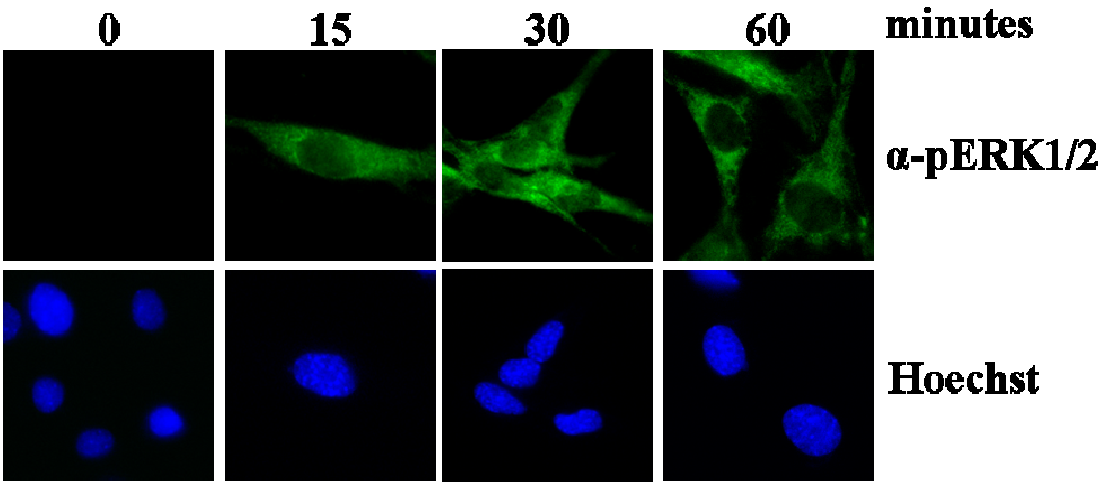

Figure 15. Localization of phospho-ERK1/2 over time. 23A2RafER^{DD} myoblasts were treated for the times shown with 1μM 4HT or vehicle-only (not shown) and immunostained for phosphoERK1/2 and Hoechst.

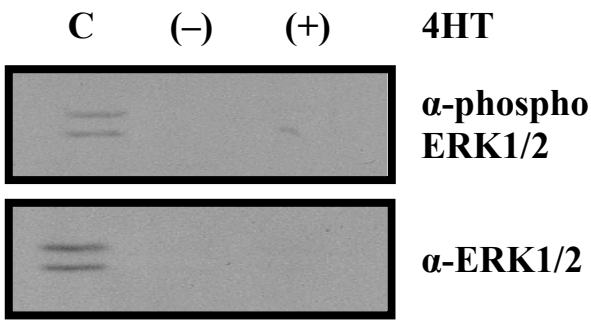

Figure 16. No phosphorylated ERK1/2 is present in control or Raf induced nuclear extracts. Nuclear extracts were isolated after 1 hour of treatment with 1μM 4HT or vehicle-only and separated over a 10% SDS gel. Western blots were probed with phosphorylated and total ERK1/2. C – control; (-) – vehicle only; (+) – 1μM 4HT

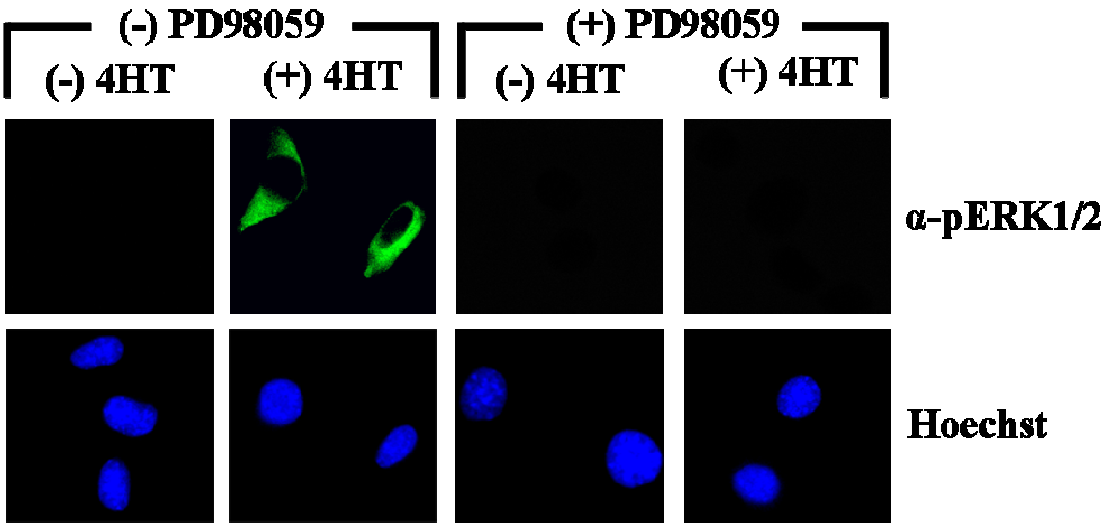

Figure 17. The presence of a MEK inhibitor blocks the activation of ERK1/2. 23A2RafER^{DD} myoblasts were treated with 1μM 4HT or vehicle-only in the presence of absence of PD98059, a MEK1 inhibitor, prior to immunostaining for phosphorylated ERK1/2.

transcriptional repressor of the E2F family. Immunostaining verified the specificity of localization changes for E2F5, as E2F4 expression does not appear to change as a function of Raf activity (Figure 21). Interestingly, a punctate ytoplasmic immunostaining pattern exists in both control and treated myoblasts that appears to co-localize with regions of rough endoplasmic reticulum. The pattern suggests that E2F4 gene expression and protein synthesis may be a product of general growth arrest.

Because the localization changes of E2F5 and pRb were found in response to high levels of ERK1/2 activity, we sought to determine whether these effects were caused by ERK1/2 phosphorylation or other cellular changes. To this end, the MEK inhibitor PD98059 was used to block ERK1/2 activation. Nuclear localization of pRb and E2F5 was blocked in the presence of PD98059 indicating that these changes are a result of Raf activation of the downstream MEK/ERK signaling axis (Figure 22).

To verify that the cells were entering a quiescent state distinct from terminal differentiation, Raf induced cells were immunostained for myogenin (mgn), an early marker of terminal differentiation. Nuclei were counterstained with Hoescht dye and a labeling index was calculated at mgn(+)/total nuclei. Twenty three percent of the control cells expressed myogenin; few (~2.5%) Raf-induced myoblasts stained positive (Figure 23A). All cells expressed MyoD (Figure 23B) indicating the effect was specific for myogenin.

To further verify that the cells were entering a state that was reversible, myoblasts were stimulated with 4HT for one hour, followed by culture in serum free media. As before, the one hour stimulation resulted in nuclear translocation of E2F5 and pRb. Removal of the stimulus partially restored the cytoplasmic location of both proteins

(Figure 24). The restoration of the cytoplasmic location of E2F5 and pRb is accompanied by the presences of less cytoplasmic protein. These proteins may potentially be targeted for degradation upon re-entrance to the cell cycle.

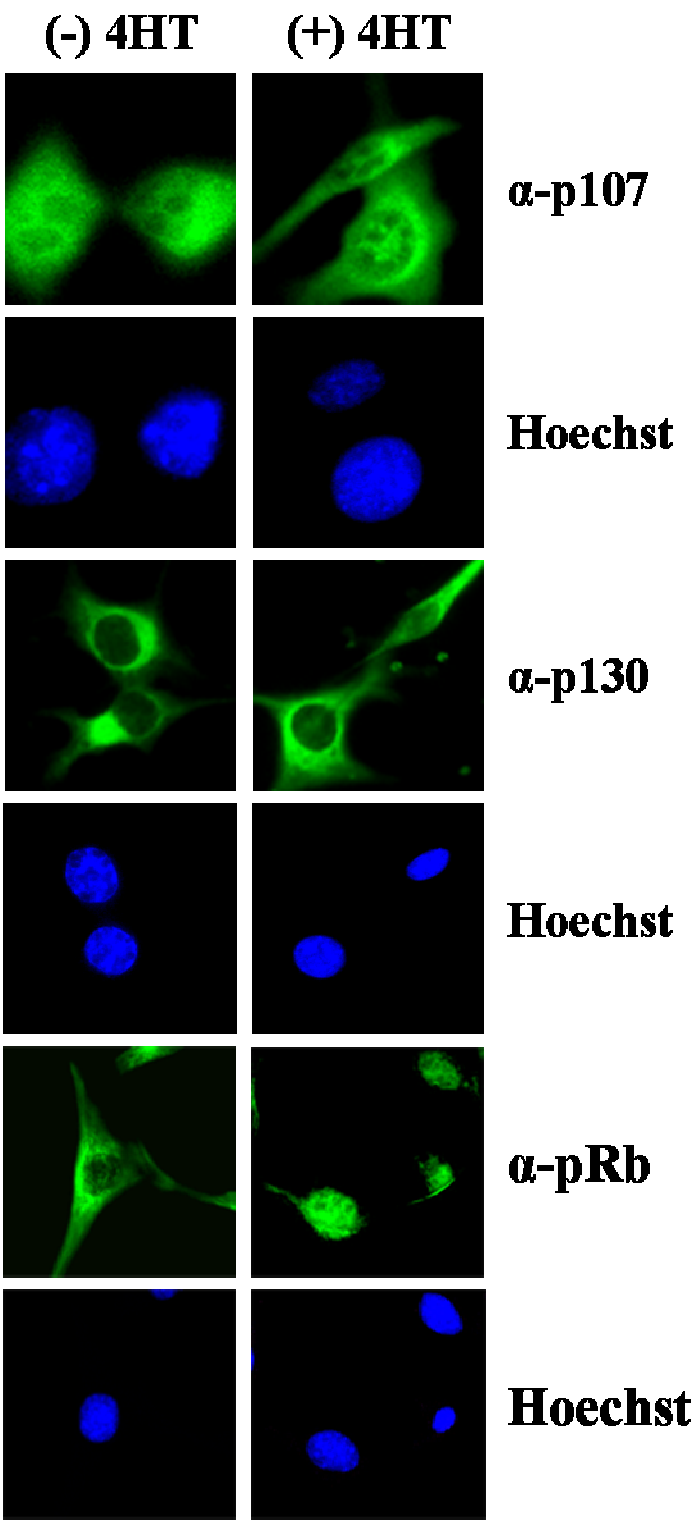

Figure 18. Pocket protein expression in control and Raf induced cells. 23A2RafER^{DD} myoblasts were treated for one hour with 1μM 4HT or vehicle-only prior to immunostaining for p107, p130, or pRb.

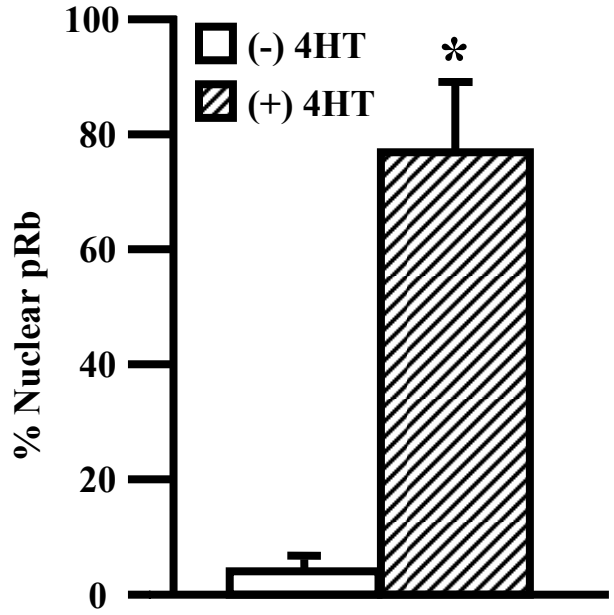

Figure 19. Differences in pRb expression in the nucleus. 23A2RafER^{DD} myoblasts were treated with 1μM 4HT or vehicle-only for one hour and immunostained for pRb. The percent of cells positive for nuclear pRb was calculated from three independent tests. Asterisk indicates a significant difference $p<0.01$.

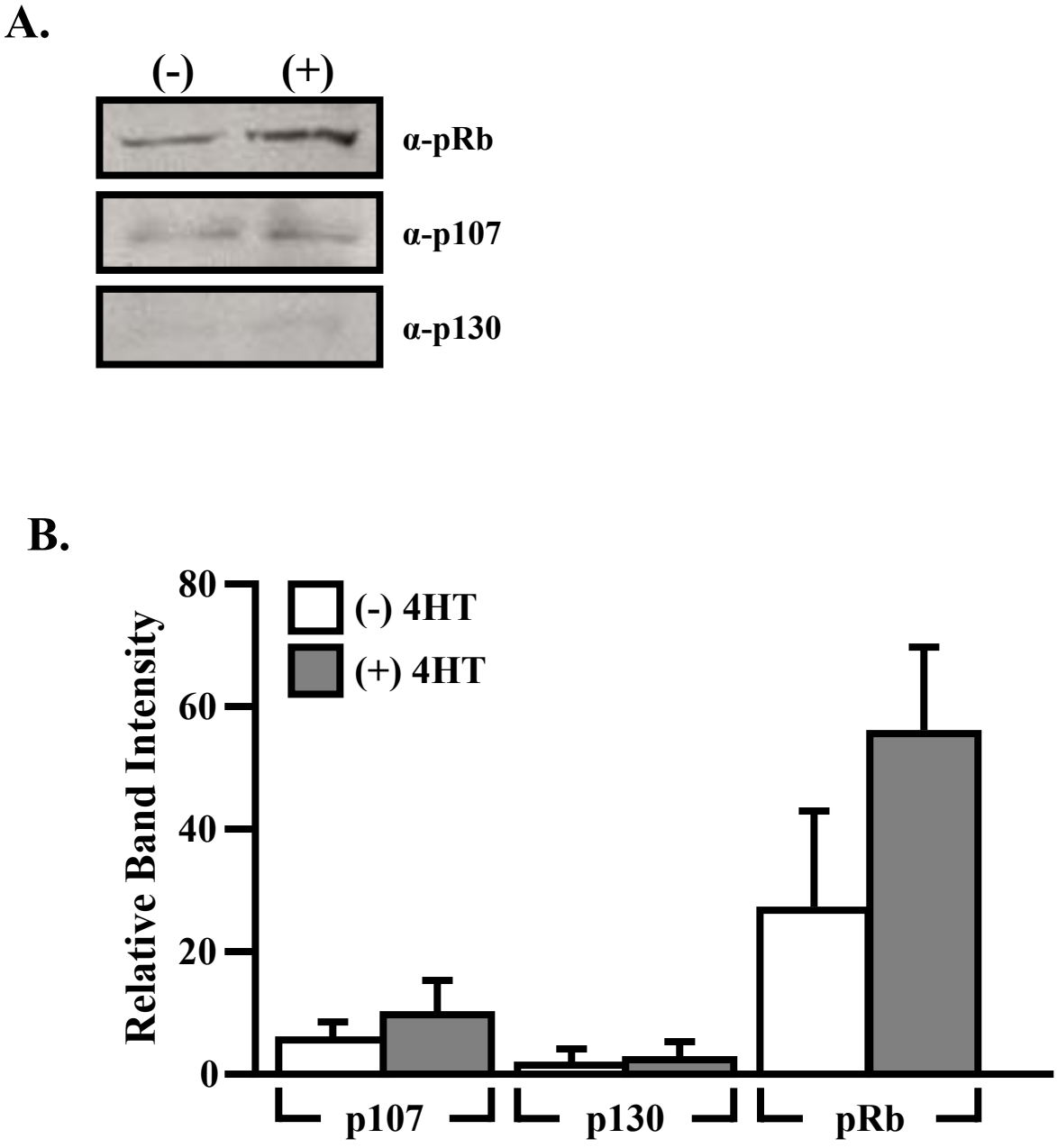

Figure 20. Pocket protein expression in nuclear extracts of control and Raf induced cells. Nuclear extracts from Raf induced (+) and control (-) myoblasts were probed for pRb, p107, and p130 (A). Densitometry performed on two independent tests reveals no significant differences in protein expression between control ((-) 4HT) and Raf induced ((+) 4HT) myoblasts, n=2 (B).

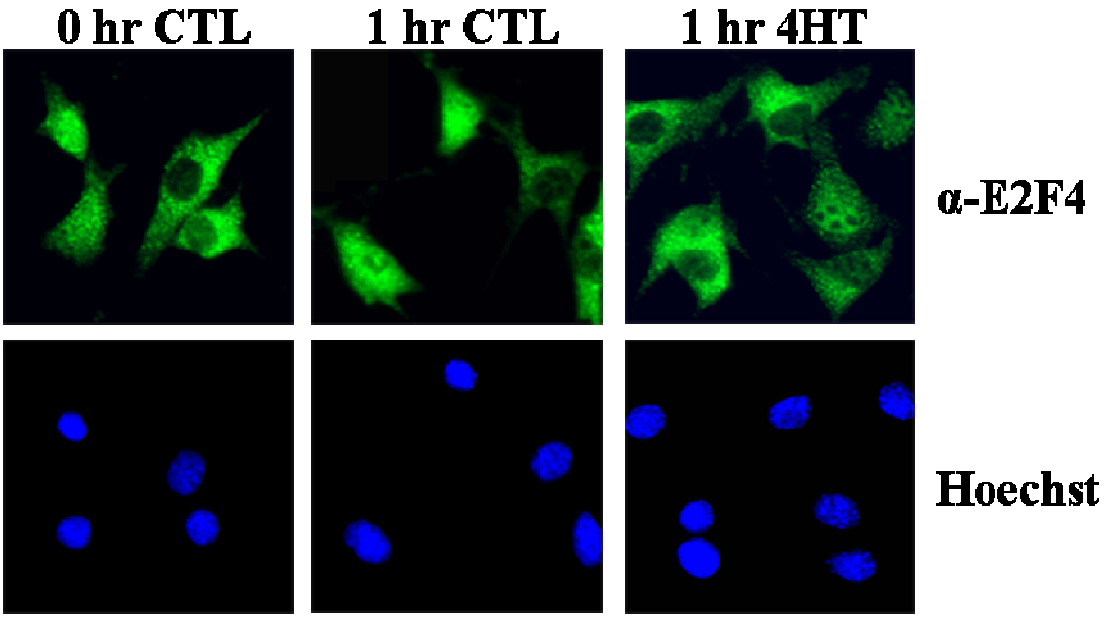

Figure 21. E2F4 expression does not change in response to Raf activity. 23A2RafER^{DD} myoblasts were treated for one hour with 1μM 4HT or vehicle-only (CTL) and immunostained for E2F4 and Hoescht.

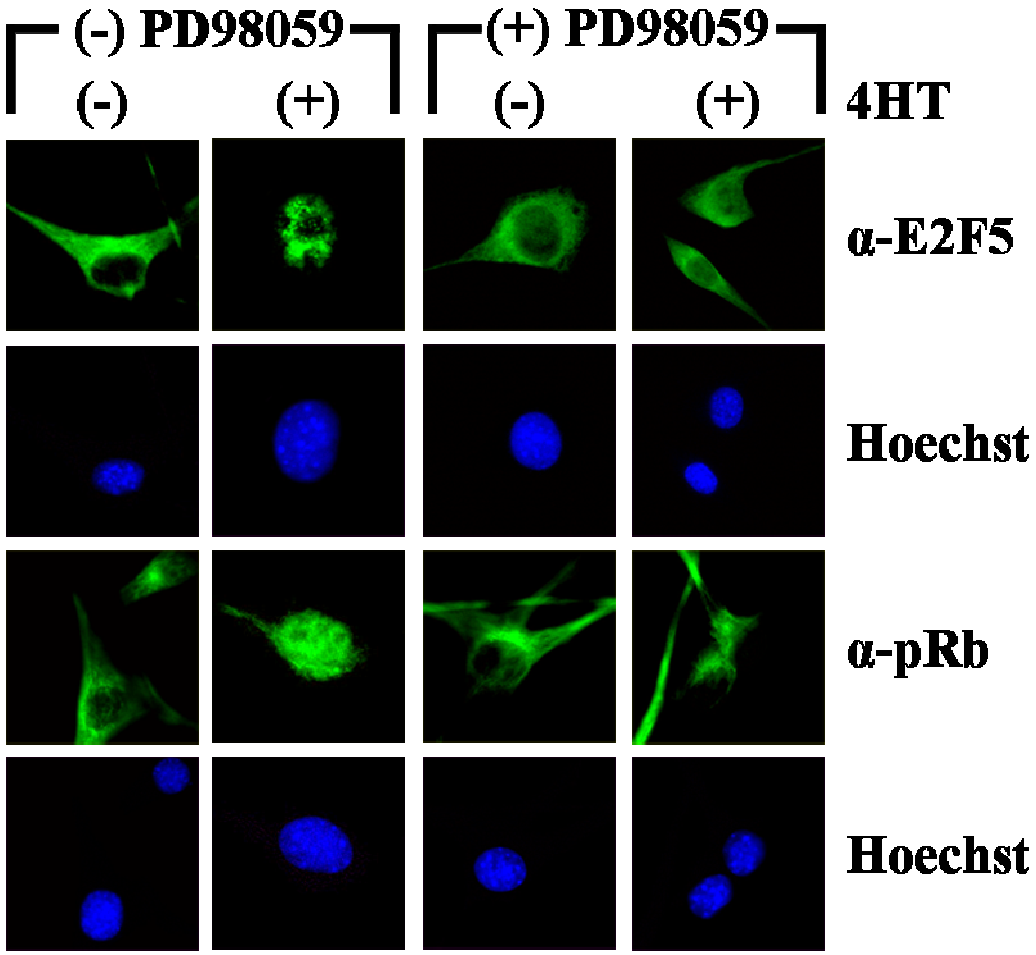

Figure 22. Inhibition of pERK1/2 blocks the translocation of E2F5 and pRb to the nucleus. 23A2RafER^{DD} myoblasts were treated with 1μM 4HT or vehicle-only for one hour in the presence or absence of PD98059 prior to immunostaining for E2F5 or pRb and Hoescht.

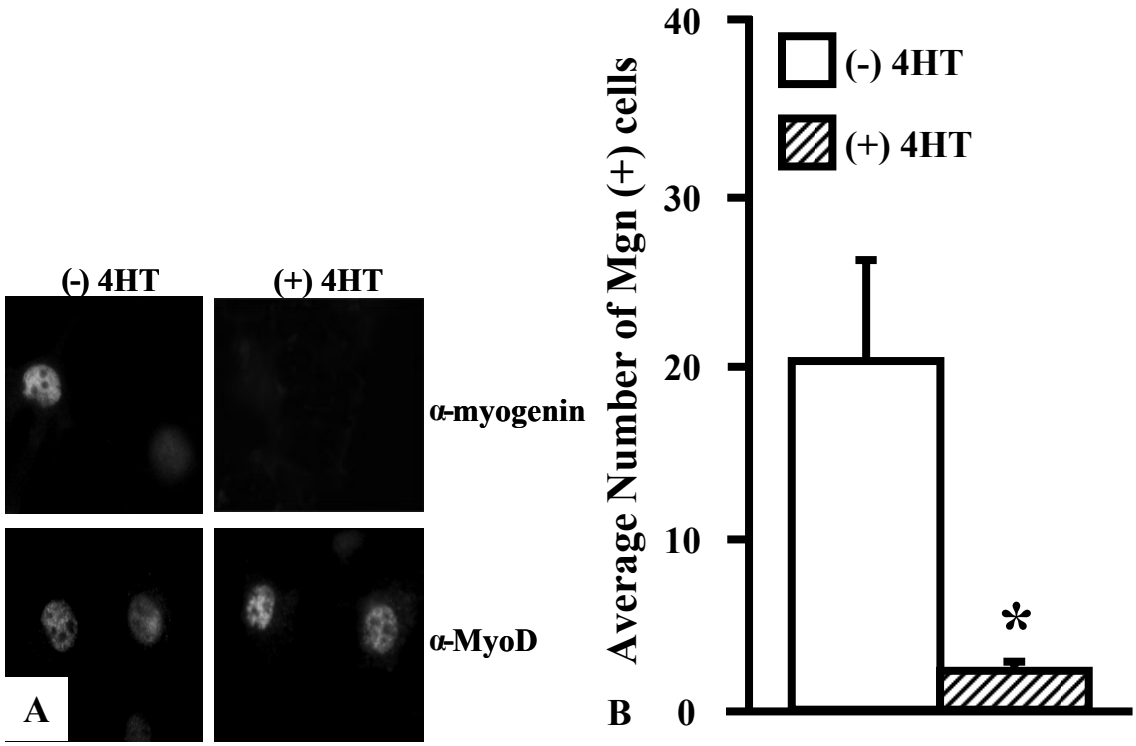

Figure 23. Myogenin is not expressed in Raf induced cells. Raf induced myoblasts were immunostained for myogenin and MyoD expression (A). The percent of myogenin positive cells was determined from three independent tests. Asterisk indicates significant difference (B).

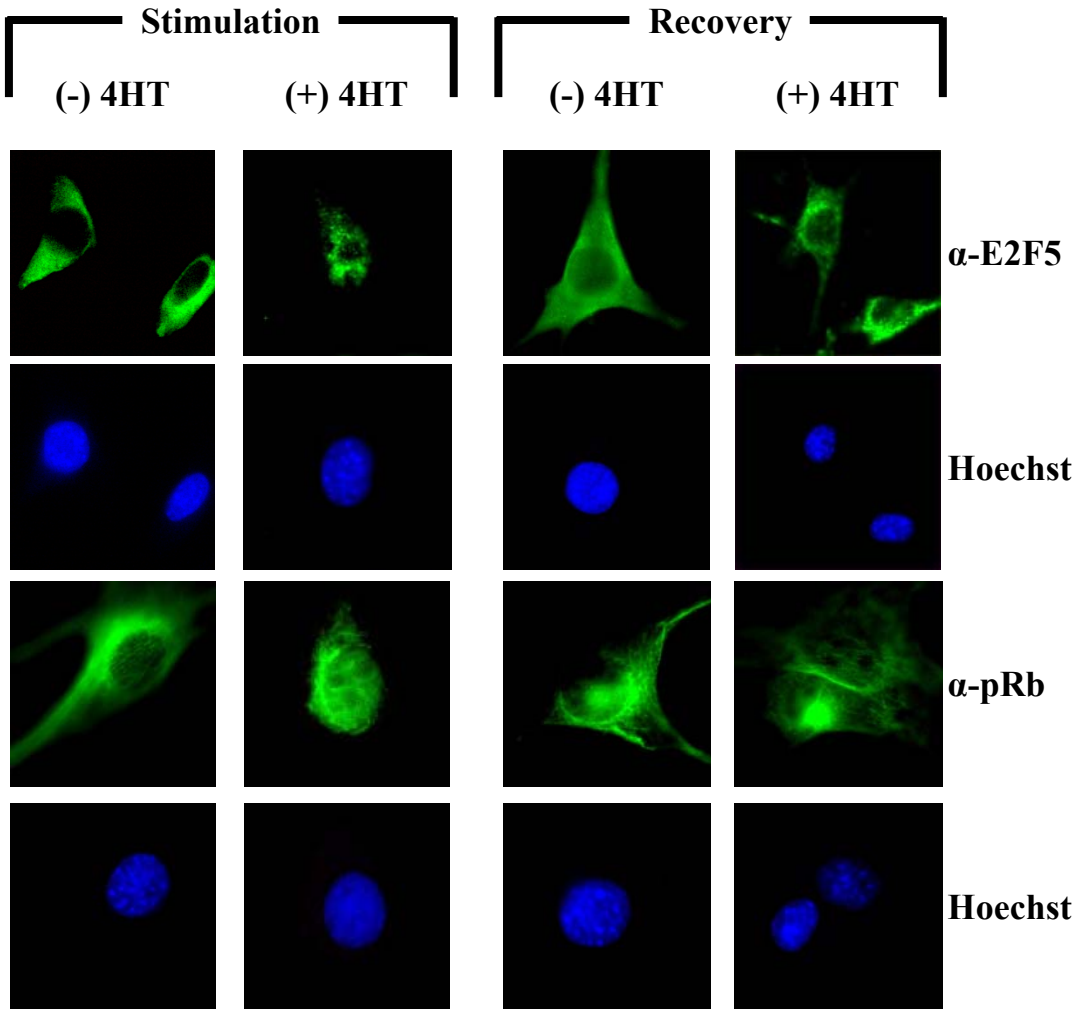

Figure 24. Recovery from ERK1/2 stimulation results in the partial restoration of cytoplasmic location of E2F5 and pRb. 23A2RafER^{DD} myoblasts were stimulated with 1μM 4HT or vehicle-only for one hour (stimulation), allowed to recover in serum free media for three hours (recovery), and immunostained for E2F5 or pRb and Hoescht.

CHAPTER 5
DISCUSSION

Embryonic myoblasts and proliferative satellite cells behave in similar manners. Proliferating satellite cells have two possible fates – terminal differentiation or return to quiescence. It is controversial whether embryonic myoblasts contribute to the satellite cell population, but it is well established that they are both capable of fusing to form myofibers. If satellite cells arise from embryonic myoblasts exiting the cell cycle to a quiescent state, determination of the causal signals would be extremely important.

The 23A2RafER^{DD} cell line was derived from an embryonic mouse myoblast population. The fusion of the Raf molecule to a tamoxifen-specific estrogen receptor allows a dose-dependent response to 4HT. High levels of Raf kinase activity over 48 hours result in cell cycle inhibition, as evidenced by a lack of proliferation in treated cells while control myoblasts proliferate. The stability of cell number in treated cells coupled with the decreased BrdU incorporation and lack of apoptosis or senescence, suggests that early changes are affecting S-phase entry. Consistent with the results of the presented work, expression of an inducible Raf molecule was not capable of inducing S-phase entry in serum starved quiescent 3T3 cells (114). In addition, a highly active Raf mutant also failed to stimulate the cell cycle entry of quiescent cells but induced the expression of cyclin D and p21^{Cip1}, which binds cyclin E/cdk2 complexes to inhibit cell cycle progression (140).

The removal of stimuli and return to a normal growth environment stimulated cell cycle re-entry. This supports the protective nature of high Raf activity against apoptosis

and suggests that the cells are becoming quiescent rather than senescent, a state from which the cell cycle cannot be re-entered. In addition, β-galactosidase staining was negative in accordance with the work of DeChant et al., a group that showed the protective effects of Raf activity against apoptosis in myoblasts (40). Furthermore, the presence of high serum media abrogated the effects of Raf induction. It is interesting to note that in serum starved 3T3 cells with high levels of Raf activity the addition of FBS allows proliferation, while the addition of other growth factors results in a retained quiescent state (114). This suggests that this pathway may be primarily active during times of non-growth. Satellite cells proliferate following activation due to growth factors and other stimuli. The presence of growth factors causes myoblasts to remain cyclic, much like the presence of growth factors in muscle activates satellite cells and causes subsequent proliferation. The abrogation of Raf induced changes by high levels of serum may be reflective of the *in vivo* state of satellite cell proliferation.

To further clarify the immediate time course of Raf pathway activation, cells were treated over time and Western blots probed for phosphorylated ERK1/2. Results indicate that a slight activation of ERK2 was occurring at thirty minutes but both kinases were strongly phosphorylated after one hour of Raf induction. The treated cells were stripped of all extracellular growth factors and starved for one hour prior to Raf induction, removing any potential mitogenic signal. The early activation of the Raf kinase suggests that this pathway plays an early role in the morphological and cell cycle related changes over time. The decrease in active ERK1/2 at 120 minutes is most likely reflective of unequal loading or detection. Interestingly, there appears to be no active ERK1/2 in the absence of stimulation suggesting a lack of ERK1/2 gene transcription and/or translation.

However, upon stimulation of upstream kinases, inactive ERK1/2 may be required to immediately upregulate its own expression. Active ERK1/2 may be required to maintain a quiescent state. In one study, the presence of ERK1/2 (regardless of phosphorylation status) was used to mark individual satellite cells on isolated rat muscle fibers. The presence of ERK1/2 may indicate that these quiescent cells require active ERK1/2 to remain unproliferative. Interestingly, the presence of phosphorylated ERK1/2 decreases from 0 minutes (the start of culture) to 24 hours of culture in satellite cells on isolated myofibers. This coincides with the time satellite cell activation following plating (143).

LEK1 Expression Changes in Response to Raf Induction

The CENP-F/mitosin/CMF1 family of proteins includes LEK1, named for the large amount of leucine (L), glutamic acid (E), and lysine (K) residues present in the protein (57, 102). Human CENP-F/mitosin, mouse LEK1, and chicken CMF1 proteins share a highly conserved C-terminus (57). CMF1 protein is 65% similar to LEK1 and CENP-F (102). The family members share an atypical Rb binding domain, an ATP/GTP binding site, a nuclear localization signal, and a predicted HLH dimerization domain distributed in a collinear fashion in the C-terminal (10, 57, 102, 110). LEK1 appears to be widely distributed amongst species with protein orthologs present in canine, mouse, and mink derived cell lines. The core region of these proteins necessary for centromere binding is conserved between species, including chickens and humans (145). LEK1 also expresses several similarities to the E2F proteins, including a Myc-type HLH motif, a similar Rb-binding site, and several leucine zippers possibly responsible for DNA binding (10) (Figure 25).

LEK1 is expressed as early as five days after the formation of the embroid body, but not in the post natal murine heart. Knockdown of LEK1 using siRNA resulted in a

severe compromise in the beating ability of embroid bodies, tightly following the time course produced in Rb null embroid bodies. Fewer embroid body cardiomyocytes are present compared to wild type and those present showed incomplete sarcomere formation (104). These results suggest that LEK1 is required for terminal differentiation.

The expression of the LEK family of proteins differs throughout the cell cycle, indicating varying functions although they belong to the same family. LEK1 is targeted to the nucleus in differentiating embroid bodies (104) and is nuclear during interphase in murine cells, showing patterns indicative of centromere localization in mitotic cells (145). In stable fibroblast lines, CMF1 is predominantly localized to nucleus (110). Similarly, LEK1 is present in the nuclei of actively dividing cells and newly differentiated myotubes, but is absent in older myotubes (57). CENP-F is present in low levels in the cytoplasm of G1 cells but increases sharply in S phase as a nuclear protein (145). CMF1 is detected in the cytoplasm of developing cardiomyocytes and is maintained in differentiated myocytes, differing significantly from other LEK family proteins (102).

In the present study, Raf induced entry into quiescence results in the majority of LEK1 protein translocating to the nucleus, while differentiating cells retain LEK1 cytoplasmically. This contrasts with previous reports of LEK1 nuclear localization in differentiated embryoid bodies and mitotic cells. These differences may be due to unique cell lines as it is well known that members of the LEK1 family have different fuctions according to their tissue of origin. In addition, the time point examined in the present study is a very short time after the initial stimulation. Other work has examined later stages of the cell cycle (104, 145). Ashe et al. report post-translational modification of

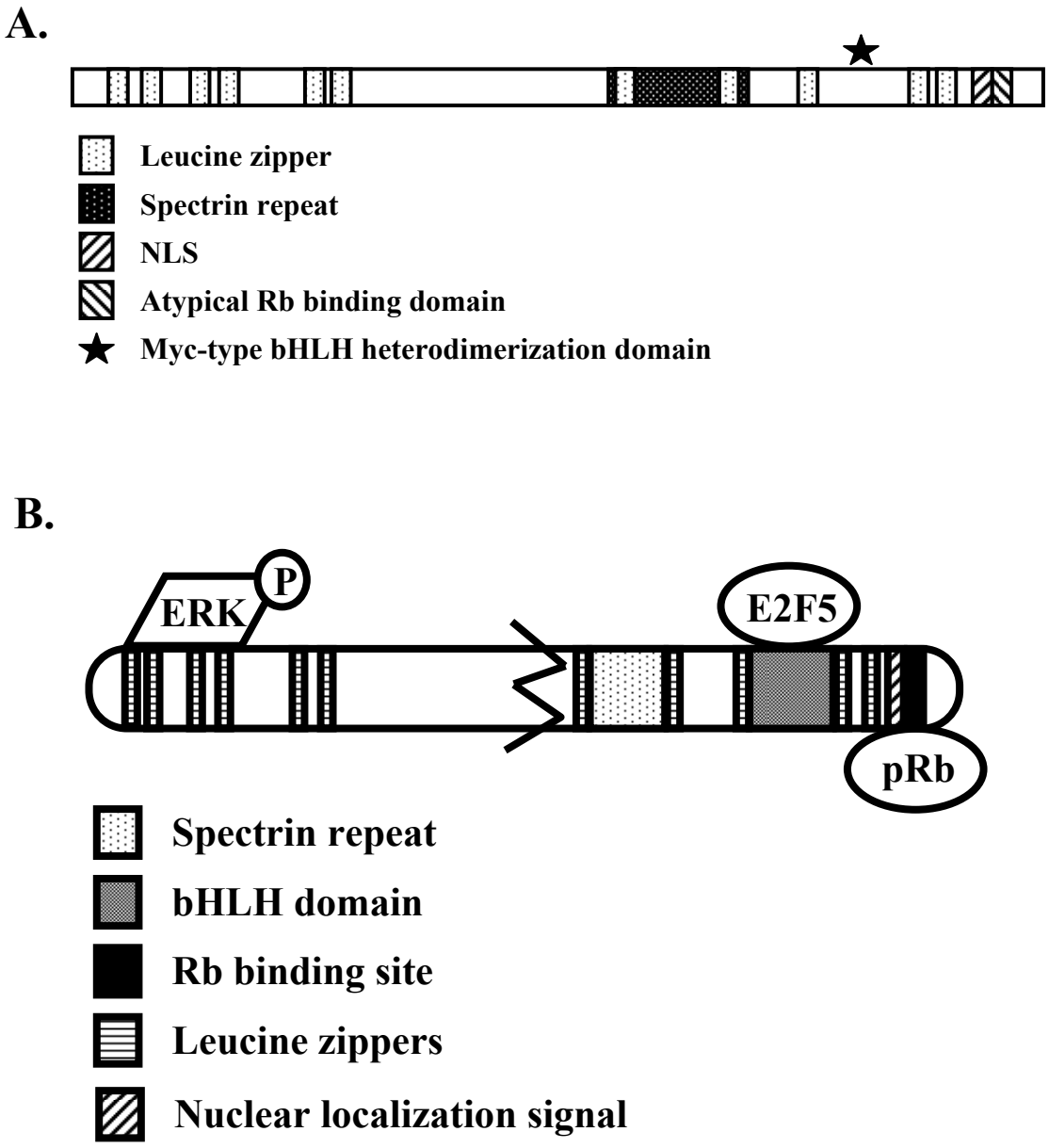

Figure 25. Schematic drawing of the conserved structures in the LEK family of proteins (A) and potential interaction sites (B). NLS, nuclear localization signal.

LEK1 in the cytoplasm, resulting in the cleavage and nuclear translocation of the C-terminus (10). Unfortunately, the exact cleavage site and mechanism of modification has yet to be determined. Immunocytochemistry indicates the presence of LEK1 in both the nucleus and cytoplasm in Raf induced quiescent cells. This is likely due to the ability of the antibody to recognize both the full length and cleaved protein as the antibody is targeted to the C-terminus of the protein.

The full function of LEK1 has yet to be determined. Despite the presence of several leucine zippers with DNA binding potential, LEK1 alone cannot directly bind DNA (10). However, LEK1 recognizes sequences in all three pRb binding pocket subdomains and complexes with active pRb, p107, and p130 in a cellular environment (10, 110). Similarly to E2F proteins, LEK1 binds the long pocket, the A/B pocket, and the C pocket regions of Rb, p107, and p130. However, LEK1 is capable of interaction with an E2F-binding incompetent Rb, which has a point mutation at amino acid 706. Pull down assays indicate that the pRb binding domain located in the C-terminus of LEK1 is essential for pocket protein binding (10). In the present work, LEK1 is accompanied by E2F5 and pRb in translocation to the nucleus. This suggests that although pRb and E2F5 may not bind preferentially, these three proteins may interact to elicit entry into quiescence.

The Rb family of proteins significantly affects the cell cycle. Knockdown of LEK1 by an antisense morpholino directed at LEK1 results in a reduced cell number and an accumulation of cells in the G_1 phase of the cell cycle, indicative of G_1/S phase arrest. Absence of LEK1 prevents cells from entering G_2 when released from serum starvation and subsequently induces apoptosis (10). LEK1 may potentially act as a pocket protein

suppressor by disrupting their association with other proteins. dnLEK1 enhanced the differentation of C2C12 myoblasts indicating that this protein may play a role in achieving or maintaining quiescence (57). In the present study, LEK1 may be sequestering pRb in the cytoplasm until appropriately stimulated and subsequently assisting or allowing nuclear translocation of this or other proteins to aid in the entrance to quiescence.

E2F5 is Involved in Cell Cycle Exit

The E2F proteins are a set of transcription factors that assist in cell cycle control. The eight proteins are divided in to three subgroups based on function. E2F1, E2F2, and E2F3 are involved in positive cell cycle control and S phase entry of quiescent cells. The second subgroup consists of E2F4 and E2F5. These proteins negatively affect the cell cycle progression. E2F6, E2F7, and E2F8 make up the third group. Although they are generally classified as repressors, the structure and function of these proteins is dramatically different from the former two groups, as none bind pocket proteins.

Closely related, 69% of the amino acids in E2F4 and E2F5 are identical and 80% are similar. The 1239 bp E2F4 cDNA open reading frame encodes a 413 amino acid protein that is approximately 44kD (115). E2F5 is a 345 amino acid protein of approximately 37.5kD encoded by a 1035bp open reading frame (63, 115). Both are constitutively synthesized (115). These two factors lack a cyclin A binding domain, resulting in shorter N-terminals than present on the other E2F factors (115). E2F5 lacks the serine repeat region found in E2F4, however both proteins contain a C-terminal transactivation domain (63)(Figure 26).

D'Souza et al. found abundant levels of E2F5 in the murine brain, heart, lung, liver, and kidney with low levels expressed in the dermis and epidermis (37). Unlike

other E2F transcription factors, E2F5 levels are detectable in adult rat cardiac myocytes (136). Murine E2F5 mRNA is transcribed and protein can be detected in the cytoplasm from pre-implantation through 11d.p.c. embryos and in gametes of both sexes (103). Upregulation of E2F5 is associated with completed neuronal circuitry in the adult murine brain (82). Actively proliferating murine keratinocytes express lower levels of E2F5, which increase upon differentiation (37).

Some controversy exists regarding the expression profile of E2F5 during the cell cycle. Several labs have found E2F5 complexes present in quiescent cells. One study found E2F5 transcript levels peaking in mid to late G_1 and returning to G_0 levels as human fibroblasts enter S phase (115). Unlike E2F1/2, little to no change in E2F4/5 mRNA expression occurred throughout the cell cycle of fibroblasts. Fugita et al. determined that in serum starved quiescent rat smooth muscle vascular cells; E2F5 was down-regulated and increased upon serum stimulation in a time dependent manner (48). Expression of E2F1-4 in serum-starved quiescent mouse and rat cardiomyocytes induces cell cycle entry, however only E2F1/2 expression can complete the cell cycle by stimulating mitotic division (44). Interestingly, a 24 hour treatment of keratinocytes with TGF-β to achieve a reversible growth arrest caused a decrease in E2F5. Forced ectopic expression of E2F5 for 24 hours in cycling keratinocytes reduced DNA synthesis (37). In another study, a variety of cell types were used to show that the E2F5-p130 complex was present in G_0 but not throughout the remainder of the cell cycle. Hypertrophic stimulus of rat cardiomyocytes promotes E2F1/3/4 and DP1 expression while down-regulating E2F5, consistent with a role for E2F5 in maintenance of growth arrest or quiescence (136). In differentiated L6 myotubes, E2F5 exists primarily in the cytoplasm, while pRb,

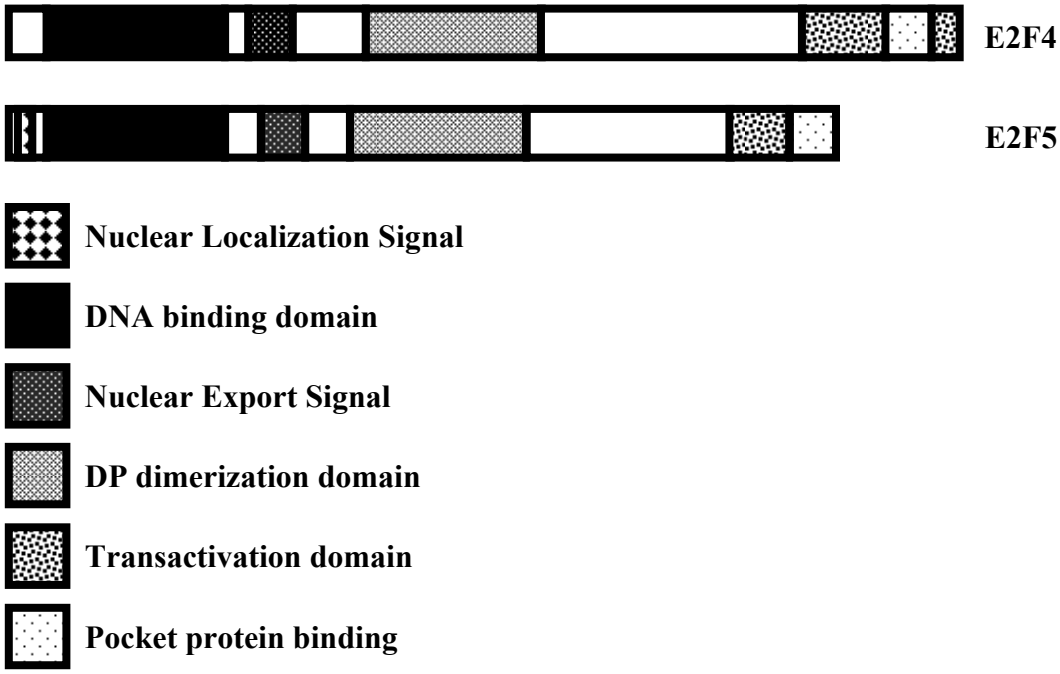

Figure 26. Schematic representation of conserved E2F4 and E2F5 domains.

p130, and p107 are present in the myonuclei (55). E2F5 may serve different purposes in individual cell types. In the present study, serum-starved myoblasts express E2F5 cytoplasmically before entering terminal differentiation. In response to high levels of Raf activity, E2F5 translocates to the nucleus. The presence of nuclear E2F5 in this study is consistent with the induction and maintenance of a quiescent state. The Raf-induced cells are likely to be entering a true quiescent state as they are capable of resuming proliferation. It is tempting to speculate that endogenous cytoplasmic E2F5 translocates to the nucleus to up regulate its own transcription in preparation for maintenance of quiescence.

It is widely accepted that E2F5 contains a nuclear export sequence (NES); however, the mechanism for nuclear entry is more controversial. Localization is mediated through the balance of import and export, as E2F5 has an atypical nuclear export sequence in a region that is poorly conserved between E2F5 and E2F4 (AA 130-154) as well as an atypical nuclear localization sequence (NLS) in AA 1-56 (8). The NES contains a high number of hydrophobic residues rather than a Rev-type Leucine-rich NES. Nuclear export is mediated through the CRM1 pathway (8). Although some groups have claimed that E2F5 translocates to the nucleus via association with pocket or DP proteins (54, 55), Apostolova et al. contend that association with pocket proteins or DP proteins is not necessary for nuclear entry (8). E2F5 enters the nucleus through nuclear pores in an energy-dependent manner. In the present study, E2F5 does not appear to require pocket proteins for nuclear entry, as p130 and p107 patterns are unchanged. pRb does translocate to the nucleus in response to high levels of Raf activity, but as E2F5 and pRb have little to no binding affinity it is unlikely that pRb is

transporting E2F5. Fujita et al. found E2F5 complexes with pRb upon serum stimulation which has not been reported by other labs (48). However, in the present work, E2F5 and pRb translocate to the nucleus in the absence of serum, further suggesting that these two proteins don't interact to elicit translocation of each other.

Serum stimulation affects the localization of E2F proteins. In media without serum supplementation, E2F1 and 4 as well as DP-1, pRb, and p130 are cytoplasmic. However, in quiescent cells supplemented with as little as 0.2% serum, both E2F1 and 4 are nuclear. This may explain the differences seen in the Raf induced cells in the presence and absence of high levels of serum in the present study. High serum concentrations that inhibit nuclear translocation of E2F5 or pocket proteins may provide mitogenic signals to the myoblast, creating inappropriate signals for cell cycle exit. In contrast, low serum conditions with high levels of Raf activity may mimic the *in vivo* environment promoting satellite cell self renewal. This may explain why Raf induced cells in high concentrations of serum continue to proliferate while Raf induced cells in low or no serum media enter quiescence. The presence of mitogens in the serum may over ride the forced Raf expression.

E2F proteins exert their major effects in two ways: (1) binding and sequestering pocket proteins and (2) binding DNA to induce or repress transcription. Members of the pocket protein family p130 and p107, but not pRb, associate with E2F4/5, although E2F5 indicates a preference for p130 binding (63, 115)(Figure 27). E2F5 stimulated transcription is inhibited by cotransfection with expression vectors containing p130, p107, and pRb (63). E2F4 can induce pocket protein independent repression during G_0 in glioblastoma cells, suggesting E2F5 may also have this capability (11)

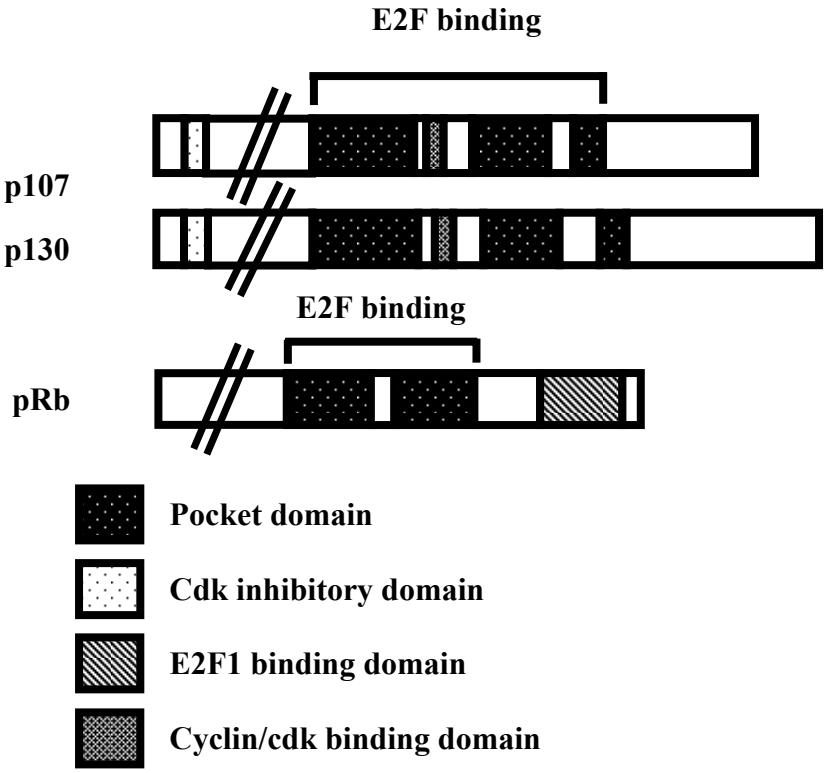

Figure 27. Comparison of pRb, p130, and p107 conserved domains.

Although E2F5 is capable of binding DNA as a homodimer, heterodimerization with one of the DP family of proteins creates a stronger bond (63, 115). DP1/2 have E2F and DNA binding regions. Heterodimers of E2F transcription factors and DP1 or DP2 cooperate in DNA transactivation (56, 62). The E2F4/DP1 heterodimer is analogous to other winged helix proteins with the exception of presenting a continuous protein surface and lacking a C-terminal wing region. The α3 helices bind the major DNA groove while the N-terminal α1 helices and portions of β sheets contact the DNA backbone. The E2F/DP residues that contact the DNA bases and backbone are identical within the E2F and DP families. This suggests that other E2F/DP dimers bind DNA in a similar manner. E2F5/DP-1 over expression increases E2F DNA binding in culture (105). Over expression of E2F5 can contribute to cell transformation in a Myc-type oncogene manner in the presence of DP-1 in primary rat BRK cells (106). How E2F5 is acting in Raf induced cells is not clear. While it is clear that E2F5 negatively affects cell cycle progression, further work needs to be completed to determine whether Raf induced E2F5 translocation affects gene transcription in a positive or negative manner.

The tumor suppressor protein p53 interacts with E2F5 to inhibit E2F5-activated transcription in a dose-dependent manner (135). p53 induces expression of p21, which then inhibits the cdks and prevents the release of free E2Fs from pRb/E2F complexes. A transactivation defective p53 is capable of inhibiting E2F5 mediated transcription, indicating that p21 is not involved in the inhibition. p53 inhibits the activity but not the expression of E2F5, having no effect on E2F5-DP1 complex formation or DNA binding, although DP1 was still required for strong binding. p53 inhibits E2F5 transcriptional activation, but does not physically interact with the protein, indicating an indirect effect.

Regulation of E2F responsive genes in cycling cells involves recruitment of co-repressors outside of the pocket protein family. HDAC1, a histone deacetylase associated with transcriptional repression stemming from histone deacetylation, complexes with E2F5 and p130 in differentiated keratinocytes (37). The reduction in DNA synthesis resulting from E2F5 over expression is abrogated in the presence of an HDAC1 inhibitor, indicating that HDAC1 is required for E2F5 mediated growth arrest (37). HDAC1 is recruited to promoters during quiescence but is absent by mid-G_1 (109). Recruitment of HDAC1 to the promoter requires the E2F4-p130 complex. In addition, histones H3 and H4 are deacetylated on certain promoters in quiescent T98G human glioblastoma cells. In contrast, these histones are extensively acetylated at E2F responsive promoters in S, G_2, and M phases. In G_1, histones H3 and H4 are deacetylated when p107 and p130 are present at the promoters.

mSin3B, a co-repressor that associates with chromatin modifying factors, occupies promoters in quiescent murine embryonic fibroblasts (MEFs). p107 or p130 is required for the recruitment of mSin3b to some but not all E2F regulated promoters (109). Although HDAC1 and mSin3b both associate with promoters during quiescence, both are equally present in quiescent and S phase nuclei. In quiescent cells, mSin3B is targeted to E2F4, E2F4/p130, and E2F4/p107 promoters. However, in early G_1 mSin3B is not present on E2F4 targets promoters. Pocket protein independent repression does not require the presence of mSin3B or the deacetylation of histones H3 and H4 in early G_1 (11).

Somatic stem cells in the drosophila ovary require hedgehog and wingless proteins for self renewal. Upon division, one stem cell remains anchored to the

germarium niche via cadherin-mediated cell adhesion and maintains stem cell identity. The other cell loses stem cell identity and differentiates. Somatic stem cells require *domino*, which encodes a transcriptional repressor, for the maintenance of the stem cell population (142). Domino effects drosophila E2F independently of Rb (Lu et al., manuscript in preparation). The mammalian homolog of Domino, Snf2 Related CBP activator protein (SRCAP), is capable of partially rescuing the lethality of domino mutants and can fully rescue the female infertility associated with domino mutations (45). SRCAP may potentially be involved in the E2F5 mediated cell cycle repression in skeletal myoblasts seen in this work. In addition, SRCAP can functionally replace Domino in drosophila Notch signaling, indicating that it is likely involved in mammalian Notch signaling as well. Indeed, SRCAP is a co-activator of *Notch* dependent gene expression in drosophila (45). In addition, another target of the Notch pathway, the HES related repressor protein (HERP), can repress gene expression through association with mSin3 and HDAC1, both of which are present in E2F5 repressor complexes (11, 37, 66, 67, 109). E2F5 repressor complexes containing SRCAP or HDAC1/mSin3/HERP may inhibit *Notch* transcription, allowing cell cycle exit. Considering that Numb, the Notch inhibitor, is present in satellite cells returning to the quiescent state, this gene repression may be an additional "off switch" for the Notch signaling pathway (28).

Methylation of certain E2F gene elements (*dhfr, E2F1,* and *cdc2*) blocks the binding of all E2F factors while other elements (*c-myb* and *c-myc* promoters) can bind all factors except E2F1 regardless of methylation status. Association with pRb family members doesn't affect the ability of E2F factors to bind methylated elements (22). Unlike pRb, p130, and E2Fs 1-3, growth inhibitory TGF-β signaling results in p107 and

E2F4/5 binding to the *c-myc* promoter. The *c-myc* promoter contains a TGF-β inhibitory element (TIE) which includes an E2F binding site flanked 5' by an imperfect Smad contact site. TGF-β induces rapid binding of Smad2/3, Smad4, E2F4/5, and p107 as a complex to the c-myc promoter *in vivo*. A site mutant that prevents E2F binding also inhibited the binding ability of Smads. The conformation of the TIE allows simultaneous binding of Smad3 and E2F4/DP1. Smad 3 is capable of establishing independent, direct associations with E2F4/5 and p107 (25).

In wild type MEFs, the cdk inhibitor p16INK4a restricts DNA synthesis, resulting in growth arrest. p16INK4a failed to inhibit DNA synthesis in E2F4$^{-/-}$5 $^{-/-}$ cells (54). Ectopic expression of E2F4/5 restores the p16INK4a mediated inhibition of DNA synthesis. Continuing MEF proliferation does not require the presence of E2F4/5. The activation of E2F4/5 requires the presence of functional pocket proteins (54). It is also interesting to note that E2F5 expression increases p16INK (44).

pRb Localization Changes in Response to Raf Activity

Because of the similar pocket protein binding abilities of E2F5 and LEK1, the expression and location of pRb, p130, and p107 were examined. Surprisingly, neither the temporal or spatial expression of p107 or p130 changed upon Raf-induced quiescence. This suggests that while p130 may be required for the maintenance of quiescence, it is not required for the early events that signal the cell to exit the cell cycle into G_0. Interestingly, the localization of pRb changes in response to Raf activity, translocating to the nucleus upon Raf induction. pRb does not commonly associate with E2F4 or E2F5, however it does play a role in cell cycle repression. Thus, while it may not be a direct response to changes in E2F5 or LEK1 translocation, pRb likely plays a significant role in the Raf induced cell cycle exit to quiescence.

Phosphorylated ERK1/2 Remains Cytoplasmic in Raf Induced Cells

The translocation of E2F5 and LEK1 prompted the examination of phosphorylated ERK1/2 location. In typical Raf-MEK-ERK1/2 signaling pathways, phosphorylated ERK1/2 translocates to the nucleus to affect gene transcription. Interestingly, phosphorylated ERK1/2 remained cytoplasmic in Raf induced myoblasts. This suggests that pERK1/2 is eliciting the phenotypic changes through a less common signaling pathway. When the sequences of E2F5 and LEK1 are examined, each has potential ERK1/2 phosphorylation and/or docking sites, insinuating the possibility of interactions (Figure 28). LEK1 has several putative N-terminal ERK1/2 binding domains that may serve to anchor ERK1/2 in the cytoplasm. Binding of ERK1/2 to LEK may also signal for the cleavage of the C-terminus. The C-terminal of E2F5 has a potential ERK1/2 phosphorylation site. It is tempting to speculate that in the absence of growth factors and the presence of high levels of Raf activity, phosphorylated ERK1/2 docks to the N-terminus of LEK1, stimulating the formation of a complex containing pRb and E2F5 (Figure 29). This results in the cleavage of the N-terminus which remains cytoplasmic while anchored to pERK1/2. The C-terminus of LEK1 (which is associated with pRb and E2F5) translocates to the nucleus. Nuclear E2F5 modifies cell cycle related gene transcription to induce the quiescent state while upregulating production of more E2F5 in preparation for the maintenance of quiescence. p130 may be recruited at a later time for maintenance of quiescence and not be necessary for the early entrance into this state. Importantly, all cells expressed MyoD in keeping with the myogenic lineage. In addition, Raf induced cells did not express myogenin, the earliest marker of terminal differentiation while over 20% of control cells expressed myogenin at this early time point.

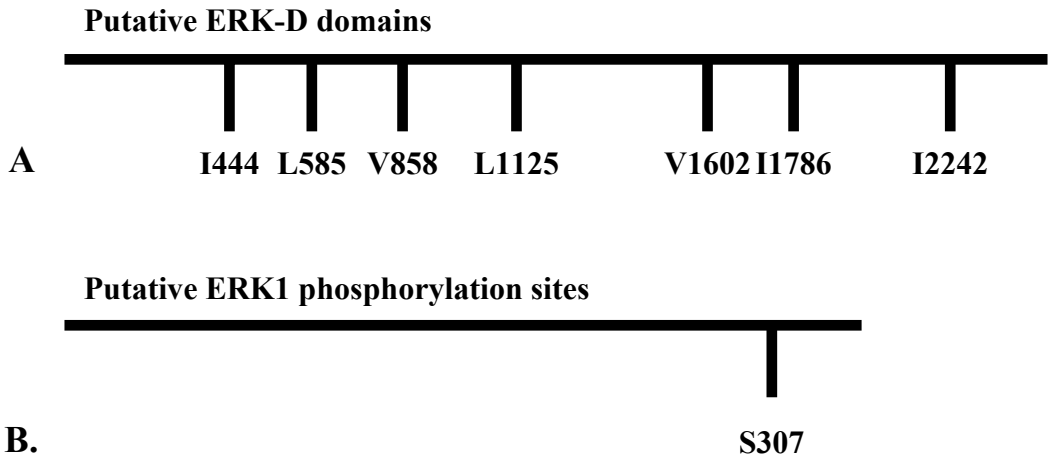

Figure 28. Potential ERK1 binding domains and phosphorylation sites on LEK1 (A) and E2F5 (B).

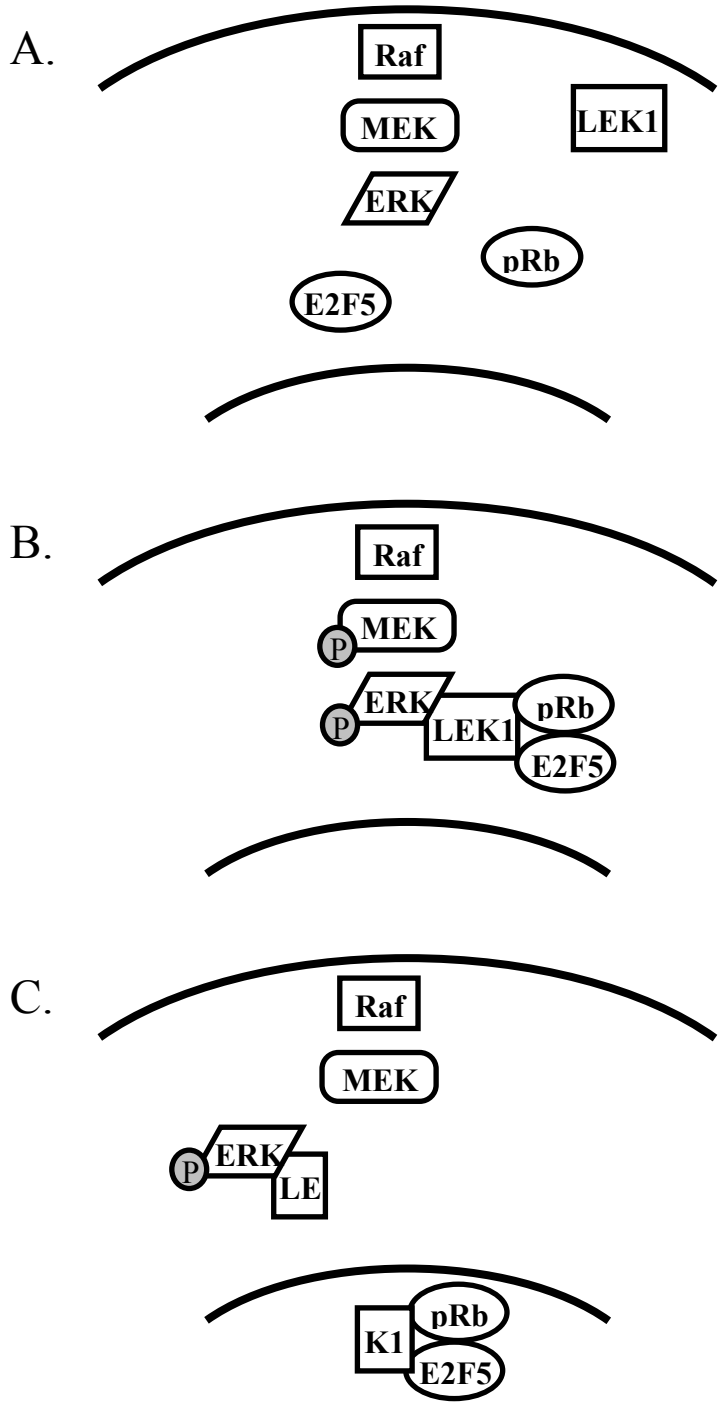

Figure 29. Proposed model. (A) The proliferative cell, lacking signal transduction through the Raf/MEK/ERK pathway. (B) Activation of Raf results in the phosphorylation of MEK and ERK1/2, causing a protein complex to form containing LEK1, pRb, and E2F5. (C) Cleavage of LEK1 results in the ERK1/2-associated N-terminus remaining in the cytoplasm and the C-terminus of LEK1 (associated with pRb and E2F5) translocating to the nucleus in the early quiescent myoblast.

CHAPTER 6
FUTURE DIRECTIONS

The two dimensional gel proteomics performed in this project led to an immense amount of data regarding the effects of high levels of Raf activity. Not only did it lead to information about proteins that were induced to translocate to the nucleus, it provided information regarding proteins that may have either been degraded or forced to exit the nucleus upon Raf stimulation. In addition, the immunochemistry performed indicated that the immediate changes identified occurred at the protein level rather than as a result of changes in gene expression. This chapter will outline future research that will aid in the understanding of the satellite cell self renewal and exit into quiescence as well as further defining the "stemness" of these cells.

Do ERK1/2, E2F5, pRb, and/or LEK1 Cooperate in Raf Induced Quiescence?

Because these proteins experience changes in phosphorylation or location in response to high levels of Raf activity, some or all may interact to elicit cell cycle exit. As mentioned previously, E2F5 and LEK1 have putative ERK1/2 phosphorylation sites and binding sites, respectively. To determine whether there are physical interactions, immunoprecipitations using each protein would identify binding partners. Both the C-terminal cleavage product and the full length LEK1 protein should be used to determine what proteins LEK1 may bind in the cytoplasm and in the nucleus. E2F5, the three pocket proteins, and pERK1/2 could be potential binding partners for LEK1 in this system. It would be expected that the N-terminus of LEK1 may bind ERK1/2, as both remain cytoplasmic in response to Raf activity. Site mutations at the essential residues of

the predicted binding sites would confirm binding site specificity. In addition to determining potential protein interactions, over-expression and under-expression studies will allow additional insight into the role of these proteins. A dominant-negative (d/n) LEK1 C-terminal protein should either remain cytoplasmic or allow the cells to proliferate even when present in the nucleus. Conversely, ectopic expression of the LEK1 C-terminus should force the cells to exit the cell cycle and remain quiescent. Overexpression of each protein and combinations of proteins would allow further clarification regarding which proteins are causing the Raf induced quiescence. Overexpression of binding deficient proteins would indicate whether heterodimerization is necessary for nuclear translocation and/or induction of quiescence.

In addition, the possibility exists that ERK1/2 phosphorylates E2F5 because of potential ERK1/2 phosphorylation sites. Western blots can determine the phosphorylation status at a variety of phosphorylation sites. In addition, phosphorylated residues can be determined by a mass spectrometry method of phosphorylation site mapping. Mutations to these sites may affect the proteins ability to translocate to the nucleus and/or affect gene transcription thereby inhibiting entrance to the quiescent state.

The Notch signaling pathway has also been implicated in satellite cell self renewal (27). As such, this pathway may be involved in Raf induced quiescence or affected by the high levels of Raf activity necessary for this quiescence. Experiments determining expression of Notch signaling molecules in response to high levels of Raf activity would indicate interaction between these pathways. Of particular interest are Numb (a Notch inhibitor), Delta (a Notch ligand) and the Notch intracellular domain (NICD). Numb is present in self renewing satellite cells and would be expected to be

present in Raf induced myoblasts (27). NICD and Delta expression should be decreased or absent in myoblasts with high Raf activity. Should these two pathways interact, elucidating whether that interaction is on the protein or gene level would lead to further experiments including whether E2F5 mediated repression is directed to Notch or Delta promoters or at what level each signaling pathway there is crosstalk, i.e. whether Raf/MEK/ERK inhibits the release of Delta and/or stimulates release or transcription of Numb.

Do High Levels of Raf Activity Promote a More Naïve State?

Induction of Raf activity resulted in the identification of several proteins present in and used to identify stem cells of non-muscle lineages. Tumor rejection antigen 1 (Tra1), Msx2 interacting nuclear target protein (MINT), and Laminin receptor 1 (Lmr1) were all identified in Raf induced cells. Tra1 has been used as a cell surface marker of undifferentiated embryonic stem cells (79, 130). Lmr1 is present in the extracellular matrix of human bone marrow derived mesenchymal stem cells and mouse embryonic stem cells, indicating that it can be used to identify both multi- and toti-potent stem cells (30, 79, 125). In addition, Kim et al. suggest that Lmr1 plays a role in stem cell self renewal, as expression of the receptor is decreased upon differentiation of human embryonic stem cells (79). MINT is an Msx2 interacting nuclear target protein identified through a mammalian two hybrid screen of a mouse brain expression library (95). It represses transcriptional activity in part through HDAC recruitment via the C-terminal recruitment domain. SHARP, the human homologue of MINT, directly interacts with the lysine-serine-aspartic acid (LSD) domains of NCoR and SMRT (123). MINT co-localizes to the nucleus with both Msx2 and Runx2 (124). BMP2/4 up-regulate the transcript levels of Msx2. Msx2 requires the presence of Smad4, another protein

involved in BMP signaling, for activation of embryonic stem cells (126). In addition, downstream targets of BMPs, Id proteins negatively regulate basic helix loop helix (bHLH) proteins which are important in inducing myogenesis (64). Inhibition of bHLH proteins may aid in inducing a more naive state. Msx2 is associated with endocrine precursor cells in the ducts of interferon gamma transgenic mice (80). Moreover, SHARP may be involved in regulating signaling from the Notch pathway through association with RBP-J, a DNA binding protein. Repression of the HES-1 promoter (a Notch responsive gene) requires the presence of a functional RBP-Jκ binding site. SKIP, an RBP-Jκ associated protein, not only co-localizes with SHARP but enhances SHARP mediated repression (99). Oswald et al. suggest that SHARP may be a general molecular switch to create repression complexes in Notch dependent pathways (99). MINT also competes for RBP-J, inhibiting Notch mediated transcriptional activity (81). As RBP-J can bind Notch or SHARP/MINT, it is likely that SHARP/MINT antagonizes Notch mediated transcription by competing for RBP-J (99).

Verification of changes in expression of Tra1, Lmr1, and MINT would indicate return to a more naïve state and a potential loss of lineage. Furthermore, additional proteins that identify pluripotent stem cells (such as Oct4, Nanog, and Sox2) could be used to further define the "stemness" of these Raf induced myoblasts. If these cells are reverting to a more naïve state, they should gain the ability to differentiate into multiple cell types. In addition, it would be interesting to determine whether these cells could contribute to non-muscle regeneration if they truly are able to differentiate into different lineages. However, a major concern that would need to be addressed is the oncogenic

potential of these cells. Raf is an oncogene and therefore has the potential to cause transformation of these cells into a cancerous line, presenting a multitude of problems.

Does High Raf Activity Correlate with Quiescence *in vivo*?

While many *in vitro* experiments could add valuable data, it is critical to verify all of this information in both a primary cell line and in the animal itself. This is especially important in this work as the cell line itself has been mutated by the addition of a constitutively active signaling molecule, even though this molecule is only stable in the presence of tamoxifen. While no side effects of tamoxifen have been seen, this remains an artificial environment which may produce artifacts of culture. The following experiments are proposed to verify and expand the presented model. Initial work should verify the presence of pERK1/2, E2F5, pRb, and LEK1 in quiescent satellite cells. These cells can be isolated from adult mouse muscle and examined before they re-enter the cell cycle. Because the changes that occur in phosphorylation and localization of these proteins occur early after stimulation, they may drive the entrance to quiescence rather than the maintenance of this state. Therefore, it is possible that healthy muscle may not strictly mimic the expression profiles observed in the culture system. Initially, cryosections of healthy adult muscle should be sufficient to examine general location of these proteins. More in depth examination will necessitate the use of isolated myofibers and mass culture of primary satellite cells. Satellite cells isolated from young mice will become active 24-36 hours after isolation, allowing time to analyze expression patterns prior to activation and proliferation. To closely examine the early stages of quiescence, it may be necessary to employ an injury model and examine satellite cells at various time points during regeneration. In addition, differences in the regeneration and activation time line in young and old mice should be characterized regarding the induction of these

proteins. Because old mice exhibit a longer lag time, it maybe be hypothesized that they express higher levels of pERK1/2, E2F5, and/or LEK1, losing expression of these proteins more slowly than young mice. It would be interesting to add a pERK1/2-specific phosphatase to satellite cells isolated from old mice in an attempt to shorten the lag phase, as high levels of phosphorylated ERK1/2 induces quiescence and a lower level allows proliferation.

The response of this panel of proteins to muscle damage may also provide valuable insight. Following injury, satellite cells become active and then proliferate, with a population fusing to the damaged fiber and a population returning to the quiescent state. A mouse injected with BrdU and then cardiotoxin would go through regeneration, incorporating BrdU into the satellite cells that enter the cell cycle. Those satellite cells that do not express BrdU and return to quiescence should be positive for LEK1, pRb, E2F5, and cytoplasmic pERK1/2. Some satellite cells may be positive for this panel of quiescent markers but still incorporate low levels BrdU due to the cells ability to divide and then return to quiescence. BrdU positive nuclei that fuse into myofibers should not express this panel of markers.

A complex but potentially revealing experiment would involve the use of an inducible Raf molecule conditionally expressed in skeletal muscle. Theoretically, if the Raf molecules in skeletal muscle were fused to the mutated estrogen receptor used in the 23A2RafER^{DD} myoblasts, injection of these muscles with 4HT should stabilize Raf expression resulting in ERK1/2 phosphorylation. Inducing high levels of Raf activity throughout an entire muscle would theoretically re-enforce the quiescent state of satellite cells. In healthy muscle, no phenotype would be expected as the satellite cells are

already quiescent. However, injection of 4HT (and thus induction of high levels of Raf activity) into an injured muscle should inhibit satellite cell activation and proliferation and thus inhibit regeneration. Alternatively, the Raf activity may not be able to overcome the myogenic signals provided by the surrounding environment, considering that mitogenic signals in culture negated the Raf induced quiescence. This may be a protective mechanism to allow for muscle regeneration.

In addition, if the transgenic mouse was induced to express high levels of Raf activity and then injured, and following the injury the Raf stimulus was removed, the muscle may exhibit delayed regeneration. Similar recovery was seen in both the 24 hour release where the cell number increased and the three hour release that partially restored the cytoplasmic location of E2F5 and pRb.

An additional component of this experiment could be the comparison of the lag phase between wild type old mice and transgenic (inducible Raf) young mice. High levels of Raf activity may mimic the extended lag phase exhibited by old mice. Furthermore, it would be interesting to examine the location, abundance, and time line of pERK1/2 expression in young and old mice. Old mice have a longer lag phase, most likely due to the existence of satellite cells in a deeper quiescent state. In theory satellite cells isolated from young mice should lose pERK1/2 expression earlier than satellite cells from old mice. Primary satellite cells from young mice forced to over express pERK1/2 should remain in the quiescent state longer.

Alternatively to the inducible Raf, a conditional knock-out model that inhibits Raf expression in skeletal muscle may prove the requirement of Raf signaling in inducing or maintaining satellite cell quiescence. If Raf activity is required for cell cycle exit,

satellite cells lacking Raf should exhibit continual proliferation. This knock out model may have a muscle phenotype similar to that seen in the Pax7 knockout mouse which has no quiescent satellite cells (119). A knockout model in which Raf could be inhibited in the skeletal muscle of aged mice may lead to a decrease in the lag time and result in more efficient regeneration of aged skeletal muscle. However, it could also result in constantly proliferating satellite cells leading to over-compensation and hypertrophy.

This work has presented a novel model of satellite cell quiescence. While there are many opportunities for future research, the most important aspect should focus on the translation of the in vitro model to the animal. It is crucial to verify the data obtained in vivo to determine both the advantages and limitations of this system.

APPENDIX A
PROTEINS IDENTIFIED IN VEHICLE-ONLY CELLS

Spot ID	Protein	Score	MW	pI	Ascension #
C1-12	1810007P19Rik -- 28175624	65	43	6.69	AAH45150
C1-18	2810406C15Rik -- 13879386	66	128	5.74	AAH06673
C1-16	4921510J17Rik	66	50	9.53	AAH50801
C1-11	aldehyde dehydrogenase AHD-M1	84	57	7.53	P47738
C1-11	Aldh2 -- 13529509	102	57	7.53	AAH05476
C1-22	Annexin A1	119	39	7.15	P10107
C1-20	Annexin A2	61	39	7.53	P07356
C2-11	Annexin a5	88	36	4.83	AAH03716
C1-2	Annexin A6	229	76	5.34	P14824
C1-8	Atp5b	218	57	5.19	P56480
C3-11		153			
C2-03	calreticulin	89	48	5.8	Q9D9Q6
C3-09		92			
C1-13	calumenin isoform 2	69	37	4.49	O35887
C2-04		76			
C3-12		65			
C1-6	casein kinase alpha 1	66	41	9.5	Q8BK63
C1-10	chaperonin subunit beta -- 20073068	99	58	5.97	AAH26918
C1-5	ERP57	88	57	5.99	P27773
C3-08		64			
C3-16	gamma actin -- 809561	113	41	5.56	CAA31455
C1-5	glucose regulated protein	175	57	5.88	AAH33439
C1-4	heat shock protein 1	137	61	5.91	P63038
C3-07		89			
C1-3	Heat shock protein 5	102	73	5.53	P17879
C3-03		139			
C3i	heterogeneous nuclear ribonucleoprotein H1 -- 37589940	80	49	5.89	AAH42187
C2-06	hypothetical protein A730012O14	66	92	9.35	BAC37916

C3-15	laminin receptor 1 -- 31560560	67	33	4.8	NP_035159
C3-15	Lamr1 protein -- 33417033	67	33	4.8	AAH55886
C1-22	lipocortin 1 -- 6754570 -- Anxa A1	97	39	6.57	NP_034860
C1-15	myomesin 2	68	166	5.83	Q62234
C1-9	none significant				
C1-17	none significant				
C1-21	none significant				
C1-23	none significant				
C1-24	none significant				
C1-26	none significant				
C1-28	none significant				
C1-29	none significant				
C1-31	none significant				
C1-32	none significant				
C2-01	none significant				
C2-02	none significant				
C2-05	none significant				
C2-07	none significant				
C2-10	none significant				
C3-01	none significant				
C3-04	none significant				
C3-06	none significant				
C3-10	none significant				
C3-13	none significant				
C3-14	none significant				
C2h	none significant				
C2i	none significant				
C2j	none significant				
C3h	none significant				
C3j	none significant				
C1-19	PCNA	64	29	4.66	P17918
C1-7	prolyl 4-hydroxylase beta	78	57	4.79	P09103
C2g		90			
C3g		116			
C3-15	protein 40kD – 226005	67	33	4.8	1405340A

C1-13	reticulocalbin	65	37	4.7	Q05186
C2-09	similar to hypothetical protein BC004409 -- 34861185	63	37	9.39	XP_238146
C1-12	SNEV	70	56	6.14	Q99KP6
C1-30	TNF alpha induced protein 1 -- 33636730	67	37	8	NP_891995
C3-15	unnamed protein product -- 12846904	67	33	4.85	BAB27355
C1-19	unnamed protein product -- 15919908	64	29	4.66	BAB28355
C2-08	unnamed protein product -- 26334119	70	44	5.17	BAC30777
C3i	unnamed protein product -- 26353116	74	51	6.33	BAC40188
C3-07	unnamed protein product -- 51452	91	59	5.48	CAA37653
C1-19	unnamed protein product -- 53600	64	27	4.66	CAA37243
C1-7	unnamed protein product -- 54777	70	57	4.79	CAA29759
C1-10	unnamed protein product -- 7670405	92	53	5.88	BAA95054
C1-14	vimentin	158	52	5.06	P20152

Scores greater than 63 indicate statistical significance. pI = isoelectric point, MW= molecular weight

APPENDIX B
PROTEINS IDENTIFIED IN RAF INDUCED CELLS

Spot ID	Protein	Score	MW	pI	Ascension #
42-09	Annexin A5	96	36	4.83	P48036
41-26	annexin a6	225	76	5.34	P14824
43-05		58			
42-04	Atp5B	220	57	5.19	P56480
43-11					
41-08	calreticulin	110	48	5.8	Q9D9Q6
43-09		112			
43b	dihydrolipoamide s-acetyltransferase 16580128		59	5.71	AAL02400
43-18	E2F5	48	152	5.17	Q61502
41-11	ERP57	134	57	5.99	P27773
41-12		88			
43-15	gamma actin -- 809561	162	41	5.56	CAA31455
43-08	glucose regulated protein -- 8393322	75	57	5.88	NP_059015
41-11	glucose regulated protein 23958822	205	57	6.79	AAH33439
41-12	glucose regulated protein 6679687	132	57	5.99	NP_031978
42-09	gprin1 34784265	64	96	6.79	AAH57044
41-07	heat shock protein 1 (chaperonin)	140	61	5.91	P63038
41-10		135			
42-03		120			
43-07		145			
41-05	heat shock protein 5	154	72	5.53	P17879
43-03		124			
43-04	heat shock protein A -- 6754256	113	74	5.91	NP_034611
41-14	heterogeneous nuclear ribonucleoprotein H1	71	49	5.89	O35737
42-10	hypothetical protein A730012o14	72	92	9.35	BAC37916
43-16	laminin receptor 1	86	33	4.96	NP_035159
43e		65			

42-06		70			
41-18	laminin receptor 1 8393693 or 31560560	67	33	4.8	NP_058834
41-18	lamr1 -- 33417033	67	33	4.74	P14206
43-16		76			
43-06	LEK1	64	284	4.94	Q9QZ84
43-14		66			
41-24	mKIAA0303 protein -- 37359892	66	101	9.53	BAC97924
42a	Msx2 interacting nuclear protein	45	390	8.65	BAB32786
43d	NAD+specific isocitrate dehydrog		40	6.46	
41-01	none significant				
41-02	none significant				
41-04	none significant				
41-06	none significant				
41-13	none significant				
41-19	none significant				
41-20	none significant				
41-23	none significant				
41-25	none significant				
42-01	none significant				
42-11	none significant				
42b	none significant				
42d	none significant				
42f	none significant				
43-02	none significant				
43-12	none significant				
43-17	none significant				
43a	none significant				
43f	none significant				
42e	none significant				
42-08	PCNA	68	30	4.66	P17918
41-09	prolyl 4-hydroxylase beta	79	57	4.79	P09103
42-02		123			
43-10		181			
41-18	protein 40kD -- 226005	67	33	4.8	1405340A

43c	see 42c				
43-13	similar to palladin -- CGI-151 protein -- 34878103	63	23	8.22	XP_344508
41-03	tumor rejection antigen gp96	113	92	4.74	P08113
43-01		114			
42c	Txndc7 -- pos ID with MS/MS		48	5.05	BC006865
41-18	U8 -- 5103680	63	51	8.74	BAA79193
43-16		67			
41-18	unnamed protein product -- 12846904	67	33	4.85	BAB27355
42-08	unnamed protein product 15919908	72	29	4.66	BAB28355
41-24	unnamed protein product -- 26328539	64	82	9.62	BAC28008
41-11	unnamed protein product -- 26353794	207	57	5.78	BAC40527
41-12		133			
42-05	vimentin	131	52	5.06	P20152
42-07	YL2/p32 RACK (pos id with MS/MS)	31		4.77	Q8R5L1

Scores greater than 63 indicate statistical significance. pI = isoelectric point, MW= molecular weight

LITERATURE CITED

1. **Adams, G. R., and S. A. McCue.** 1998. Localized infusion of IGF-I results in skeletal muscle hypertrophy in rats. J. Appl. Physiol. **84:**1716-22.

2. **Allegra, S., J. Y. Li, J. M. Saez, and D. Langlois.** 2004. Terminal differentiation of Sol 8 myoblasts is retarded by a transforming growth factor-beta autocrine regulatory loop. Biochem. J. **381:**429-36.

3. **Allen, R. E., and L. K. Boxhorn.** 1989. Regulation of skeletal muscle satellite cell proliferation and differentiation by transforming growth factor-beta, insulin-like growth factor I, and fibroblast growth factor. J. Cell Physiol. **138:**311-5.

4. **Anderson, J., and O. Pilipowicz.** 2002. Activation of muscle satellite cells in single-fiber cultures. Nitric Oxide. **7:**36-41.

5. **Anderson, J. E.** 2000. A role for nitric oxide in muscle repair: nitric oxide-mediated activation of muscle satellite cells. Mol. Biol. Cell **11:**1859-74.

6. **Anderson, J. E., C. M. Mitchell, J. K. McGeachie, and M. D. Grounds.** 1995. The time course of basic fibroblast growth factor expression in crush-injured skeletal muscles of SJL/J and BALB/c mice. Exp. Cell Res. **216:**325-34.

7. **Anderson, J. E., and C. Vargas.** 2003. Correlated NOS-Imu and myf5 expression by satellite cells in mdx mouse muscle regeneration during NOS manipulation and deflazacort treatment. Neuromuscul. Disord. **13:**388-96.

8. **Apostolova, M. D., I. A. Ivanova, C. Dagnino, S. J. D'Souza, and L. Dagnino.** 2002. Active nuclear import and export pathways regulate E2F-5 subcellular localization. J. Biol. Chem. **277:**34471-9.

9. **Asakura, A., P. Seale, A. Girgis-Gabardo, and M. A. Rudnicki.** 2002. Myogenic specification of side population cells in skeletal muscle. J. Cell Biol. **159:**123-34.

10. **Ashe, M., L. Pabon-Pena, E. Dees, K. L. Price, and D. Bader.** 2004. LEK1 is a potential inhibitor of pocket protein-mediated cellular processes. J. Biol. Chem. **279:**664-76.

11. **Balciunaite, E., A. Spektor, N. H. Lents, H. Cam, H. Te Riele, A. Scime, M. A. Rudnicki, R. Young, and B. D. Dynlacht.** 2005. Pocket protein complexes are recruited to distinct targets in quiescent and proliferating cells. Mol. Cell Biol. **25:**8166-78.

12. **Barani, A. E., A. C. Durieux, O. Sabido, and D. Freyssenet.** 2003. Age-related changes in the mitotic and metabolic characteristics of muscle-derived cells. J. Appl. Physiol. **95:**2089-98.

13. **Barton-Davis, E. R., D. I. Shoturma, and H. L. Sweeney.** 1999. Contribution of satellite cells to IGF-I induced hypertrophy of skeletal muscle. Acta. Physiol. Scand. **167:**301-5.

14. **Barton, E. R., L. Morris, M. Kawana, L. T. Bish, and T. Toursel.** 2005. Systemic administration of L-arginine benefits mdx skeletal muscle function. Muscle Nerve. **32**:751-60.

15. **Beauchamp, J. R., L. Heslop, D. S. Yu, S. Tajbakhsh, R. G. Kelly, A. Wernig, M. E. Buckingham, T. A. Partridge, and P. S. Zammit.** 2000. Expression of CD34 and Myf5 defines the majority of quiescent adult skeletal muscle satellite cells. J. Cell Biol. **151:**1221-34.

16. **Bischoff, R.** 1990. Cell cycle commitment of rat muscle satellite cells. J. Cell Biol. **111:**201-7.

17. **Bischoff, R.** 1986. Proliferation of muscle satellite cells on intact myofibers in culture. Dev. Biol. **115:**129-39.

18. **Bischoff, R.** 1986. A satellite cell mitogen from crushed adult muscle. Dev. Biol. **115:**140-7.

19. **Bladt, F., D. Riethmacher, S. Isenmann, A. Aguzzi, and C. Birchmeier.** 1995. Essential role for the c-met receptor in the migration of myogenic precursor cells into the limb bud. Nature. **376:**768-71.

20. **Bonavaud, S., P. Thibert, R. K. Gherardi, and G. Barlovatz-Meimon.** 1997. Primary human muscle satellite cell culture: variations of cell yield, proliferation and differentiation rates according to age and sex of donors, site of muscle biopsy, and delay before processing. Biol. Cell. **89:**233-40.

21. **Bottaro, D. P., J. S. Rubin, D. L. Faletto, A. M. Chan, T. E. Kmiecik, G. F. Vande Woude, and S. A. Aaronson.** 1991. Identification of the hepatocyte growth factor receptor as the c-met proto-oncogene product. Science. **251:**802-4.

22. **Campanero, M. R., M. I. Armstrong, and E. K. Flemington.** 2000. CpG methylation as a mechanism for the regulation of E2F activity. Proc. Natl. Acad. Sci. U. S. A. **97:**6481-6.

23. **Campbell, J. S., M. P. Wenderoth, S. D. Hauschka, and E. G. Krebs.** 1995. Differential activation of mitogen-activated protein kinase in response to basic fibroblast growth factor in skeletal muscle cells. Proc. Natl. Acad. Sci. U. S. A. **92:**870-4.

24. **Chakravarthy, M. V., B. S. Davis, and F. W. Booth.** 2000. IGF-I restores satellite cell proliferative potential in immobilized old skeletal muscle. J. Appl. Physiol. **89:**1365-79.

25. **Chen, C. R., Y. Kang, P. M. Siegel, and J. Massague.** 2002. E2F4/5 and p107 as Smad cofactors linking the TGFbeta receptor to c-myc repression. Cell. **110:**19-32.

26. **Clegg, C. H., T. A. Linkhart, B. B. Olwin, and S. D. Hauschka.** 1987. Growth factor control of skeletal muscle differentiation: commitment to terminal differentiation occurs in G1 phase and is repressed by fibroblast growth factor. J. Cell Biol. **105:**949-56.

27. **Conboy, I. M., M. J. Conboy, G. M. Smythe, and T. A. Rando.** 2003. Notch-mediated restoration of regenerative potential to aged muscle. Science. **302:**1575-7.

28. **Conboy, I. M., M. J. Conboy, A. J. Wagers, E. R. Girma, I. L. Weissman, and T. A. Rando.** 2005. Rejuvenation of aged progenitor cells by exposure to a young systemic environment. Nature. **433:**760-4.

29. **Conboy, I. M., and T. A. Rando.** 2002. The regulation of Notch signaling controls satellite cell activation and cell fate determination in postnatal myogenesis. Dev. Cell. **3:**397-409.

30. **Cooper, H. M., R. N. Tamura, and V. Quaranta.** 1991. The major laminin receptor of mouse embryonic stem cells is a novel isoform of the alpha 6 beta 1 integrin. J. Cell Biol. **115:**843-50.

31. **Cooper, R. N., S. Tajbakhsh, V. Mouly, G. Cossu, M. Buckingham, and G. S. Butler-Browne.** 1999. In vivo satellite cell activation via Myf5 and MyoD in regenerating mouse skeletal muscle. J. Cell Sci. **112 (Pt 17):**2895-901.

32. **Corbel, S. Y., A. Lee, L. Yi, J. Duenas, T. R. Brazelton, H. M. Blau, and F. M. Rossi.** 2003. Contribution of hematopoietic stem cells to skeletal muscle. Nat. Med. **9:**1528-32.

33. **Cornelison, D. D., M. S. Filla, H. M. Stanley, A. C. Rapraeger, and B. B. Olwin.** 2001. Syndecan-3 and syndecan-4 specifically mark skeletal muscle satellite cells and are implicated in satellite cell maintenance and muscle regeneration. Dev. Biol. **239:**79-94.

34. **Cornelison, D. D., S. A. Wilcox-Adelman, P. F. Goetinck, H. Rauvala, A. C. Rapraeger, and B. B. Olwin.** 2004. Essential and separable roles for Syndecan-3 and Syndecan-4 in skeletal muscle development and regeneration. Genes Dev. **18:**2231-6.

35. **Cornelison, D. D., and B. J. Wold.** 1997. Single-cell analysis of regulatory gene expression in quiescent and activated mouse skeletal muscle satellite cells. Dev. Biol. **191:**270-83.

36. **Crameri, R. M., H. Langberg, P. Magnusson, C. H. Jensen, H. D. Schroder, J. L. Olesen, C. Suetta, B. Teisner, and M. Kjaer.** 2004. Changes in satellite cells in human skeletal muscle after a single bout of high intensity exercise. J. Physiol. **558:**333-40.

37. **D'Souza, S. J., A. Pajak, K. Balazsi, and L. Dagnino.** 2001. Ca2+ and BMP-6 signaling regulate E2F during epidermal keratinocyte differentiation. J. Biol. Chem. **276:**23531-8.

38. **Dasarathy, S., M. Dodig, S. M. Muc, S. C. Kalhan, and A. J. McCullough.** 2004. Skeletal muscle atrophy is associated with an increased expression of myostatin and impaired satellite cell function in the portacaval anastamosis rat. Am. J. Physiol. Gastrointest. Liver. Physiol. **287:**G1124-30.

39. **Deasy, B. M., B. M. Gharaibeh, J. B. Pollett, M. M. Jones, M. A. Lucas, Y. Kanda, and J. Huard.** 2005. Long-term self-renewal of postnatal muscle-derived stem cells. Mol. Biol. Cell. **16:**3323-33.

40. **DeChant, A. K., K. Dee, and C. M. Weyman.** 2002. Raf-induced effects on the differentiation and apoptosis of skeletal myoblasts are determined by the level of Raf signaling: abrogation of apoptosis by Raf is downstream of caspase 3 activation. Oncogene. **21:**5268-79.

41. **Doyonnas, R., M. A. LaBarge, A. Sacco, C. Charlton, and H. M. Blau.** 2004. Hematopoietic contribution to skeletal muscle regeneration by myelomonocytic precursors. Proc. Natl. Acad. Sci. U. S. A. **101:**13507-12.

42. **Dupont-Versteegden, E. E., J. D. Houle, C. M. Gurley, and C. A. Peterson.** 1998. Early changes in muscle fiber size and gene expression in response to spinal cord transection and exercise. Am. J. Physiol. **275:**C1124-33.

43. **Dusterhoft, S., C. T. Putman, and D. Pette.** 1999. Changes in FGF and FGF receptor expression in low-frequency-stimulated rat muscles and rat satellite cell cultures. Differentiation. **65:**203-8.

44. **Ebelt, H., N. Hufnagel, P. Neuhaus, H. Neuhaus, P. Gajawada, A. Simm, U. Muller-Werdan, K. Werdan, and T. Braun.** 2005. Divergent siblings: E2F2 and E2F4 but not E2F1 and E2F3 induce DNA synthesis in cardiomyocytes without activation of apoptosis. Circ. Res. **96:**509-17.

45. **Eissenberg, J. C., M. Wong, and J. C. Chrivia.** 2005. Human SRCAP and Drosophila melanogaster DOM are homologs that function in the notch signaling pathway. Mol. Cell Biol. **25:**6559-69.

46. **Flanagan-Steet, H., K. Hannon, M. J. McAvoy, R. Hullinger, and B. B. Olwin.** 2000. Loss of FGF receptor 1 signaling reduces skeletal muscle mass and disrupts myofiber organization in the developing limb. Dev. Biol. **218:**21-37.

47. **Florini, J. R., A. B. Roberts, D. Z. Ewton, S. L. Falen, K. C. Flanders, and M. B. Sporn.** 1986. Transforming growth factor-beta. A very potent inhibitor of myoblast differentiation, identical to the differentiation inhibitor secreted by Buffalo rat liver cells. J. Biol. Chem. **261:**16509-13.

48. **Fujita, N., Y. Furukawa, N. Itabashi, K. Okada, T. Saito, and S. Ishibashi.** 2002. Differences in E2F subunit expression in quiescent and proliferating vascular smooth muscle cells. Am. J. Physiol. Heart Circ. Physiol. **283:**H204-12.

49. **Gal-Levi, R., Y. Leshem, S. Aoki, T. Nakamura, and O. Halevy.** 1998. Hepatocyte growth factor plays a dual role in regulating skeletal muscle satellite cell proliferation and differentiation. Biochim. Biophys. Acta. **1402:**39-51.

50. **Gallegly, J. C., N. A. Turesky, B. A. Strotman, C. M. Gurley, C. A. Peterson, and E. E. Dupont-Versteegden.** 2004. Satellite cell regulation of muscle mass is altered at old age. J. Appl. Physiol. **97:**1082-90.

51. **Garrett, K. L., and J. E. Anderson.** 1995. Colocalization of bFGF and the myogenic regulatory gene myogenin in dystrophic mdx muscle precursors and young myotubes in vivo. Dev. Biol. **169:**596-608.

52. **Garry, D. J., A. Meeson, J. Elterman, Y. Zhao, P. Yang, R. Bassel-Duby, and R. S. Williams.** 2000. Myogenic stem cell function is impaired in mice lacking the forkhead/winged helix protein MNF. Proc. Natl. Acad. Sci. U. S. A. **97:**5416-21.

53. **Garry, D. J., Q. Yang, R. Bassel-Duby, and R. S. Williams.** 1997. Persistent expression of MNF identifies myogenic stem cells in postnatal muscles. Dev. Biol. **188:**280-94.

54. **Gaubatz, S., G. J. Lindeman, S. Ishida, L. Jakoi, J. R. Nevins, D. M. Livingston, and R. E. Rempel.** 2000. E2F4 and E2F5 play an essential role in pocket protein-mediated G1 control. Mol. Cell. **6:**729-35.

55. **Gill, R. M., and P. A. Hamel.** 2000. Subcellular compartmentalization of E2F family members is required for maintenance of the postmitotic state in terminally differentiated muscle. J. Cell Biol. **148:**1187-201.

56. **Girling, R., J. F. Partridge, L. R. Bandara, N. Burden, N. F. Totty, J. J. Hsuan, and N. B. La Thangue.** 1993. A new component of the transcription factor DRTF1/E2F. Nature. **362:**83-7.

57. **Goodwin, R. L., L. M. Pabon-Pena, G. C. Foster, and D. Bader.** 1999. The cloning and analysis of LEK1 identifies variations in the LEK/centromere protein F/mitosin gene family. J. Biol. Chem. **274:**18597-604.

58. **Gospodarowicz, D., J. Weseman, J. S. Moran, and J. Lindstrom.** 1976. Effect of fibroblast growth factor on the division and fusion of bovine myoblasts. J. Cell Biol. **70:**395-405.

59. **Greene, E. A., and R. E. Allen.** 1991. Growth factor regulation of bovine satellite cell growth in vitro. J. Anim. Sci. **69:**146-52.

60. **Halevy, O., Y. Piestun, M. Z. Allouh, B. W. Rosser, Y. Rinkevich, R. Reshef, I. Rozenboim, M. Wleklinski-Lee, and Z. Yablonka-Reuveni.** 2004. Pattern of Pax7 expression during myogenesis in the posthatch chicken establishes a model for satellite cell differentiation and renewal. Dev. Dyn. **231:**489-502.

61. **Hannon, K., A. J. Kudla, M. J. McAvoy, K. L. Clase, and B. B. Olwin.** 1996. Differentially expressed fibroblast growth factors regulate skeletal muscle development through autocrine and paracrine mechanisms. J. Cell Biol. **132:**1151-9.

62. **Helin, K., C. L. Wu, A. R. Fattaey, J. A. Lees, B. D. Dynlacht, C. Ngwu, and E. Harlow.** 1993. Heterodimerization of the transcription factors E2F-1 and DP-1 leads to cooperative trans-activation. Genes Dev. **7:**1850-61.

63. **Hijmans, E. M., P. M. Voorhoeve, R. L. Beijersbergen, L. J. van 't Veer, and R. Bernards.** 1995. E2F-5, a new E2F family member that interacts with p130 in vivo. Mol. Cell Biol. **15:**3082-9.

64. **Hollnagel, A., V. Oehlmann, J. Heymer, U. Ruther, and A. Nordheim.** 1999. Id genes are direct targets of bone morphogenetic protein induction in embryonic stem cells. J. Biol Chem. **274:**19838-45.

65. **Huh, C. G., V. M. Factor, A. Sanchez, K. Uchida, E. A. Conner, and S. S. Thorgeirsson.** 2004. Hepatocyte growth factor/c-met signaling pathway is required for efficient liver regeneration and repair. Proc. Natl. Acad. Sci. U. S. A. **101:**4477-82.

66. **Iso, T., V. Sartorelli, G. Chung, T. Shichinohe, L. Kedes, and Y. Hamamori.** 2001. HERP, a new primary target of Notch regulated by ligand binding. Mol. Cell Biol. **21:**6071-9.

67. **Iso, T., V. Sartorelli, C. Poizat, S. Iezzi, H. Y. Wu, G. Chung, L. Kedes, and Y. Hamamori.** 2001. HERP, a novel heterodimer partner of HES/E(spl) in Notch signaling. Mol. Cell Biol. **21:**6080-9.

68. **Jankowski, R. J., B. M. Deasy, B. Cao, C. Gates, and J. Huard.** 2002. The role of CD34 expression and cellular fusion in the regeneration capacity of myogenic progenitor cells. J. Cell Sci. **115:**4361-74.

69. **Jesse, T. L., R. LaChance, M. F. Iademarco, and D. C. Dean.** 1998. Interferon regulatory factor-2 is a transcriptional activator in muscle where It regulates expression of vascular cell adhesion molecule-1. J. Cell Biol. **140:**1265-76.

70. **Johnson, S. E., and R. E. Allen.** 1995. Activation of skeletal muscle satellite cells and the role of fibroblast growth factor receptors. Exp. Cell Res. **219:**449-53.

71. **Johnson, S. E., and R. E. Allen.** 1993. Proliferating cell nuclear antigen (PCNA) is expressed in activated rat skeletal muscle satellite cells. J. Cell Physiol. **154:**39-43.

72. **Kadi, F., N. Charifi, C. Denis, and J. Lexell.** 2004. Satellite cells and myonuclei in young and elderly women and men. Muscle Nerve. **29:**120-7.

73. **Kadi, F., P. Schjerling, L. L. Andersen, N. Charifi, J. L. Madsen, L. R. Christensen, and J. L. Andersen.** 2004. The effects of heavy resistance training and detraining on satellite cells in human skeletal muscles. J. Physiol. **558:**1005-12.

74. **Kadi, F., and L. E. Thornell.** 2000. Concomitant increases in myonuclear and satellite cell content in female trapezius muscle following strength training. Histochem. Cell Biol. **113:**99-103.

75. **Kamanga-Sollo, E., M. S. Pampusch, M. E. White, and W. R. Dayton.** 2003. Role of insulin-like growth factor binding protein (IGFBP)-3 in TGF-beta- and GDF-8 (myostatin)-induced suppression of proliferation in porcine embryonic myogenic cell cultures. J. Cell Physiol. **197:**225-31.

76. **Kamanga-Sollo, E., M. S. Pampusch, G. Xi, M. E. White, M. R. Hathaway, and W. R. Dayton.** 2004. IGF-I mRNA levels in bovine satellite cell cultures: effects of fusion and anabolic steroid treatment. J. Cell Physiol. **201:**181-9.

77. **Kastner, S., M. C. Elias, A. J. Rivera, and Z. Yablonka-Reuveni.** 2000. Gene expression patterns of the fibroblast growth factors and their receptors during myogenesis of rat satellite cells. J. Histochem. Cytochem. **48:**1079-96.

78. **Kim, J. S., J. M. Cross, and M. M. Bamman.** 2005. Impact of resistance loading on myostatin expression and cell cycle regulation in young and older men and women. Am. J. Physiol. Endocrinol. Metab. **288:**E1110-9.

79. **Kim, S. J., S. H. Cheon, S. J. Yoo, J. Kwon, J. H. Park, C. G. Kim, K. Rhee, S. You, J. Y. Lee, S. I. Roh, and H. S. Yoon.** 2005. Contribution of the PI3K/Akt/PKB signal pathway to maintenance of self-renewal in human embryonic stem cells. FEBS Lett. **579:**534-40.

80. **Kritzik, M. R., E. Jones, Z. Chen, M. Krakowski, T. Krahl, A. Good, C. Wright, H. Fox, and N. Sarvetnick.** 1999. PDX-1 and Msx-2 expression in the regenerating and developing pancreas. J. Endocrinol. **163:**523-30.

81. **Kuroda, K., H. Han, S. Tani, K. Tanigaki, T. Tun, T. Furukawa, Y. Taniguchi, H. Kurooka, Y. Hamada, S. Toyokuni, and T. Honjo.** 2003. Regulation of marginal zone B cell development by MINT, a suppressor of Notch/RBP-J signaling pathway. Immunity. **18:**301-12.

82. **Kusek, J. C., R. M. Greene, and M. M. Pisano.** 2001. Expression of the E2F and retinoblastoma families of proteins during neural differentiation. Brain. Res. Bull. **54:**187-98.

83. **LaBarge, M. A., and H. M. Blau.** 2002. Biological progression from adult bone marrow to mononucleate muscle stem cell to multinucleate muscle fiber in response to injury. Cell. **111:**589-601.

84. **LaFramboise, W. A., R. D. Guthrie, D. Scalise, V. Elborne, K. L. Bombach, C. S. Armanious, and J. A. Magovern.** 2003. Effect of muscle origin and phenotype on satellite cell muscle-specific gene expression. J. Mol. Cell Cardiol. **35:**1307-18.

85. **Lee, J. Y., Z. Qu-Petersen, B. Cao, S. Kimura, R. Jankowski, J. Cummins, A. Usas, C. Gates, P. Robbins, A. Wernig, and J. Huard.** 2000. Clonal isolation of muscle-derived cells capable of enhancing muscle regeneration and bone healing. J. Cell Biol. **150:**1085-100.

86. **Lefaucheur, J. P., and A. Sebille.** 1995. Basic fibroblast growth factor promotes in vivo muscle regeneration in murine muscular dystrophy. Neurosci. Lett. **202:**121-4.

87. **Machida, S., and F. W. Booth.** 2004. Increased nuclear proteins in muscle satellite cells in aged animals as compared to young growing animals. Exp. Gerontol. **39:**1521-5.

88. **Malm, C., P. Nyberg, M. Engstrom, B. Sjodin, R. Lenkei, B. Ekblom, and I. Lundberg.** 2000. Immunological changes in human skeletal muscle and blood after eccentric exercise and multiple biopsies. J. Physiol. **529 Pt 1:**243-62.

89. **Mauro, A.** 1961. Satellite cell of skeletal muscle fibers. J. Biophys. Biochem. Cytol. **9:**493-5.

90. **McCroskery, S., M. Thomas, L. Maxwell, M. Sharma, and R. Kambadur.** 2003. Myostatin negatively regulates satellite cell activation and self-renewal. J. Cell Biol. **162:**1135-47.

91. **McFarland, D. C., X. Liu, S. G. Velleman, C. Zeng, C. S. Coy, and J. E. Pesall.** 2003. Variation in fibroblast growth factor response and heparan sulfate proteoglycan production in satellite cell populations. Comp. Biochem. Physiol. C. Toxicol. Pharmacol. **134:**341-51.

92. **Miller, K. J., D. Thaloor, S. Matteson, and G. K. Pavlath.** 2000. Hepatocyte growth factor affects satellite cell activation and differentiation in regenerating skeletal muscle. Am. J. Physiol. Cell. Physiol. **278:**C174-81.

93. **Moss, F. P., and C. P. Leblond.** 1971. Satellite cells as the source of nuclei in muscles of growing rats. Anat. Rec. **170:**421-35.

94. **Naldini, L., K. M. Weidner, E. Vigna, G. Gaudino, A. Bardelli, C. Ponzetto, R. P. Narsimhan, G. Hartmann, R. Zarnegar, G. K. Michalopoulos, and et al.** 1991. Scatter factor and hepatocyte growth factor are indistinguishable ligands for the MET receptor. Embo. J. **10:**2867-78.

95. **Newberry, E. P., T. Latifi, and D. A. Towler.** 1999. The RRM domain of MINT, a novel Msx2 binding protein, recognizes and regulates the rat osteocalcin promoter. Biochemistry. **38:**10678-90.

96. **Olguin, H. C., and B. B. Olwin.** 2004. Pax-7 up-regulation inhibits myogenesis and cell cycle progression in satellite cells: a potential mechanism for self-renewal. Dev. Biol. **275:**375-88.

97. **Olwin, B. B., and S. D. Hauschka.** 1988. Cell surface fibroblast growth factor and epidermal growth factor receptors are permanently lost during skeletal muscle terminal differentiation in culture. J. Cell. Biol. **107:**761-9.

98. **Olwin, B. B., and A. Rapraeger.** 1992. Repression of myogenic differentiation by aFGF, bFGF, and K-FGF is dependent on cellular heparan sulfate. J. Cell. Biol. **118:**631-9.

99. **Oswald, F., U. Kostezka, K. Astrahantseff, S. Bourteele, K. Dillinger, U. Zechner, L. Ludwig, M. Wilda, H. Hameister, W. Knochel, S. Liptay, and R. M. Schmid.** 2002. SHARP is a novel component of the Notch/RBP-Jkappa signalling pathway. Embo. J. **21:**5417-26.

100. **Oustanina, S., G. Hause, and T. Braun.** 2004. Pax7 directs postnatal renewal and propagation of myogenic satellite cells but not their specification. Embo. J. **23:**3430-9.

101. **Owino, V., S. Y. Yang, and G. Goldspink.** 2001. Age-related loss of skeletal muscle function and the inability to express the autocrine form of insulin-like growth factor-1 (MGF) in response to mechanical overload. FEBS Lett. **505:**259-63.

102. **Pabon-Pena, L. M., R. L. Goodwin, L. J. Cise, and D. Bader.** 2000. Analysis of CMF1 reveals a bone morphogenetic protein-independent component of the cardiomyogenic pathway. J. Biol. Chem. **275:**21453-9.

103. **Palena, A., R. Mangiacasale, A. R. Magnano, L. Barberi, R. Giordano, C. Spadafora, and P. Lavia.** 2000. E2F transcription factors are differentially expressed in murine gametes and early embryos. Mech. Dev. **97:**211-5.

104. **Papadimou, E., C. Menard, C. Grey, and M. Puceat.** 2005. Interplay between the retinoblastoma protein and LEK1 specifies stem cells toward the cardiac lineage. Embo. J.

105. **Pierce, A. M., R. Schneider-Broussard, J. L. Philhower, and D. G. Johnson.** 1998. Differential activities of E2F family members: unique functions in regulating transcription. Mol. Carcinog. **22:**190-8.

106. **Polanowska, J., L. Le Cam, B. Orsetti, H. Valles, E. Fabbrizio, L. Fajas, S. Taviaux, C. Theillet, and C. Sardet.** 2000. Human E2F5 gene is oncogenic in primary rodent cells and is amplified in human breast tumors. Genes Chromosomes Cancer. **28:**126-30.

107. **Rao, S. S., and D. S. Kohtz.** 1995. Positive and negative regulation of D-type cyclin expression in skeletal myoblasts by basic fibroblast growth factor and transforming growth factor beta. A role for cyclin D1 in control of myoblast differentiation. J. Biol. Chem. **270:**4093-100.

108. **Rathbone, C. R., J. C. Wenke, G. L. Warren, and R. B. Armstrong.** 2003. Importance of satellite cells in the strength recovery after eccentric contraction-induced muscle injury. Am. J. Physiol. Regul. Integr. Comp. Physiol. **285:**R1490-5.

109. **Rayman, J. B., Y. Takahashi, V. B. Indjeian, J. H. Dannenberg, S. Catchpole, R. J. Watson, H. te Riele, and B. D. Dynlacht.** 2002. E2F mediates cell cycle-dependent transcriptional repression in vivo by recruitment of an HDAC1/mSin3B corepressor complex. Genes Dev. **16:**933-47.

110. **Redkar, A., J. K. deRiel, Y. S. Xu, M. Montgomery, V. Patwardhan, and J. Litvin.** 2002. Characterization of cardiac muscle factor 1 sequence motifs: retinoblastoma protein binding and nuclear localization. Gene. **282:**53-64.

111. **Relaix, F., D. Rocancourt, A. Mansouri, and M. Buckingham.** 2005. A Pax3/Pax7-dependent population of skeletal muscle progenitor cells. Nature. **435:**948-53.

112. **Renault, V., G. Piron-Hamelin, C. Forestier, S. DiDonna, S. Decary, F. Hentati, G. Saillant, G. S. Butler-Browne, and V. Mouly.** 2000. Skeletal muscle regeneration and the mitotic clock. Exp. Gerontol. **35:**711-9.

113. **Royer, C. L., J. C. Howell, P. R. Morrison, E. F. Srour, and M. C. Yoder.** 2002. Muscle-derived CD45-SCA-1+c-kit- progenitor cells give rise to skeletal muscle myotubes in vitro. In Vitro Cell Dev. Biol. Anim. **38:**512-7.

114. **Samuels, M. L., and M. McMahon.** 1994. Inhibition of platelet-derived growth factor- and epidermal growth factor-mediated mitogenesis and signaling in 3T3 cells expressing delta Raf-1:ER, an estradiol-regulated form of Raf-1. Mol. Cell. Biol. **14:**7855-66.

115. **Sardet, C., M. Vidal, D. Cobrinik, Y. Geng, C. Onufryk, A. Chen, and R. A. Weinberg.** 1995. E2F-4 and E2F-5, two members of the E2F family, are expressed in the early phases of the cell cycle. Proc. Natl. Acad. Sci. U. S. A. **92:**2403-7.

116. **Schmalbruch, H., and U. Hellhammer.** 1976. The number of satellite cells in normal human muscle. Anat. Rec. **185:**279-87.

117. **Schultz, E., M. C. Gibson, and T. Champion.** 1978. Satellite cells are mitotically quiescent in mature mouse muscle: an EM and radioautographic study. J. Exp. Zool. **206:**451-6.

118. **Seale, P., J. Ishibashi, C. Holterman, and M. A. Rudnicki.** 2004. Muscle satellite cell-specific genes identified by genetic profiling of MyoD-deficient myogenic cell. Dev. Biol. **275:**287-300.

119. **Seale, P., L. A. Sabourin, A. Girgis-Gabardo, A. Mansouri, P. Gruss, and M. A. Rudnicki.** 2000. Pax7 is required for the specification of myogenic satellite cells. Cell. **102:**777-86.

120. **Sellman, J. E., K. C. Deruisseau, J. L. Betters, V. A. Lira, Q. A. Soltow, J. T. Selsby, and D. S. Criswell.** 2005. In vivo inhibition of nitric oxide synthase impairs up-regulation of contractile protein mRNA in overloaded plantaris muscle. J. Appl. Physiol.

121. **Sheehan, S. M., and R. E. Allen.** 1999. Skeletal muscle satellite cell proliferation in response to members of the fibroblast growth factor family and hepatocyte growth factor. J. Cell Physiol. **181:**499-506.

122. **Sheehan, S. M., R. Tatsumi, C. J. Temm-Grove, and R. E. Allen.** 2000. HGF is an autocrine growth factor for skeletal muscle satellite cells in vitro. Muscle Nerve. **23:**239-45.

123. **Shi, Y., M. Downes, W. Xie, H. Y. Kao, P. Ordentlich, C. C. Tsai, M. Hon, and R. M. Evans.** 2001. Sharp, an inducible cofactor that integrates nuclear receptor repression and activation. Genes Dev. **15:**1140-51.

124. **Sierra, O. L., S. L. Cheng, A. P. Loewy, N. Charlton-Kachigian, and D. A. Towler.** 2004. MINT, the Msx2 interacting nuclear matrix target, enhances Runx2-dependent activation of the osteocalcin fibroblast growth factor response element. J. Biol. Chem. **279:**32913-23.

125. **Silva, W. A., Jr., D. T. Covas, R. A. Panepucci, R. Proto-Siqueira, J. L. Siufi, D. L. Zanette, A. R. Santos, and M. A. Zago.** 2003. The profile of gene expression of human marrow mesenchymal stem cells. Stem Cells. **21:**661-9.

126. **Sirard, C., S. Kim, C. Mirtsos, P. Tadich, P. A. Hoodless, A. Itie, R. Maxson, J. L. Wrana, and T. W. Mak.** 2000. Targeted disruption in murine cells reveals variable requirement for Smad4 in transforming growth factor beta-related signaling. J. Biol. Chem. **275:**2063-70.

127. **Smith, H. K., L. Maxwell, C. D. Rodgers, N. H. McKee, and M. J. Plyley.** 2001. Exercise-enhanced satellite cell proliferation and new myonuclear accretion in rat skeletal muscle. J. Appl. Physiol. **90:**1407-14.

128. **Snow, M. H.** 1977. Myogenic cell formation in regenerating rat skeletal muscle injured by mincing. II. An autoradiographic study. Anat. Rec. **188:**201-17.

129. **Stewart, J. D., T. L. Masi, A. E. Cumming, G. M. Molnar, B. M. Wentworth, K. Sampath, J. M. McPherson, and P. C. Yaeger.** 2003. Characterization of proliferating human skeletal muscle-derived cells in vitro: differential modulation of myoblast markers by TGF-beta2. J. Cell Physiol. **196:**70-8.

130. **Stojkovic, M., M. Lako, P. Stojkovic, R. Stewart, S. Przyborski, L. Armstrong, J. Evans, M. Herbert, L. Hyslop, S. Ahmad, A. Murdoch, and T. Strachan.** 2004. Derivation of human embryonic stem cells from day-8 blastocysts recovered after three-step in vitro culture. Stem Cells. **22:**790-7.

131. **Tatsumi, R., and R. E. Allen.** 2004. Active hepatocyte growth factor is present in skeletal muscle extracellular matrix. Muscle Nerve. **30:**654-8.

132. **Tatsumi, R., J. E. Anderson, C. J. Nevoret, O. Halevy, and R. E. Allen.** 1998. HGF/SF is present in normal adult skeletal muscle and is capable of activating satellite cells. Dev. Biol. **194:**114-28.

133. **Tatsumi, R., A. Hattori, Y. Ikeuchi, J. E. Anderson, and R. E. Allen.** 2002. Release of hepatocyte growth factor from mechanically stretched skeletal muscle satellite cells and role of pH and nitric oxide. Mol. Biol. Cell **13:**2909-18.

134. **Vaidya, T. B., S. J. Rhodes, E. J. Taparowsky, and S. F. Konieczny.** 1989. Fibroblast growth factor and transforming growth factor beta repress transcription of the myogenic regulatory gene MyoD1. Mol. Cell Biol. **9:**3576-9.

135. **Vaishnav, Y. N., and V. Pant.** 1999. Differential regulation of E2F transcription factors by p53 tumor suppressor protein. DNA Cell Biol **18:**911-22.

136. **Vara, D., K. A. Bicknell, C. H. Coxon, and G. Brooks.** 2003. Inhibition of E2F abrogates the development of cardiac myocyte hypertrophy. J. Biol. Chem. **278:**21388-94.

137. **Villena, J., and E. Brandan.** 2004. Dermatan sulfate exerts an enhanced growth factor response on skeletal muscle satellite cell proliferation and migration. J. Cell Physiol. **198:**169-78.

138. **Walsh, F. S., C. Hobbs, D. J. Wells, C. R. Slater, and S. Fazeli.** 2000. Ectopic expression of NCAM in skeletal muscle of transgenic mice results in terminal sprouting at the neuromuscular junction and altered structure but not function. Mol. Cell Neurosci. **15:**244-61.

139. **Wang, X., S. R. Thomson, J. D. Starkey, J. L. Page, A. D. Ealy, and S. E. Johnson.** 2004. Transforming growth factor beta1 is up-regulated by activated Raf in skeletal myoblasts but does not contribute to the differentiation-defective phenotype. J. Biol. Chem. **279:**2528-34.

140. **Woods, D., D. Parry, H. Cherwinski, E. Bosch, E. Lees, and M. McMahon.** 1997. Raf-induced proliferation or cell cycle arrest is determined by the level of Raf activity with arrest mediated by p21Cip1. Mol. Cell Biol. **17:**5598-611.

141. **Wozniak, A. C., O. Pilipowicz, Z. Yablonka-Reuveni, S. Greenway, S. Craven, E. Scott, and J. E. Anderson.** 2003. C-Met expression and mechanical activation of satellite cells on cultured muscle fibers. J. Histochem. Cytochem. **51:**1437-45.

142. **Xi, R., and T. Xie.** 2005. Stem cell self-renewal controlled by chromatin remodeling factors. Science **310:**1487-9.

143. **Yablonka-Reuveni, Z., R. Seger, and A. J. Rivera.** 1999. Fibroblast growth factor promotes recruitment of skeletal muscle satellite cells in young and old rats. J. Histochem. Cytochem. **47:**23-42.

144. **Yang, Q., R. Bassel-Duby, and R. S. Williams.** 1997. Transient expression of a winged-helix protein, MNF-beta, during myogenesis. Mol. Cell. Biol. **17:**5236-43.

145. **Yang, Z. Y., J. Guo, N. Li, M. Qian, S. N. Wang, and X. L. Zhu.** 2003. Mitosin/CENP-F is a conserved kinetochore protein subjected to cytoplasmic dynein-mediated poleward transport. Cell Res. **13:**275-83.

146. **Yi, Z., M. R. Hathaway, W. R. Dayton, and M. E. White.** 2001. Effects of growth factors on insulin-like growth factor binding protein (IGFBP) secretion by primary porcine satellite cell cultures. J. Anim. Sci. **79:**2820-6.

147. **Zammit, P. S., J. P. Golding, Y. Nagata, V. Hudon, T. A. Partridge, and J. R. Beauchamp.** 2004. Muscle satellite cells adopt divergent fates: a mechanism for self-renewal? J. Cell Biol. **166:**347-57.

BIOGRAPHICAL SKETCH

Sarah Reed was born in Bellefonte, Pennsylvania, to Lisa and Howard Grove, Jr. She grew up riding and showing Quarter Horses and was a member of 4-H and the American Quarter Horse Youth Association. Sarah graduated summa cum laude from Delaware Valley College with her B.S. in equine science in December 2003. While at DVC, Sarah was involved in the Equine Science Organization and Delta Tau Alpha. Following graduation, she worked as a laboratory technician for Dr. Sally E. Johnson at the Pennsylvania State University. Upon Dr. Johnson's move to the University of Florida, Sarah enrolled as a master's student in Dr. Johnson's laboratory. Sarah currently resides in Alachua, Florida, with her husband, Jared, and their two dogs, Annie and Bella.